
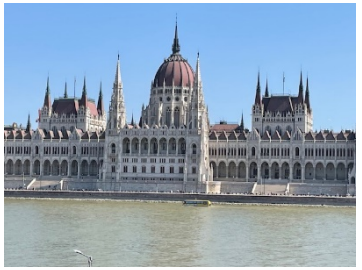
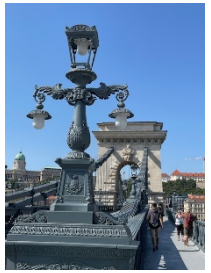

POLITECNICO DI MILANO

MŰEGYETEM 1782

15th fib PhD Symposium 2024 Budapest - Overview

BME, 1111 Budapest, Műegyetem rkp. 3.

fib CEB-FIP

POLITECNICO MILANO 1863

UHPFRC for sustainability: a high-performance material for new and existing structures

M. di Prisco

Politecnico di Milano

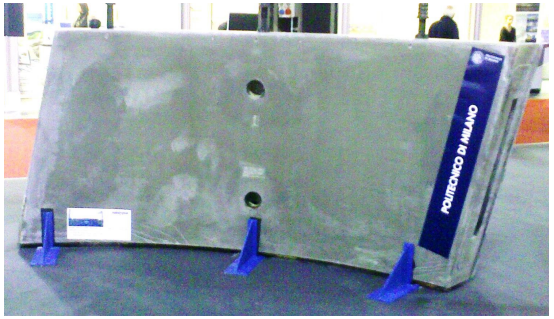

M. Colombo

G. Zani

M.C. Rampini

Material	R/C	P/C	FRC
Idea birth	1850	1888	Last 1950's
Preliminary applications	1861	1935	1960
First patent	1867	1927	1975
Scientific papers	1877	1949	1963
Design guidelines	German 1903	CEB-FIP 1970	ACI 544 - 1982 RILEM - 1995
Massive applications	1905	1945	1975

2 chapters in the fib Model Code 2010

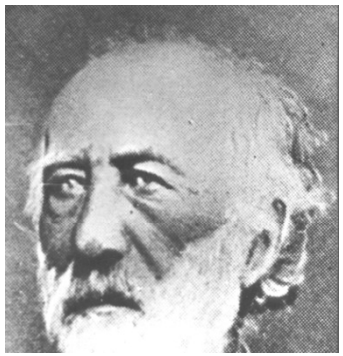

J. L. Lambot (1814-1887)

E. Freyssinet (1879 1962)

G. B. Batson

Romualdi, and Batson, ASCE Proc. Vol. 89, EM3, June 1963.

✓A long history ...

Ferrocement

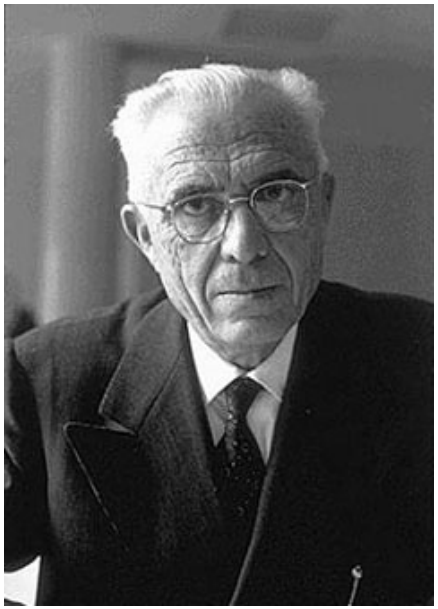

"We wondered if, increasing significantly the diffusion of the steel and its percentage (i.e. reinforcement ratio), it could not be possible to create a new material characterized by a higher strength and especially a larger elasticity and elongation ...".

Pier Luigi Nervi, 1940

t = 38 mm!

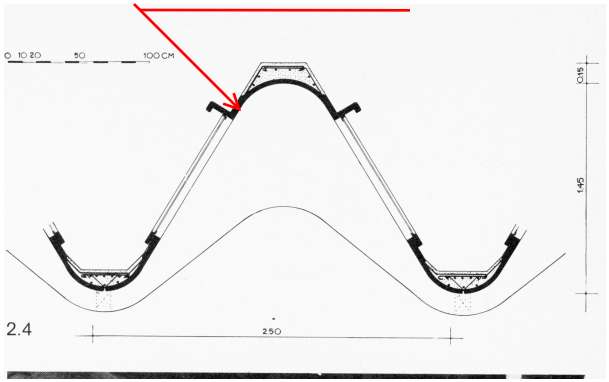

Vault span 94 m!

Exposition Palace: B Pavilion, Torino, 1949-50

Reconstruction stadium Jean Bouin, Paris (2012)

- Envelope 23,000 m^2, roof 12,000 m^2
- 3600 triangular precast UHPC elements for roof
- All elements precast

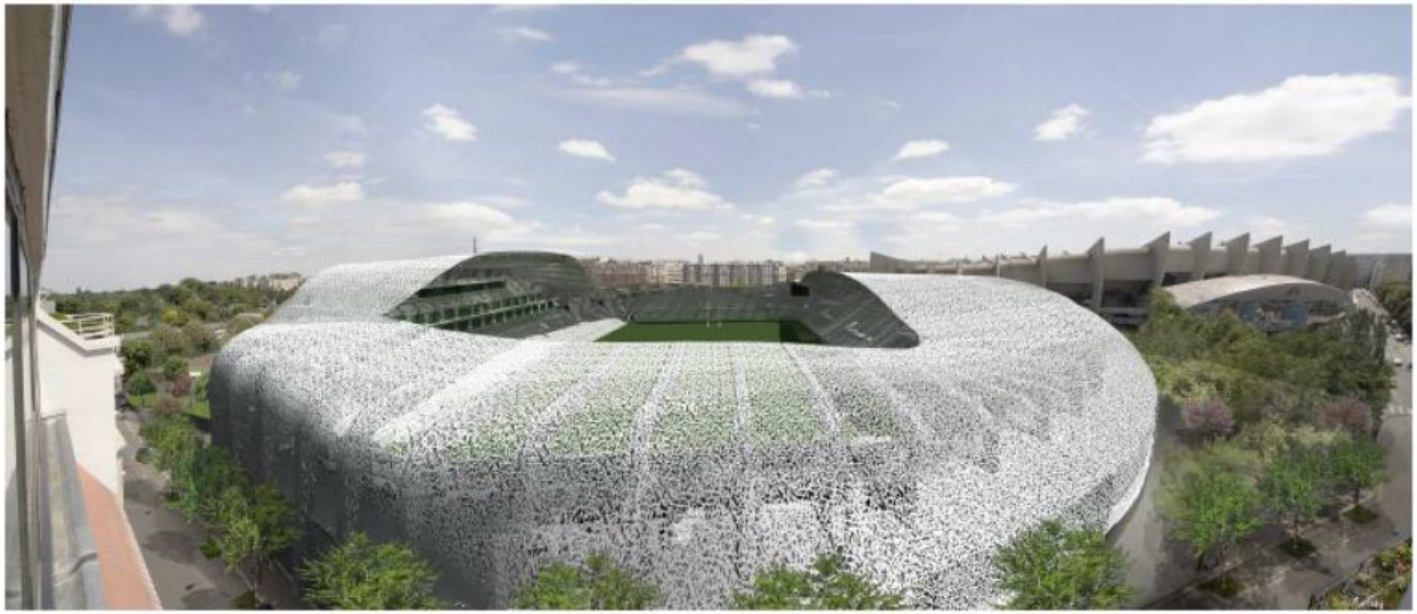

Architect Rudy Ricciotti

courtesy by J. Walraven

Stadium Jean Bouin, Paris (2012)

1900 elements for roof
1600 elements for facade

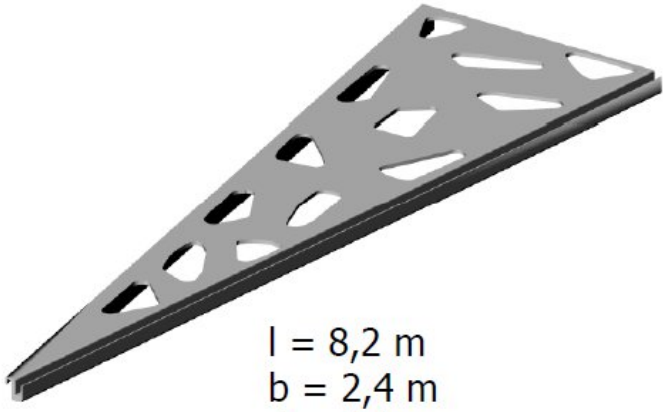

l = 8,2 m
b = 2,4 m
d = 35mm

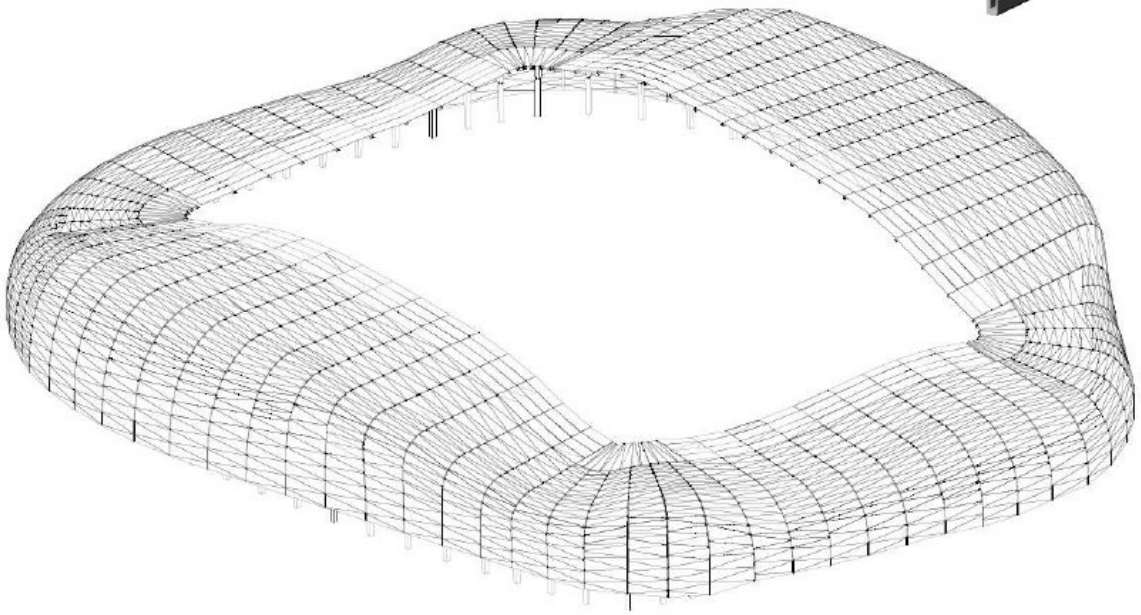

courtesy by J. Walraven

Stade Jean Bouin, Paris (2012)

23000 m² lattice envelope and roof

(left): UHPC lattice roof system with glass inserts

(right): sunlight filtering through the facade

courtesy by J. Walraven

UHPC Building structures (2014)

MuCEM: Musée des Civilisations de l'Europe et de la Méditerranée, Marseille 2014

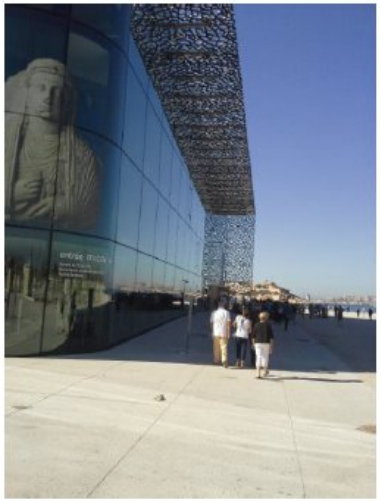

The load bearing structure of this building consist to a large extent of UHPC components such as tree-like columns, the edge beams to the suspended floors, the facade elements and the 78m footbridge to the neighbouring fort Saint Jean.

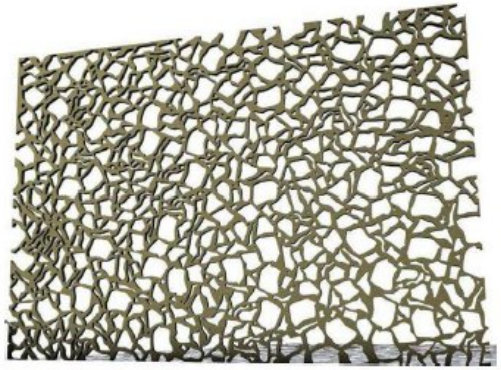

courtesy by J. Walraven

UHPC Building Structures (2014)

MuCem under construction 2012

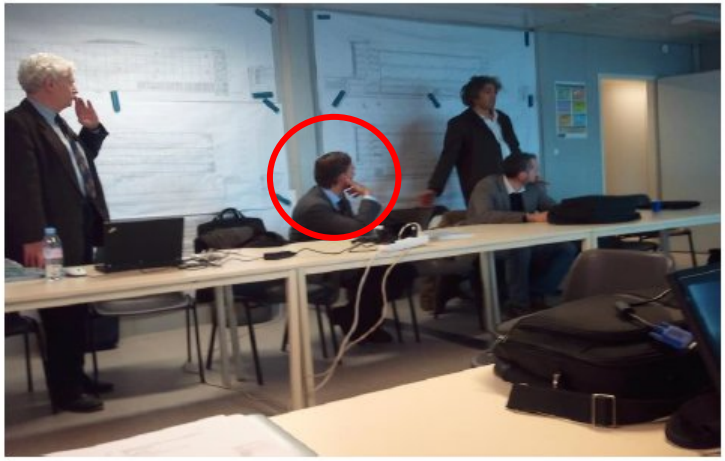

courtesy by J. Walraven

UHPFRC roof Montpellier TGV Station 2017

Concrete Ductal White B3, 1.75% fibres;
f_{ck} = 130 Mpa
LoP (tension) = 5.5 Mpa.

Roof made of 115 beams ("palms")

Roof made of 115 modular double cambered self-supporting elements in precast white UHPFRC, filtering the strong southern light. Span = 20m , width = 2.4m, thickness 4 cm. All roofing elements (10.000 m^2) were produced in 5 months and installed in 2 weeks.

courtesy by J. Walraven

UHPFRC roof Montpellier TGV Station (2017)

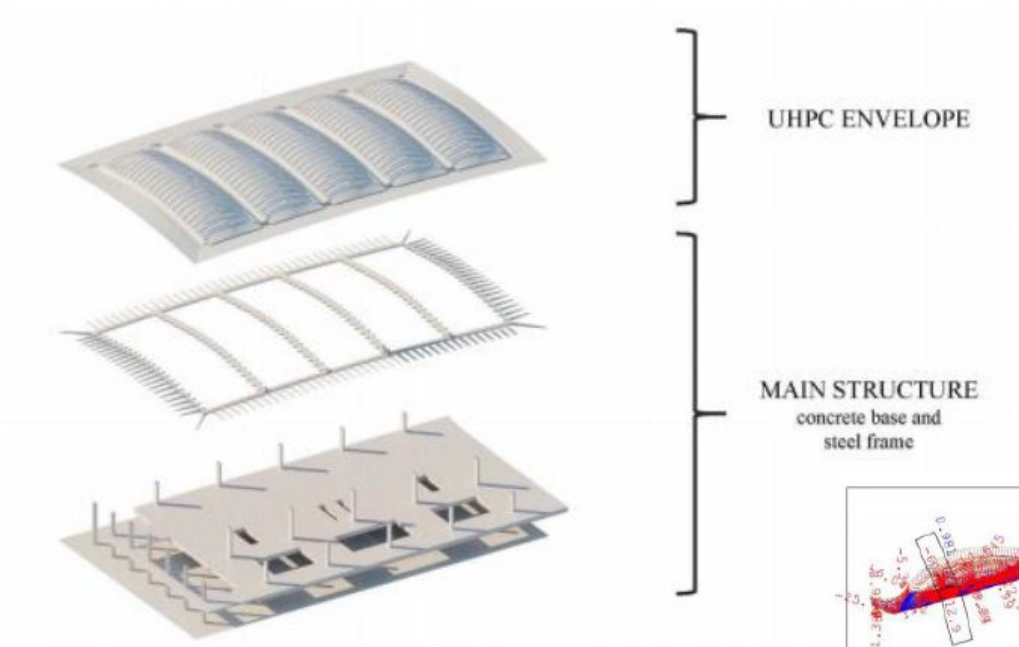

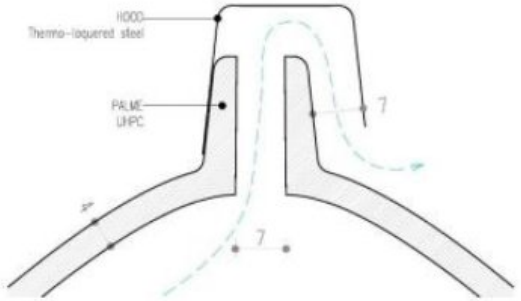

"Porous roof", with detail for climate regulation. Natural ventilation verified b fluid dynamics computational analysis

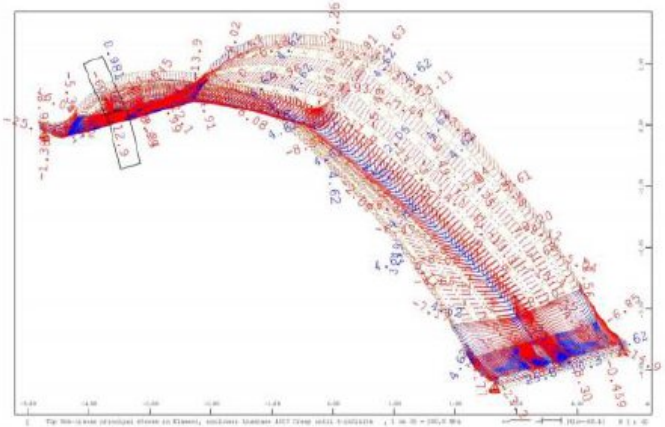

Nonlinear analysis of roof;

Maximum admissible SLS concrete stress $\sigma_{ct,SLS}$ = 4.75 Mpa, and maximum compressive stress $\sigma_{cc,SLS}$ = 78 Mpa;

W < 0.1mm, δ_{max} = 6.8mm = l/1200

courtesy by J. Walraven

UHPFRC roof Montpellier TGV Station 2017

Full scale testing of a beam, subjected to several load-bearing configurations, with data corresponding to deformations and deflections of the structure and natural frequence, in order to confirm the static and dynamic behaviour.

courtesy by J. Walraven

Outline

- ✓ HPFRC sustainability
- ✓ hybrid solution to optimize mechanical performance
- ✓ constitutive law identification and modelling problems
- ✓ applications:
  - precast light roofing: a synergic solution for industrial building rehabilitation
  - light floors partially prefabricated
  - UHPFRC panels as loss formworks to protect bridge deck
  - UHPFRC to strengthen damaged half-joints
  - tunnel segments
  - HPFRC for retrofitting
- ✓ Concluding remarks

Concrete evolution

Development of compressive strength of concrete since 1950

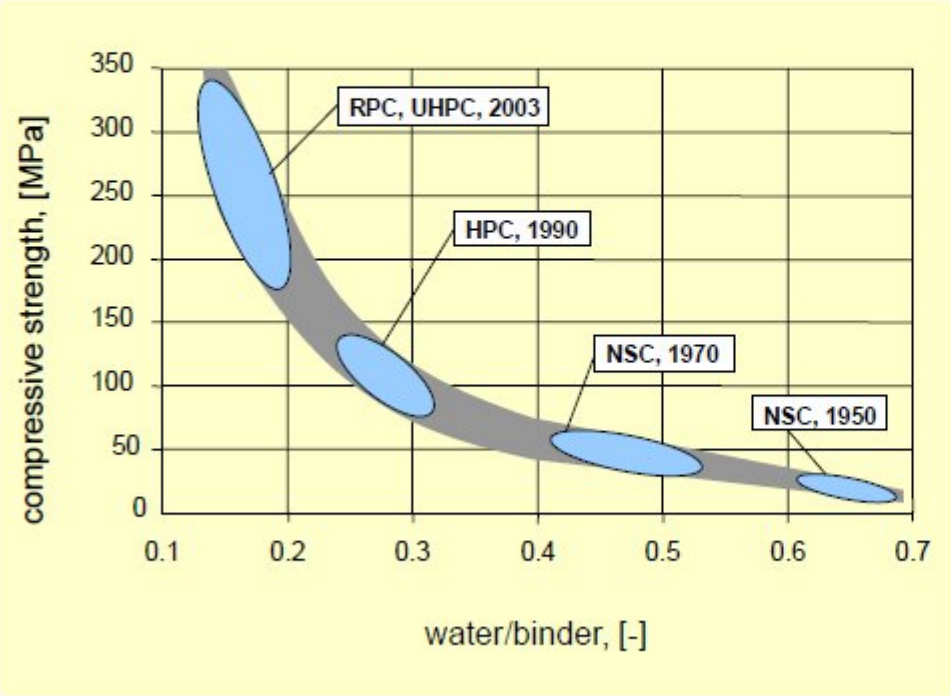

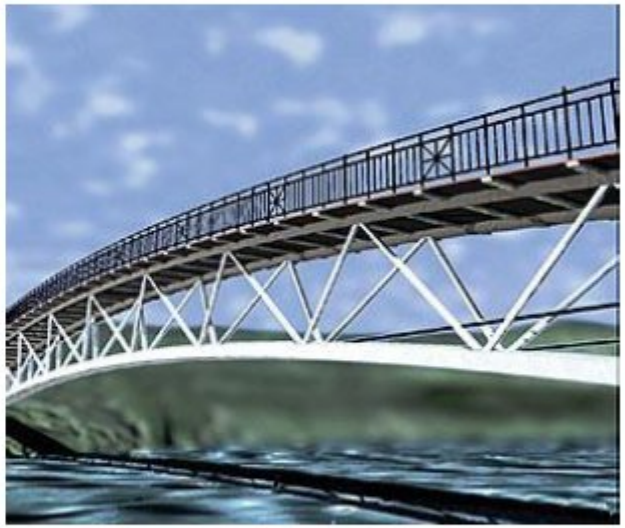

courtesy by J. Walraven

Maximum strength by optimization packing density

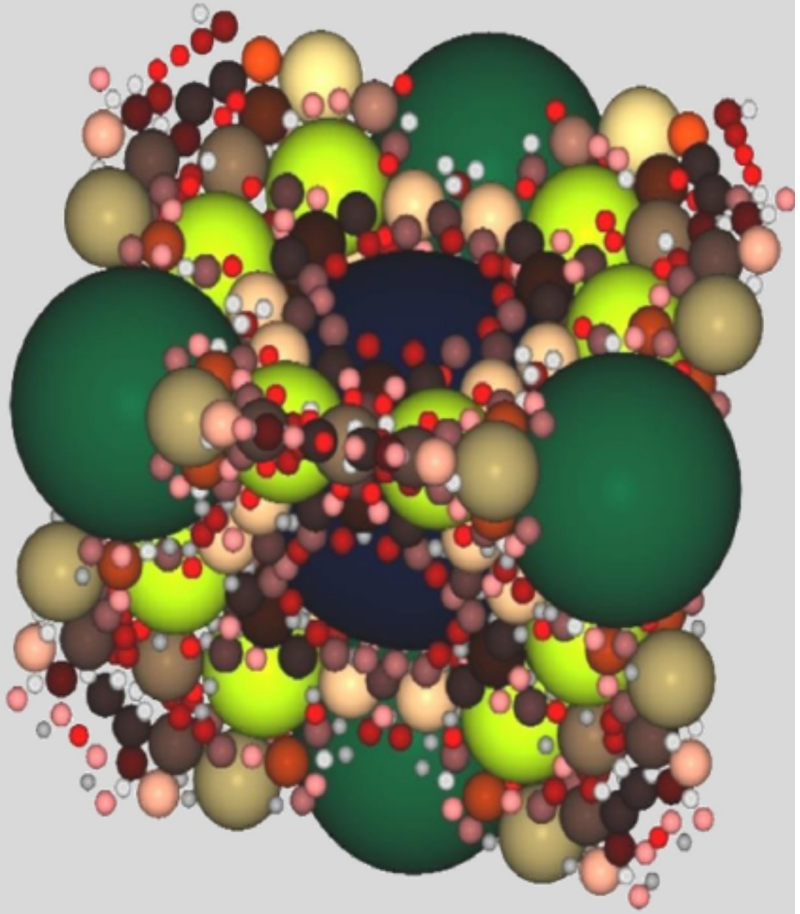

Figure: University Kassel

	Dosage (kg/m^3)
Cement type I 52.5	**600**
Slag	500
Water	200
Superplasticizer	33 (l/m^3)
Sand 0-2 mm	983
Fibers (l_f = 13mm; d_f = 0.16mm)	100

 = 2450 – 2530 kg/m^3

$R_{cm,\ 24h}$ = 66.3 Mpa
$R_{cm,\ 7d}$ = 99.1 Mpa
$R_{cm,\ 28d}$ = 116.5 Mpa
E_{sm} = 45249 Mpa

Around 600 kg of CO_2 for 1 m^3 of UHPFRC

- **> durability (life time extension)**
- **< volume (structure optimization)**

To have a daily-life comparison, we have to take into account that:

1 km with a hybrid car = 0.1 kg of CO_2 emission

1 km with a modern plane = 0.25 kg/pass

1 km with a modern cruise ship = 0.4 kg/pass

1 km with a train = 0.024 kg/pass

1 kwh = 0.3 kg

In Italy the whole emission of CO_2 / habitant for the whole production of concrete is around 1.5 kg

CASE STUDY: ROOF ELEMENT

Roof systems are an important component of the building envelope, since they are specifically designed to separate the living spaces from the natural environment. **They should ensure: adequate mechanical performances, energy efficiency, sound insulation, durability and aesthetics**.

HOW CAN WE MEET THE REQUIREMENTS OF THE REVISED NATIONAL CODES?

A retrofitting strategy that might be successfully applied to several precast structures in northern Italy is represented by the substitution of the unsafe tertiary roofing elements with **innovative multilayer panels** characterized by lightness and remarkable structural performances.

HPFRC + INSULATING CORE + TRC

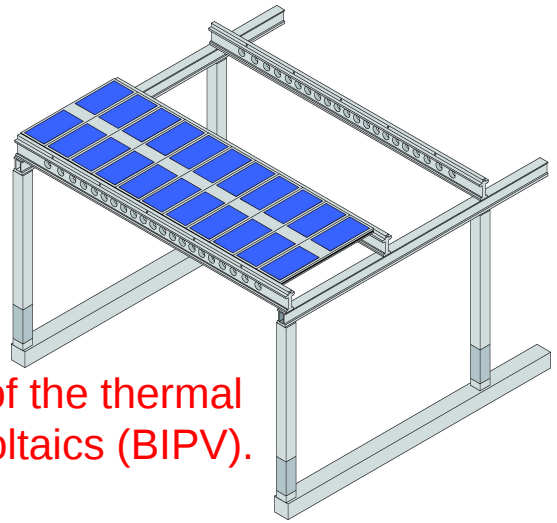

- self-weight reduction;
- global cost reduction;
- fire safety;
- no need of waterproofing layer;
- environmental sustainability, relying both on the improvement of the thermal performances and on the design of Building-Integrated Photovoltaics (BIPV).

MATERIALS

HPFRCC

w/b=0.19 and SP/c=5.5%.

Component	Content
Cement I 52.5	600 kg/m^3
Sand $0 \div 2$ mm	977 kg/m^3
Water	200 l/m^3
Superplasticizer	33 l/m^3
Slag	500 kg/m^3
Steel fibers	100 kg/m^3

Flexural residual strengths.

Specimen	f_{R1} [MPa]	$f_{R1,av}$ [MPa] (std)	f_{R3} [MPa]	$f_{R3,av}$ [MPa] (std)
H1_a1_1	15.90	15.46	14.51	12.87
H1_a1_2	15.11	(0.40)	12.27	(1.44)
H1_a1_3	15.38		11.82	

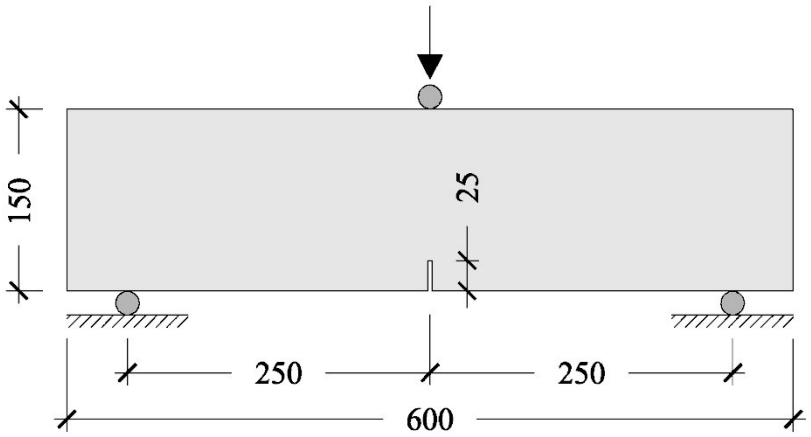

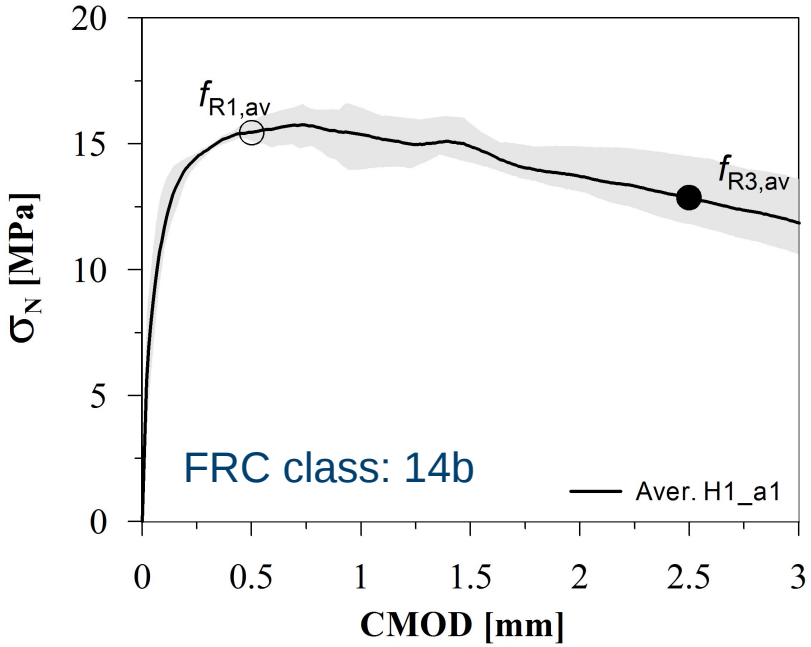

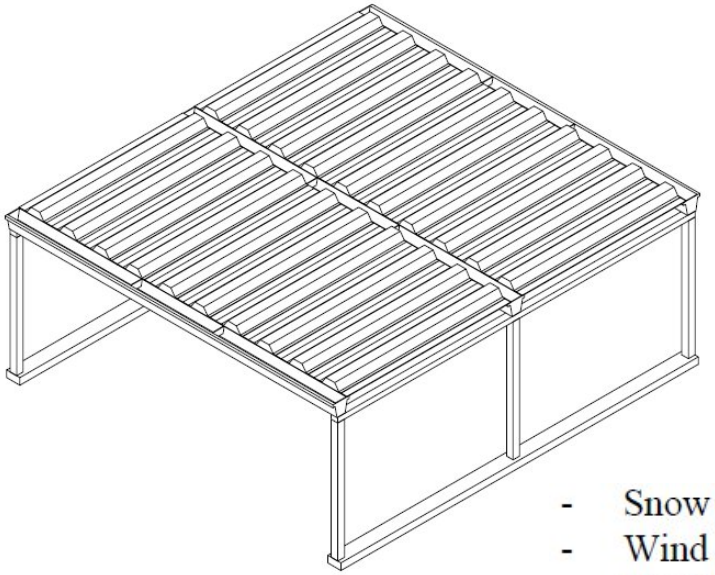

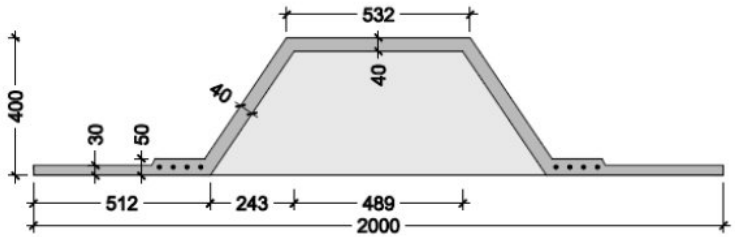

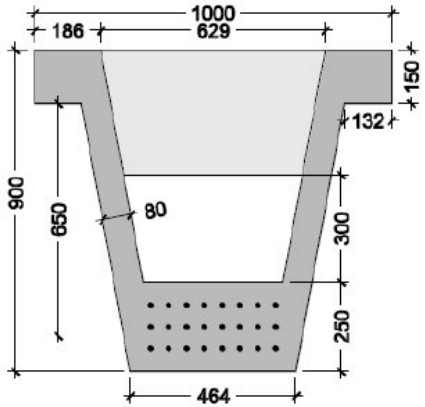

- Snow load: 1.2 kN/m^2
- Wind load: 0.64 kN/m^2
- Distributed maintenance load: 0.5 kN/m^2
- Seismic acceleration: $S_d = 0{,}07$ g

Table 3. Materials costs

Conventional Concrete C50/60 (€/m^3)	VHPFRC (fibers incl.) (€/m^3)	Steel Bars (€/kg)	Prestressed Tendons (€/kg)	Fiber Reinforced Concrete (€/m^3)
50	440	0.65	1.00	150

Table 7 – Structure costs

	Material Cost (€)	Labor Cost (€)	Transport Cost (€)	Storage Cost (€)	Assembly Cost (€)	**Structure Cost (€)**
Traditional	22.401	21.728	5.601	6.301	7.002	**63.033**
New Solution	24.037	8.175	3.075	3.459	7.002	**45.748**

di Prisco et al., CIC 2014

ODP = Ozono Depleting Potential
GWP = Global Warming Potential
PED = Primary Energy Demand

Computation for a specific volume

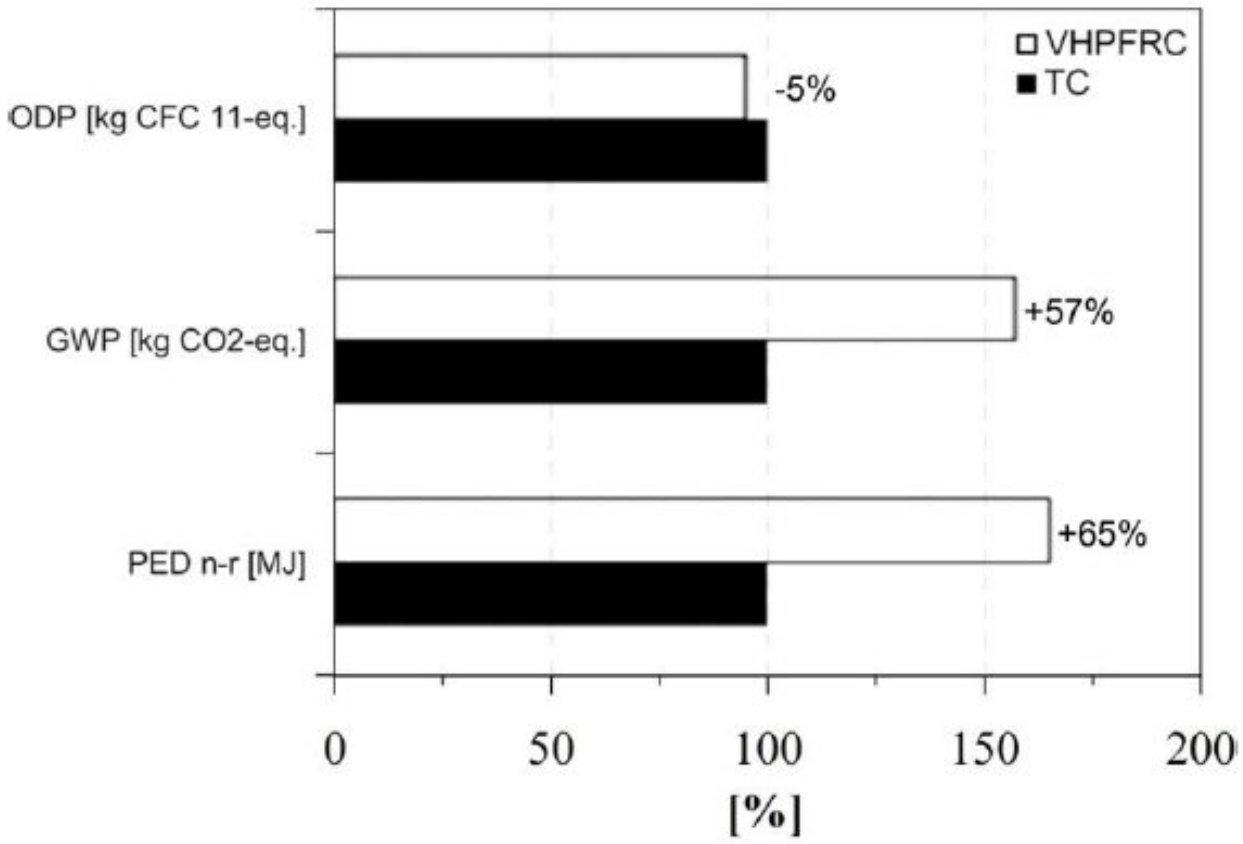

di Prisco M., Moro S., Bayard O., Zani G., (2014), New Industrial Building Designed with Very High Performance Fiber Reinforced Concrete, Concrete Innovation Concrete, Oslo, June 2014

ODP = Ozono Depleting Potential
GWP = Global Warming Potential
PED = Primary Energy Demand

Computation for the whole structure

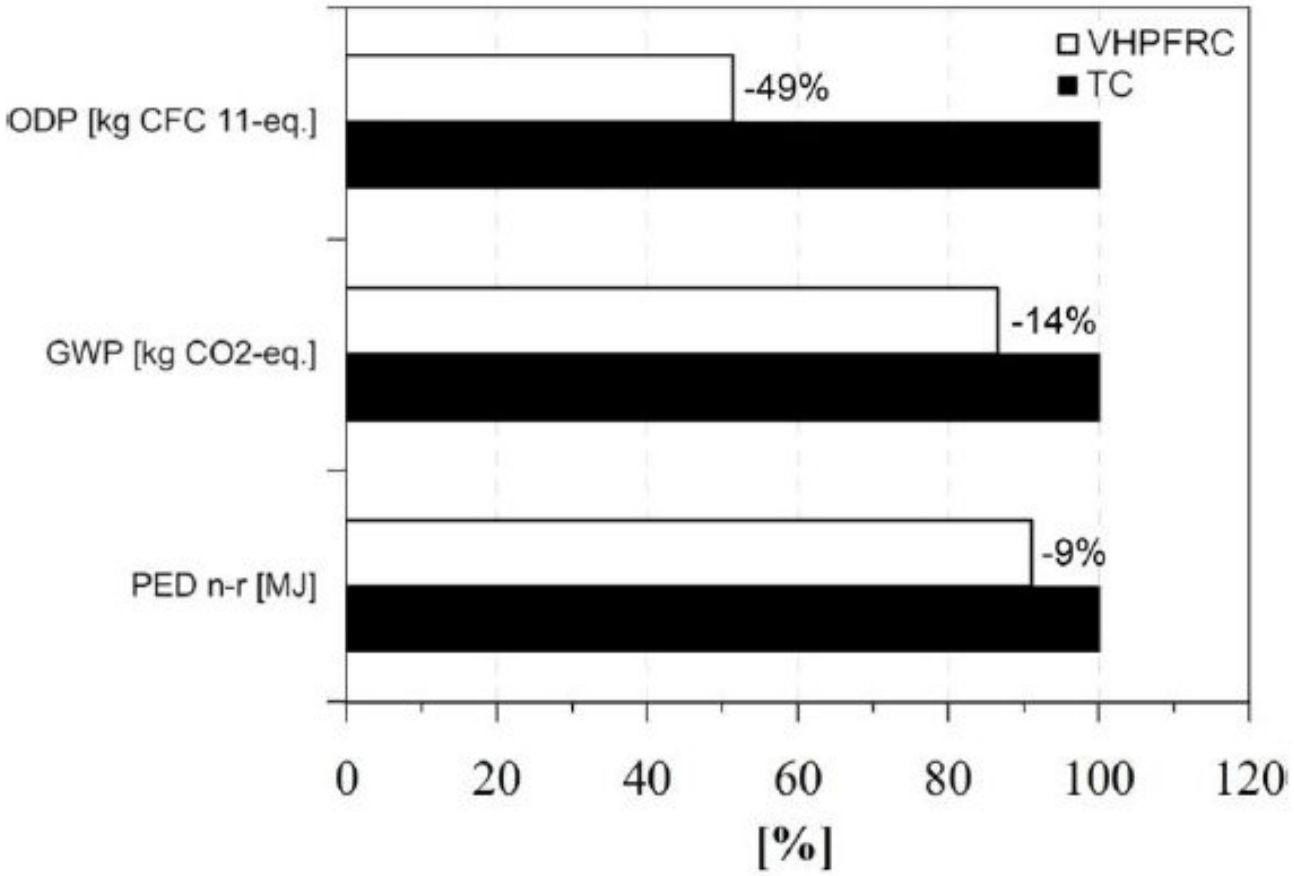

di Prisco M., Moro S., Bayard O., Zani G., (2014), New Industrial Building Designed with Very High Performance Fiber Reinforced Concrete, Concrete Innovation Concrete, Oslo, June 2014

4PB tests on ‘structural’ unnotched specimens

HPFRCC - Randomly oriented fibers

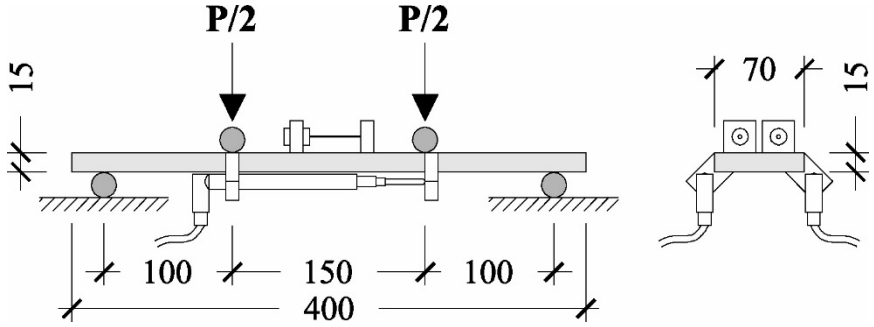

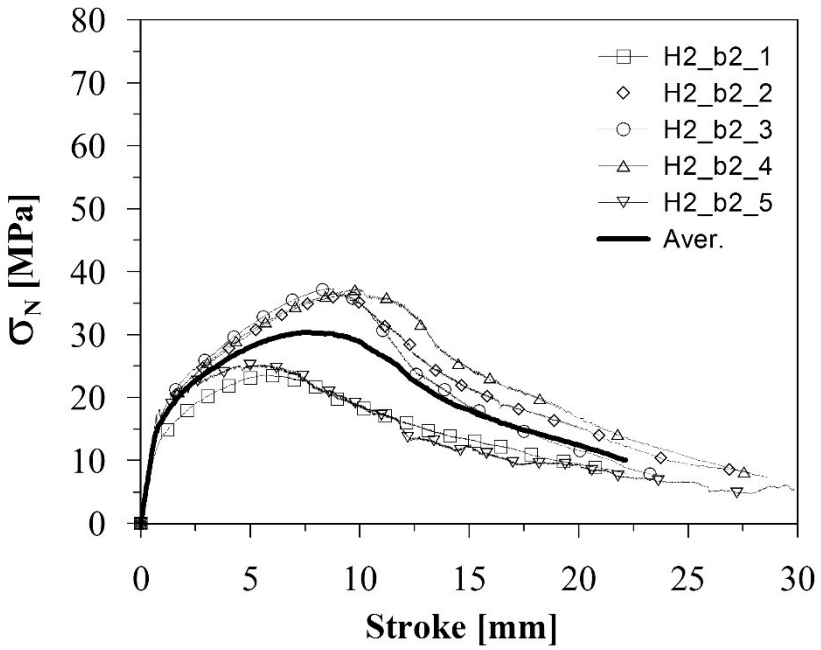

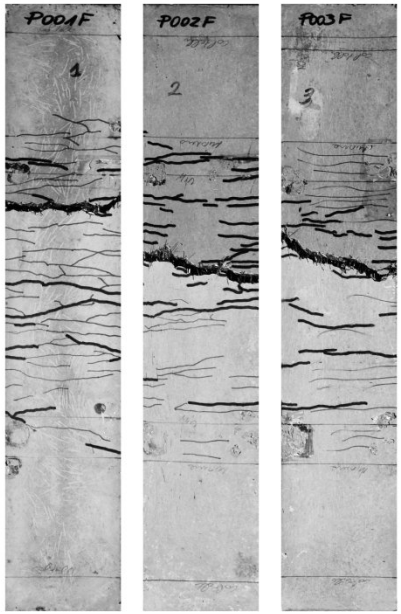

4PB tests on ‘structural’ unnotched specimens

HPFRCC - Oriented fibers

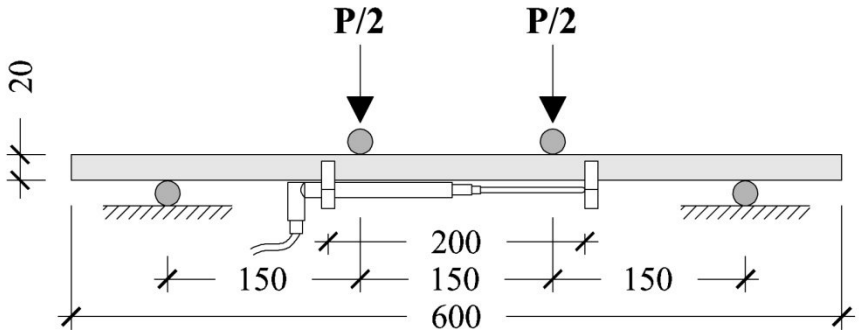

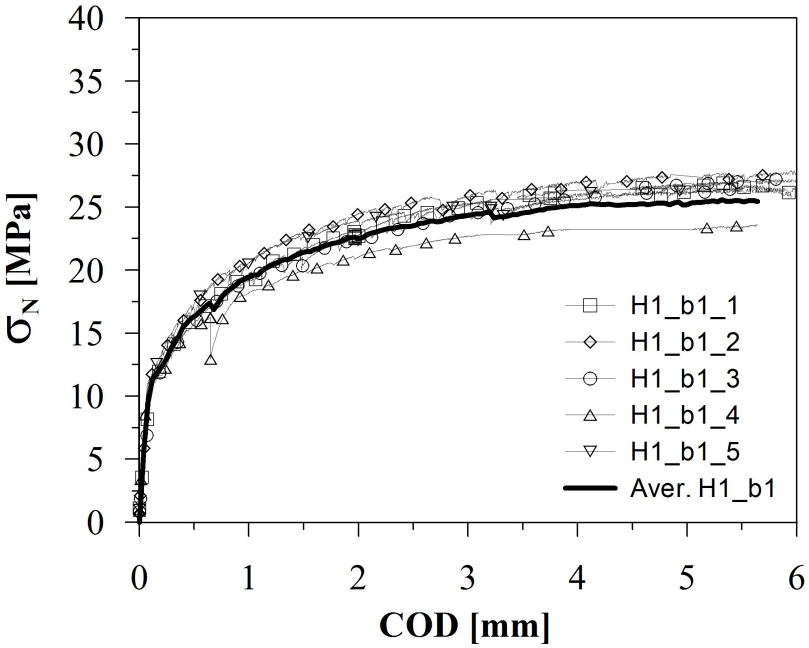

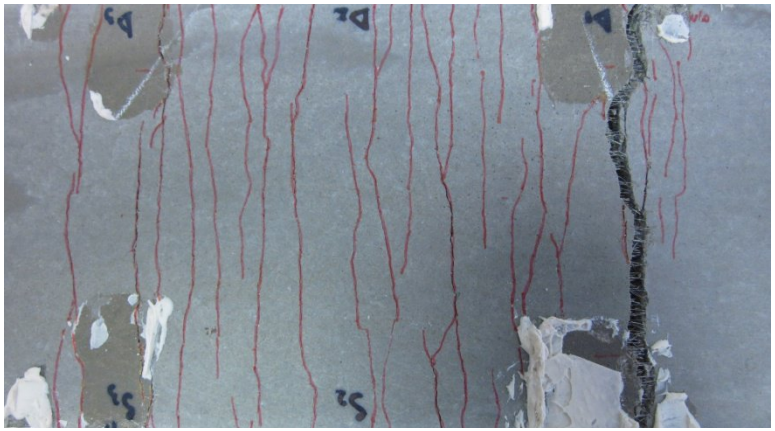

HyFRC

MATERIALS

- High Peformance Concrete (HPC)
  w/b=0.19 and SP/c=5.5%

- Straight high carbon steel microfibers (randomly dispersed)
  Content: 100 kg/m^3 (1.2% by volume)
  Length 13 mm, diameter 0.16 mm, aspect ratio (l_f/d_f) 80

- Alkali-resistant (AR) glass fabrics

Component	Content
Cement I 52.5	600 kg/m^3
Sand 0–2 mm	977 kg/m^3
Water	212.7 kg/m^3
Superplasticizer	33 kg/m^3
Slag	500 kg/m^3

Material	AR-glass
Fabrication technique	Leno weave
Warp wire spacing [mm]	4.9
Weft wire spacing [mm]	10.1
Warp fineness [Tex]	2 x 1200
Weft fineness [Tex]	1200
Warp filament [µm]	19
Weft filament [µm]	19
Maximum tensile load on 70 mm [kN]	11.02

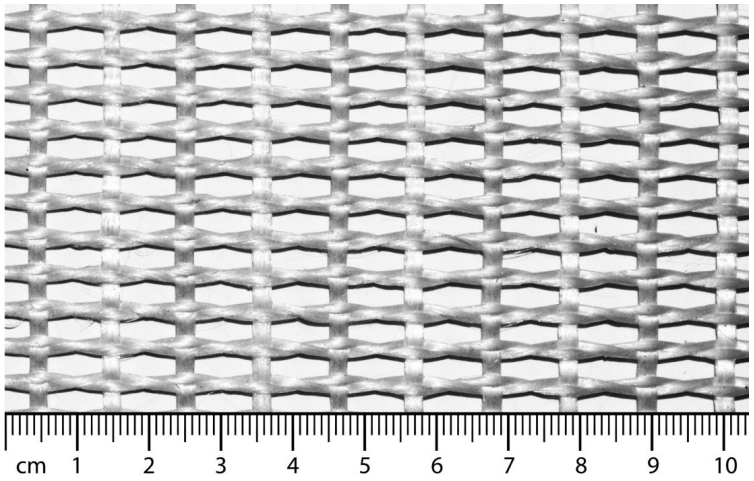

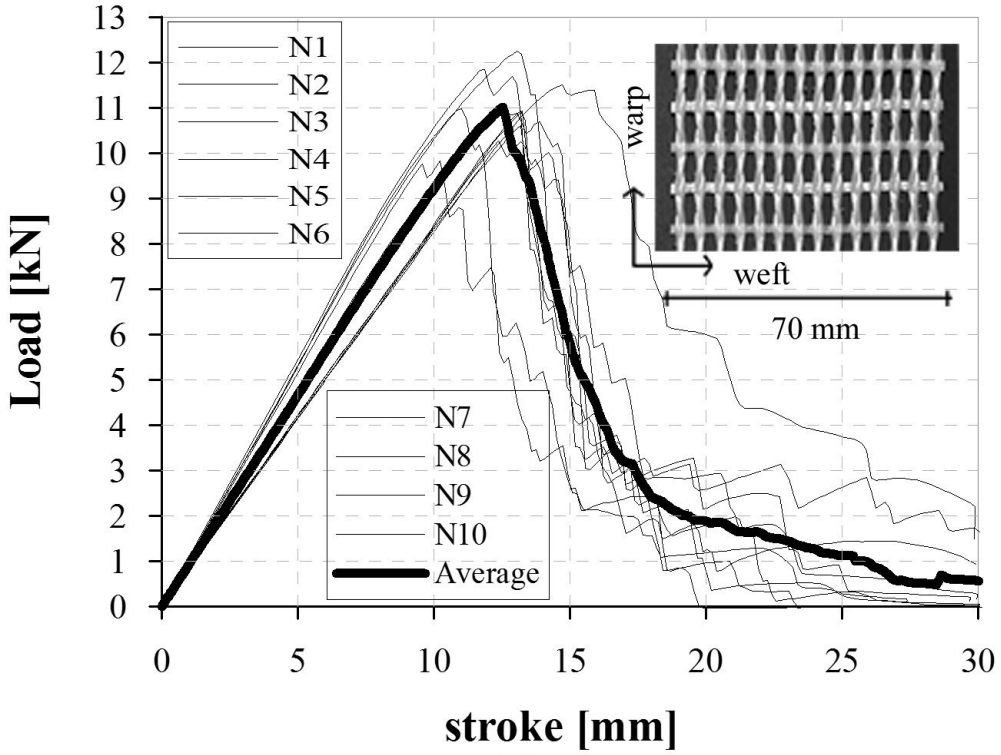
Load [kN]
stroke [mm]
N1
N2
N3
N4
N5
N6
N7
N8
N9
N10
Average
warp
weft
70 mm

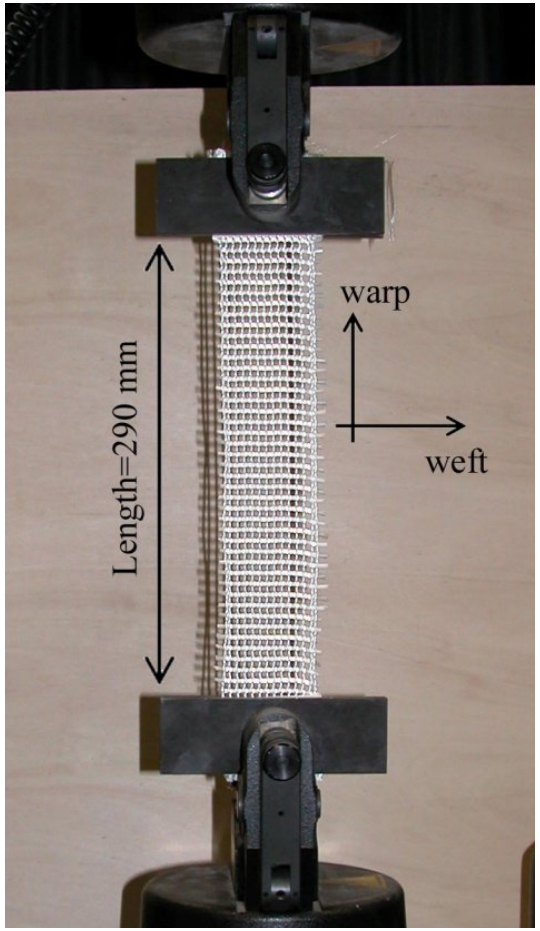
Length=290 mm
warp
weft

HyFRC

SPECIMENS PREPARATION

Code	Steel fibers content [kg/m^3]	Glass textiles layers
F	100	0
T	0	2
FT	100	2

Reinforcement layouts

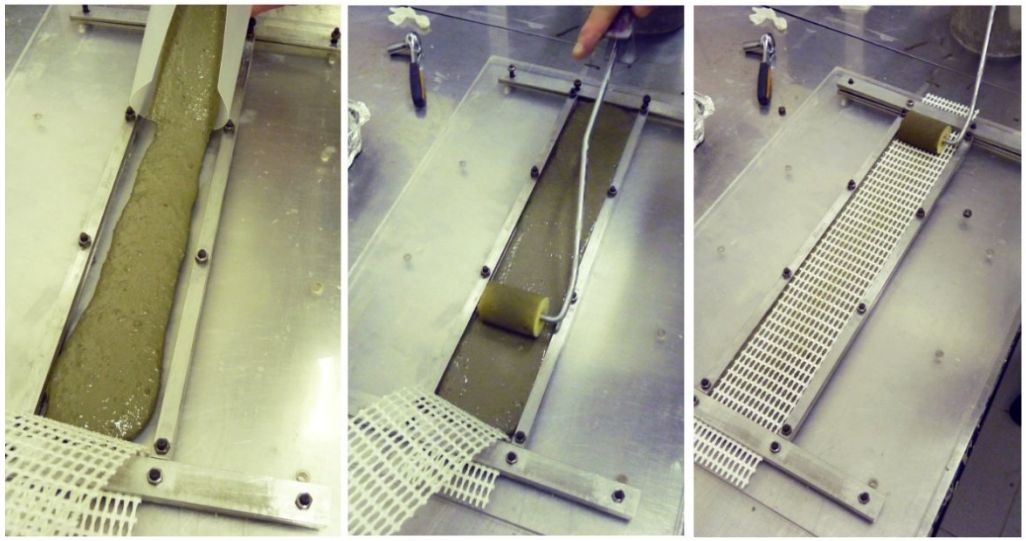

Hand lay-up technique

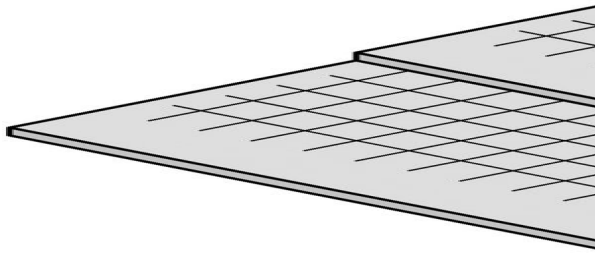

Global thickness = 15 mm

The thickness of the concrete layer embedded between the two fabrics and of the concrete cover was set equal to 5 mm.

HyFRC

TESTING

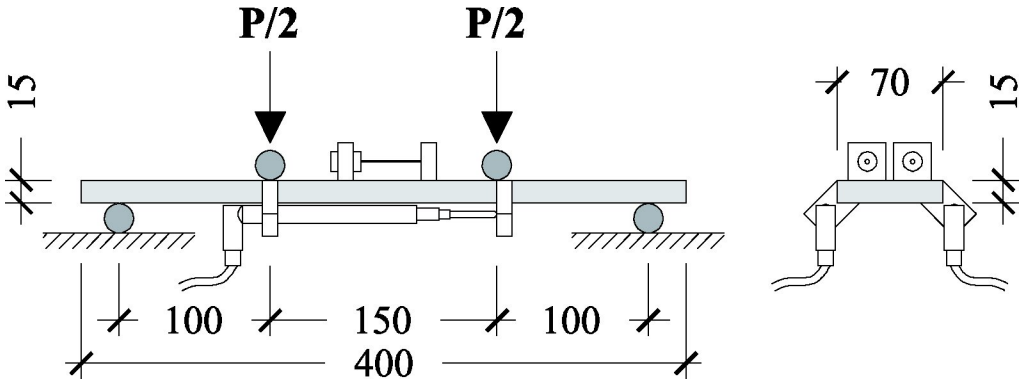

Four point bending test setup

Displacement controlled closed-loop tests rates:

- **$4 \cdot 10^{-3}$ mm/sec up to a 20 mm stroke.**
- **$1.2 \cdot 10^{-2}$ mm/sec up to the specimen failure.**

Cement-based composites

Hybrid composites

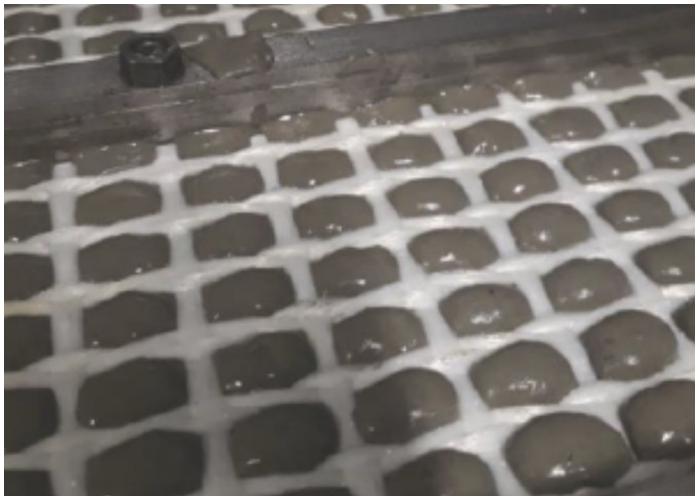

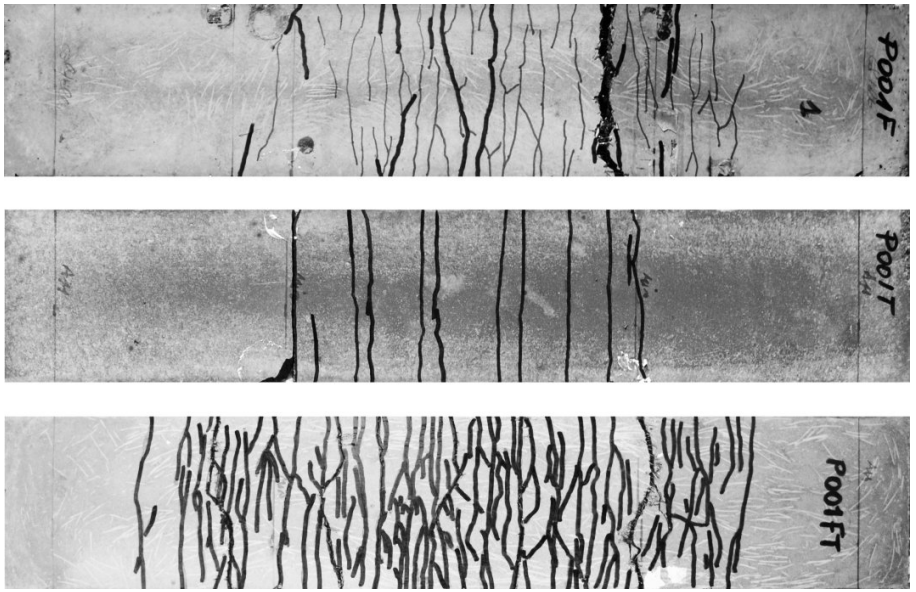

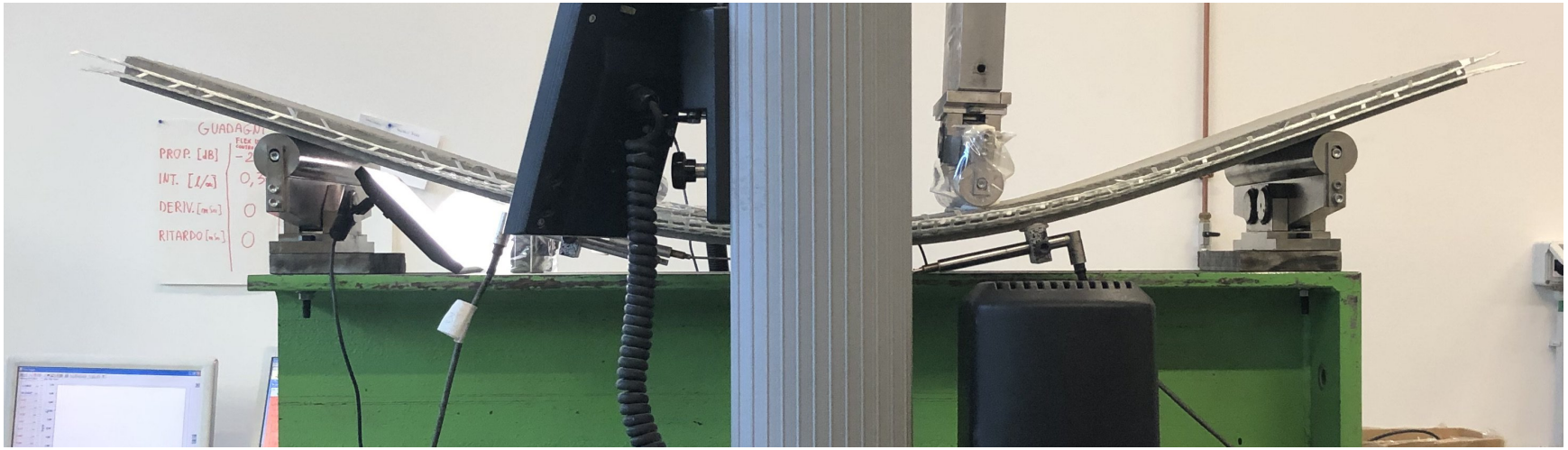

Experimental results

STEEL FIBERS REINFORCEMENT

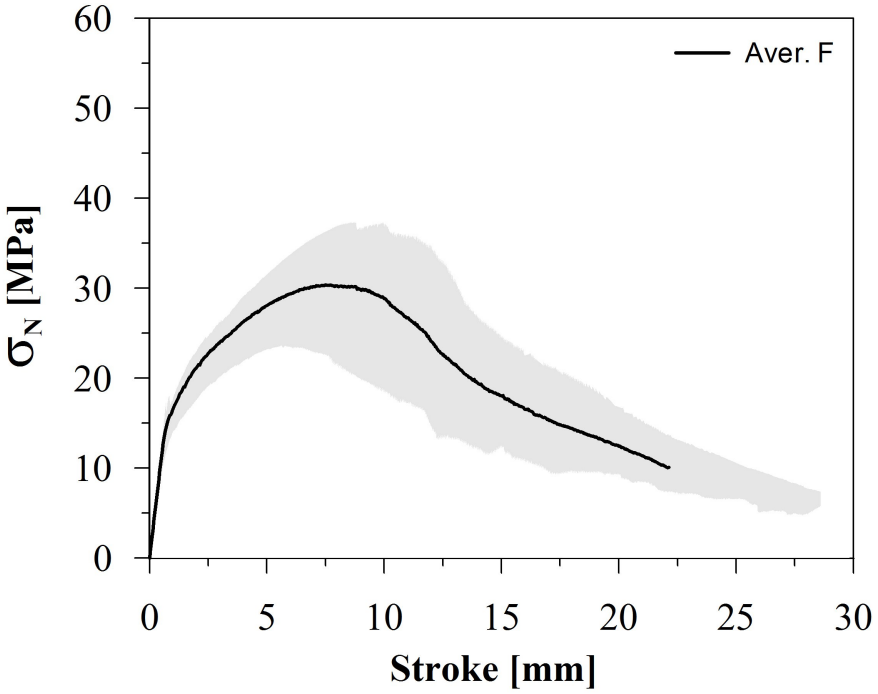

TEXTILE REINFORCEMENT

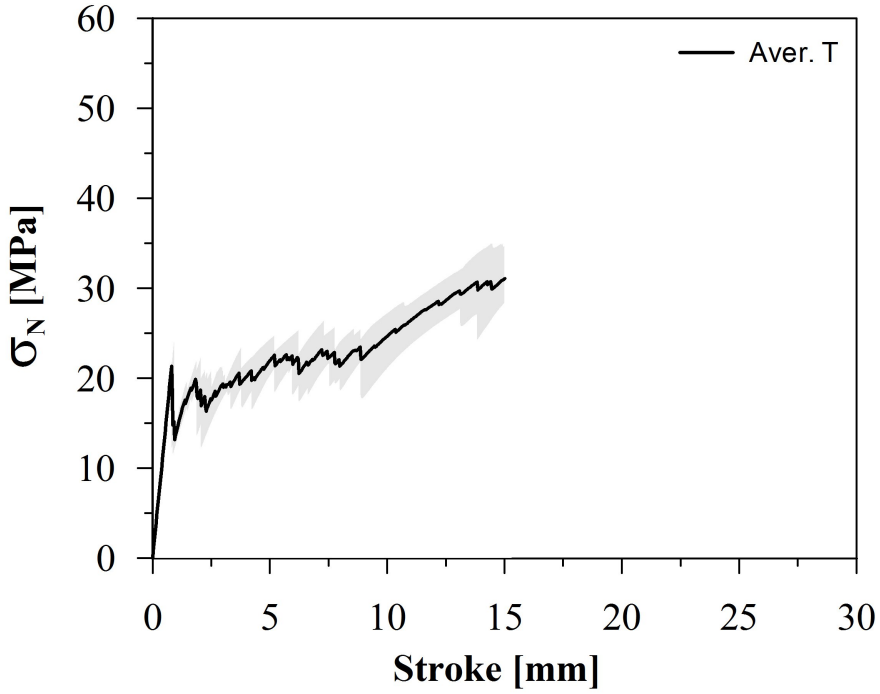

Nominal Stress vs. Stroke curves

4PB tests on ‘structural’ unnotched specimens

HyFRCC: HPFRCC + 2 layers of AR glass fabrics - Randomly oriented fibers

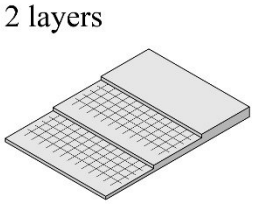

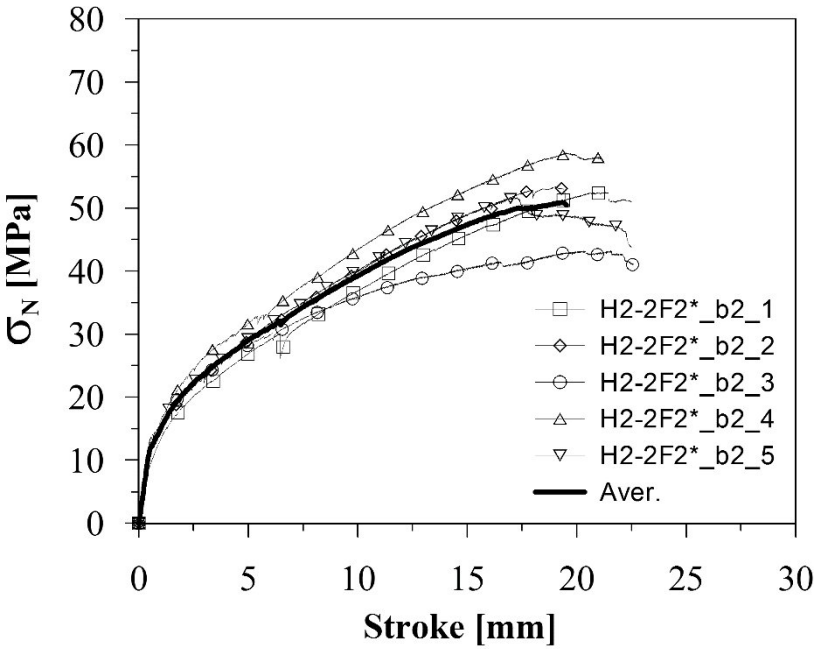

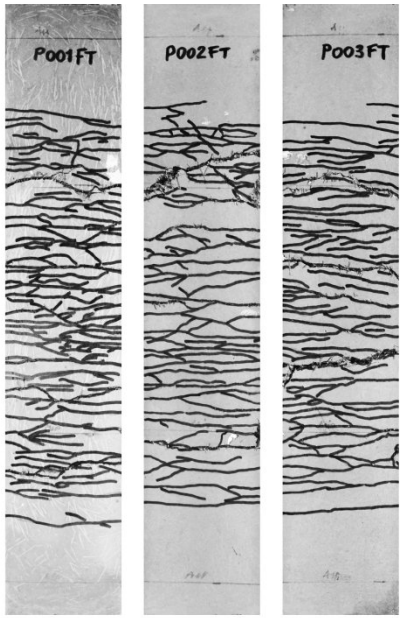

HyFRC

EXPERIMENTAL RESULTS

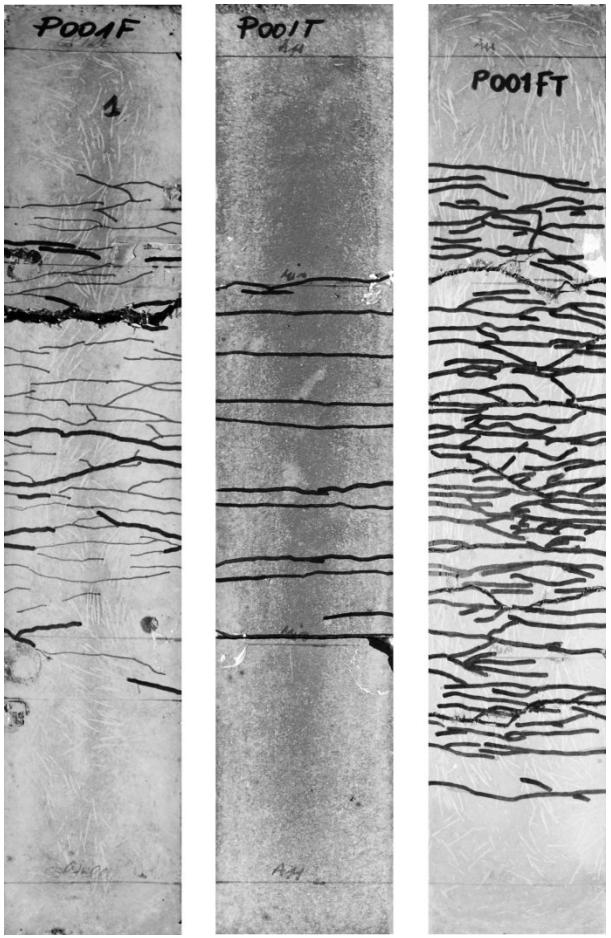

F T FT

TYPICAL CRACK PATTERNS

AVERAGE DATA

Set	$\sigma_{N;peak;av}$ (std) [MPa]	$\varepsilon^*_{peak;av}$ [%]
F	32.2 (6.6)	2.1
T	36.1 (2.9)	5.8
FT	52.4 (5.6)	> 6

$$\sigma_{N;peak} = \frac{P_{peak}}{\frac{b \cdot h^2}{6}}$$

$$\varepsilon^*_{peak} = \frac{COD_{peak}}{\ell_{COD}}$$

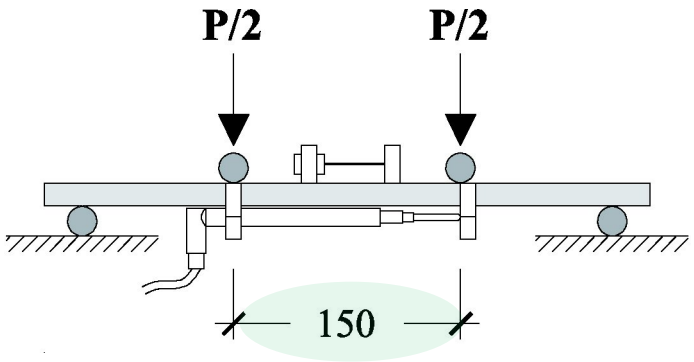

Experimental results

CUMULATIVE AVERAGE CURVE (F+T)

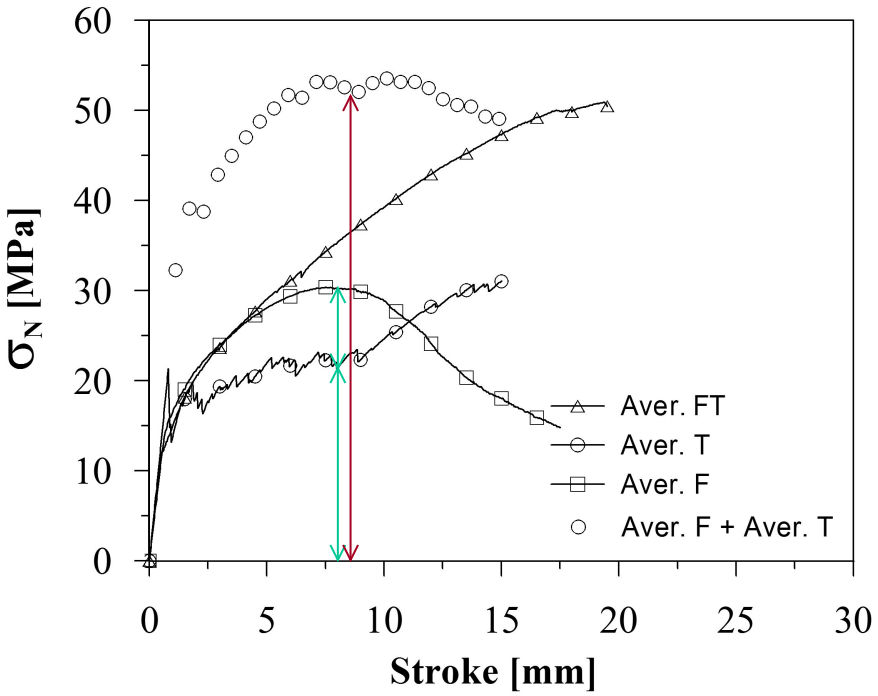

SHIFTED T CURVE

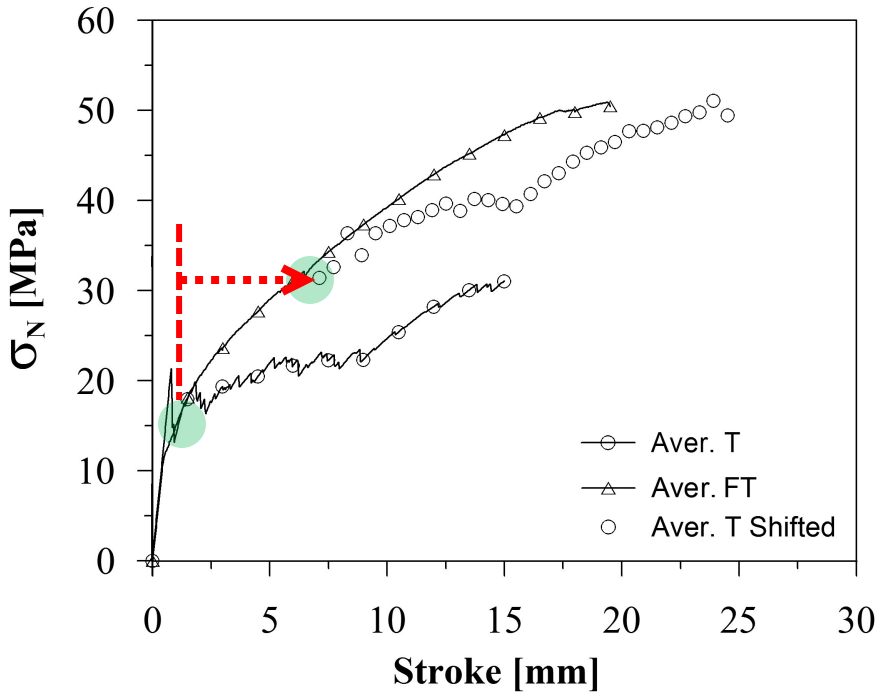

No clear synergic effects (as the ones highlighted in direct tension)

The response of the lower glass fabric took place after the onset of a diffuse micro-cracking, that was found to be close to an equivalent strain ε* of about 2.7%.

constitutive law identification and modelling problems

Table 1
Direct tension test setups – dogbone shaped specimens.

Shape dogbone	Material (–)	Performance level (–)	Length, width and depth of constant area (total specimen) in (mm)			Diff. area	Grip/attachment	DOF[a] top–bottom	Ref.
			L	W	D				
	UHP-FRC	4	80 (330)	30 (60)	13 (13)	50%	Fixed	0–0	[12,13]
	HPFRCC	3–4	80 (240)	24 (40)	40 (40)	60%	Fixed	0–0	[14]
	HPFRCC	4	152 (457)	38 (76)	76 (76)	50%	Self-clamping friction grip[b]	1–1	[16]
	HPFRCC	3	150 (200)	25 (40)	25 (25)	63%	Anchored/pinned	1–1	[17]
	HPFRCC	3	200 (525)	50 (125)	13 (13)	40%	Anchored/pinned	1–1	[17]
	UHP-FRC	3–4	178 (525)	51 (125)	25 (25)	41%	Anchored/pinned	1–1	[7]
	UHP-FRC	3–4	200 (750)	100 (300)	50 (50)	33%	Top glued/anchored	0–0	[18]
	UHP-FRC	3	250 (740)	100 (200)	35 (35)	50%	Side glued/pinned	1–1	[19]
	UHP-FRC	3	200 (700)	160 (200)	45 (45)	80%	Side glued + anchored (greased)	0–0	[3]
	HPFRCC	3–4	80 (330)	30 (60)	13/30 (13/30)	50%	Clamped/fixed/pinned	0/2–0/2	[11]
	Plain concrete	0	200 (400)	60 (100)	100 (100)	60%	Top glued	0–0	[20]
	Plain concrete	0	0[c] (150)[c]	60[c] (100)[c]	100[c] (100)[c]	60%	Top glued/pinned	2–2	[21]
	Plain lightweight concrete	0	0 (270)	80[d] (100)[d]	–	64%	Top glued/fixed	0–0	[22]

[a] DOF – degree of freedom.
[b] Similar to Saito and Imai [15].
[c] Other sizes were also investigated.
[d] Diameter of the cylinder.

by Naaman Cement & Concrete Composites 48 (2014) 53–66

CrossMark

Properties of strain hardening ultra high performance fiber reinforced concrete (UHP-FRC) under direct tensile loading

K. Wille [a,*], S. El-Tawil [b], A.E. Naaman [b]

[a] Department of Civil & Environmental Engineering, University of Connecticut, 261 Glenbrook Road Unit 2037, Storrs, CT 06269-3037, USA
[b] Department of Civil & Environmental Engineering, University of Michigan, 2350 Hayward, G.G. Brown, Ann Arbor, MI 48109-2125, USA

Table 2
Direct tension test setups – unnotched prism/cylinder specimens.

Shape unnotched prism/cylinder	Material (–)	Performance level (–)	Length, width and depth of constant area (total specimen) in (mm)			Diff. area	Grip/attachment	DOF[a] top–bottom	Ref.
			L	W	D				
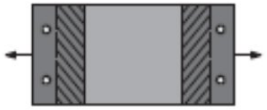	FRC	<3	127 (330)	127 (127)	28 (28)	100%	Side glued/pinned	0–0	[23]
	FRC/ECC	3/4	205 (305)	76 (76)	13 (13)	100%	Side glued/pinned	0–0	[24,25]
	UHP-FRC	3	102 (432)	51 (51)	51 (51)	100%	Side glued + clamped /fixed	0–0	[26]
	UHP-FRC	3	160 (160)	70 (70)	70 (70)	100%	Top glued	0–0	[27]
	Plain concrete/UHP-FRC	0/3	200 (200)	100[b] (100)[b]	–	100%	op glued	0–0	[28,29]

[a] DOF – degree of freedom.
[b] Diameter of the cylinder.

K. Wille et al. / Cement & Concrete Composites 48 (2014) 53–66

Table 3
Direct tension test setups – notched prism/cylinder specimens.

Shape notched prism/cylinder	Material (–)	Performance level (–)	Length, width and depth of constant area (total specimen) in (mm)			Diff. area	Grip/attachment	DOF[a] top–bottom	Ref.
			L	W	D				
	FRC	<3	2 (152)	51 (76)	51 (76)	44%	Top glued	0–0	[30]
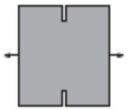	FRC	<3	3 (55)	42 (60)	50 (50)	70%	Top glued	0–0	[31]
	FRC	2	1 (254)	51 (76)	13 (13)	67%	Top glued	0–0	[32]
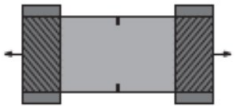	UHP-FRC	3–4	~5 (500)	160 (200)	50 (50)	80%	Side glued + anchored (greased)	0–0	[33,34]
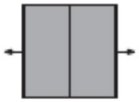	FRC/UHP-FRC	2/3	2–5 (150)	135[a] (150)[b]	–	81%	Top glued	0–0	[29,35–37]
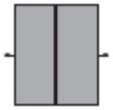	UHP-FRC	3–4	2 (60)	44[b] (74)[b]	–	35%	Top glued	0–0	[38]

[a] DOF – degree of freedom.
[b] Diameter of the cylinder.

K. Wille et al. / Cement & Concrete Composites 48 (2014) 53–66

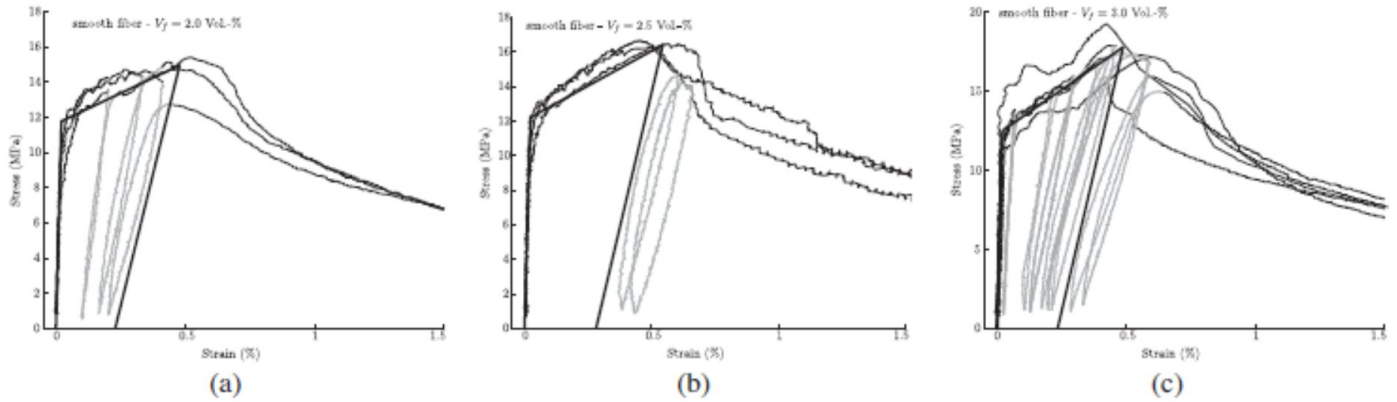

Fig. 8. Test data for U-S-specimens and bi-linear model including unloading line, (a) U-S-2, (b) U-S-25 and (c) U-S-3.

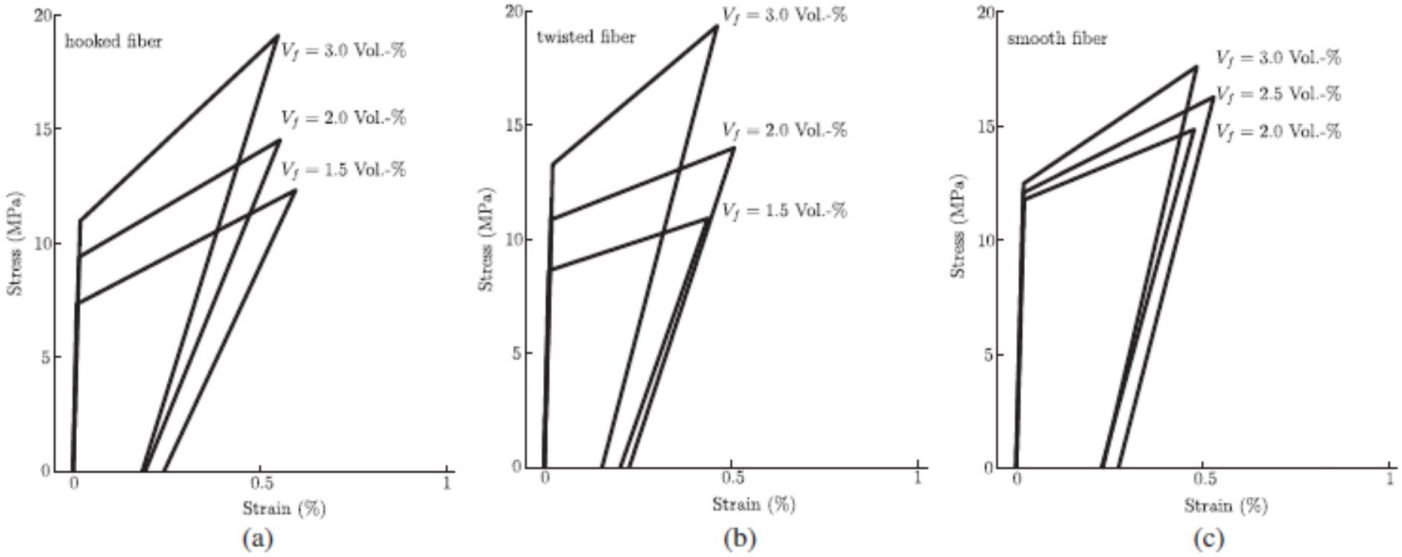

K. Wille et al. / Cement & Concrete Composites 48 (2014) 53–66

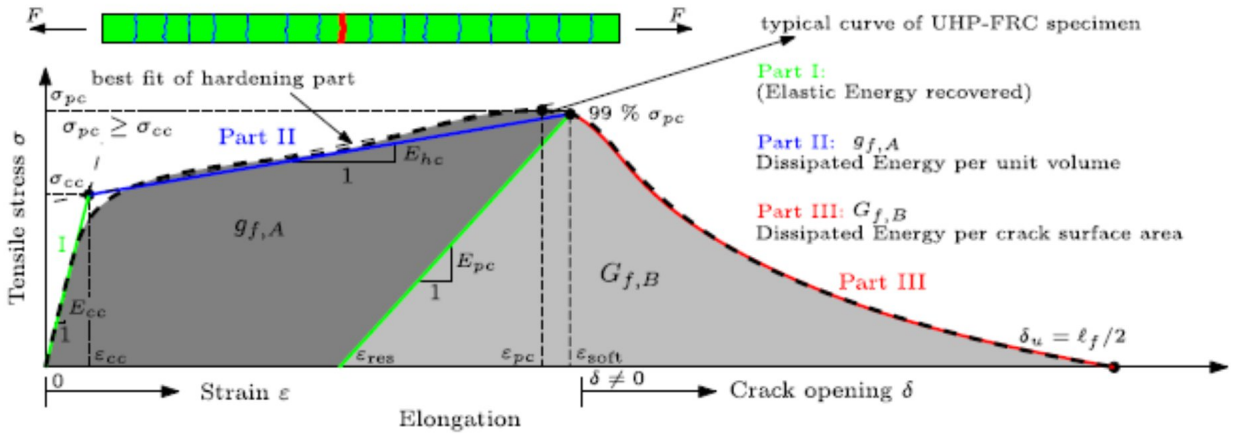

Fig. 3. Strain hardening tensile behavior of UHP-FRC and idealized modeling approach (horizontal axis scale magnified for clarity).

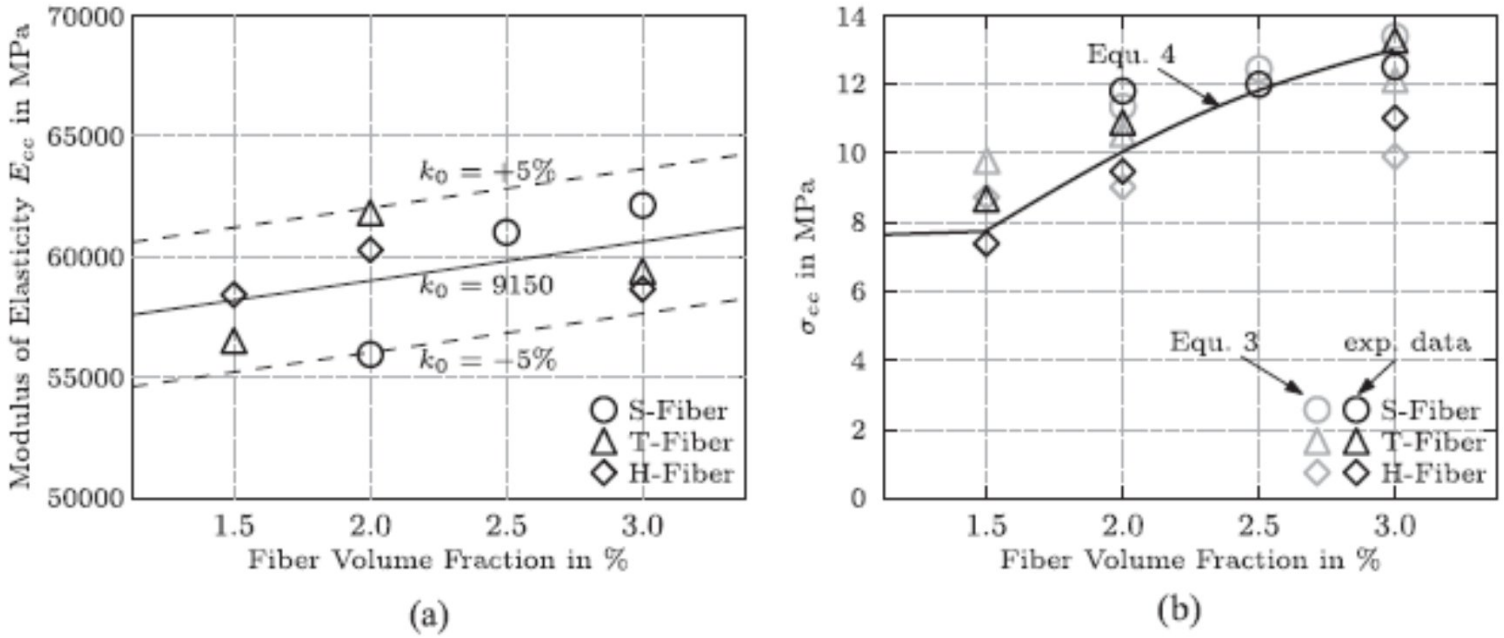

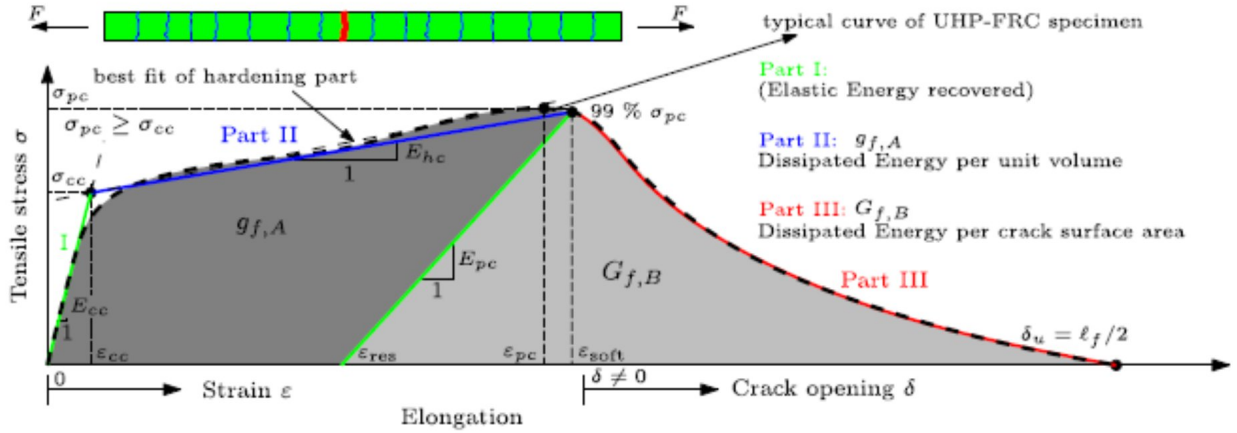

Fig. 3. Strain hardening tensile behavior of UHP-FRC and idealized modeling approach (horizontal axis scale magnified for clarity).

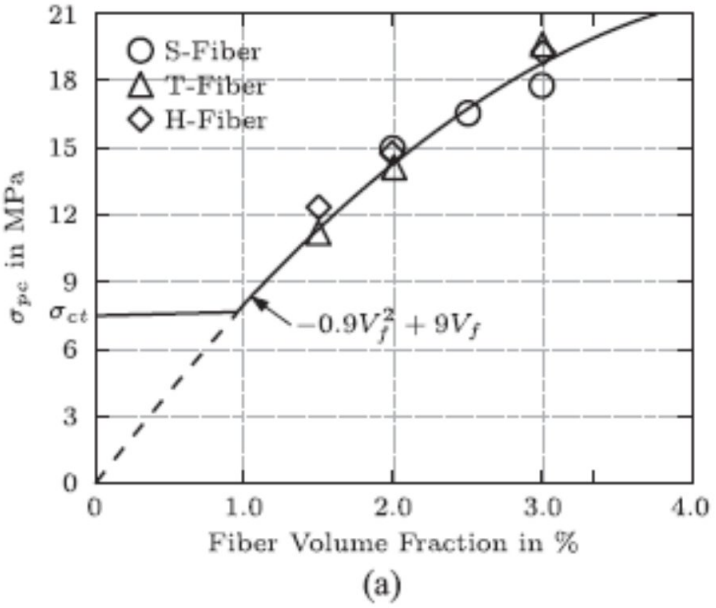

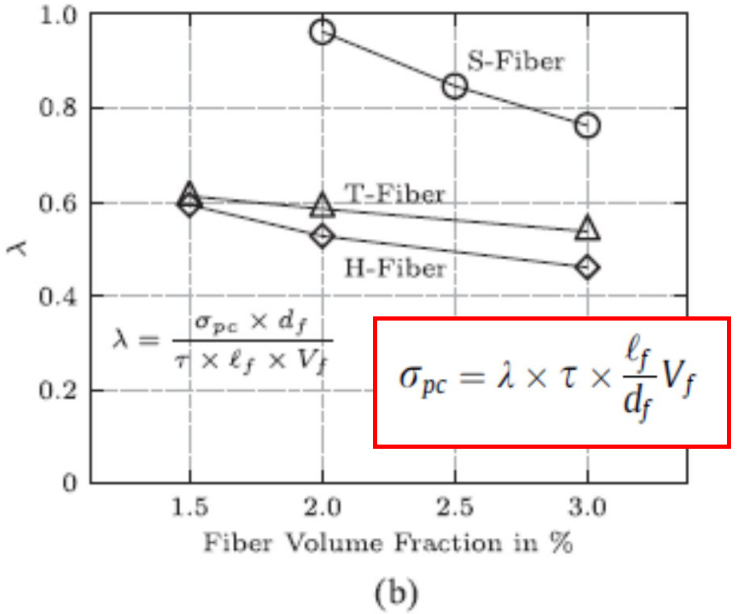

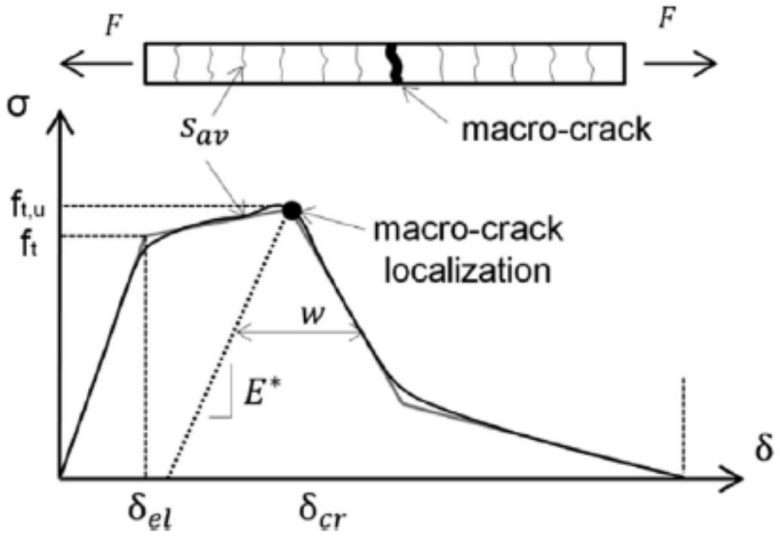

Fig. 2. Typical strain-hardening tensile response of UHPFRC.

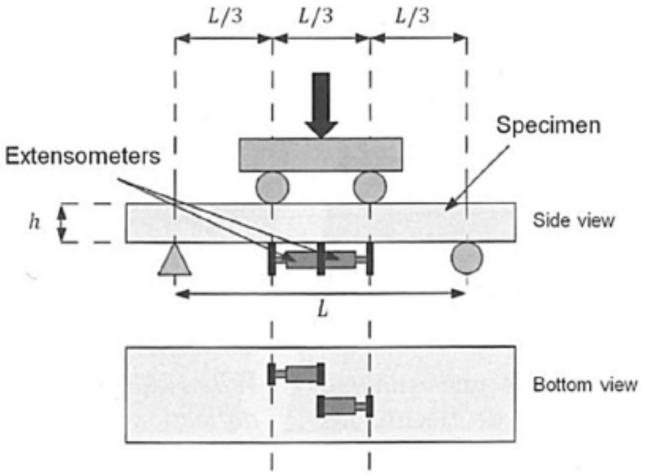

Fig. 17. Crack localisation measurement staggers the extensometers on the tensile face [1].

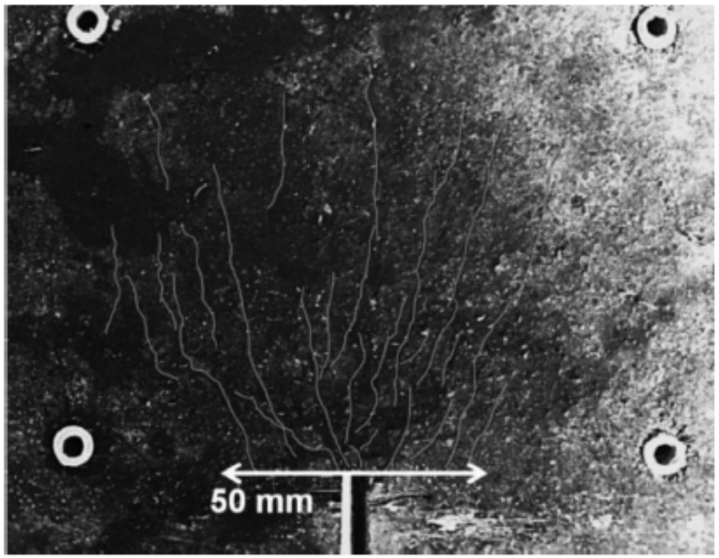

Fig. 1. Multi-microcracking in a UHPFRC specimen notched three-point bending test.

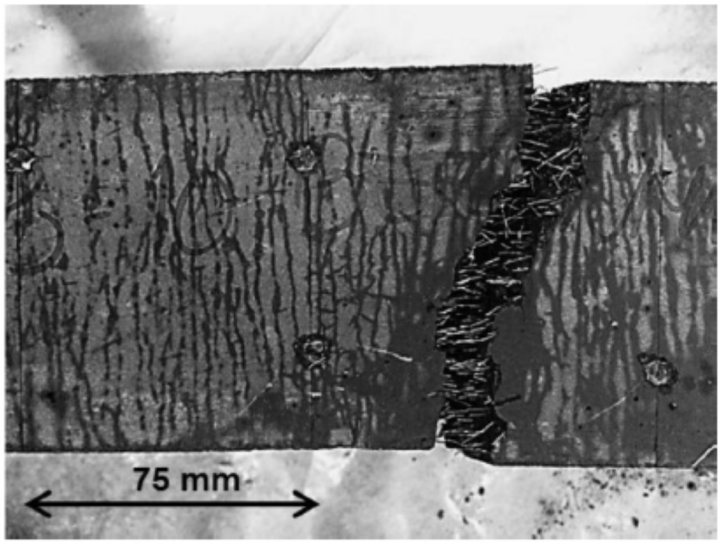

Fig. 23. Average crack spacing determination after FPBT (bottom view of the specimen).

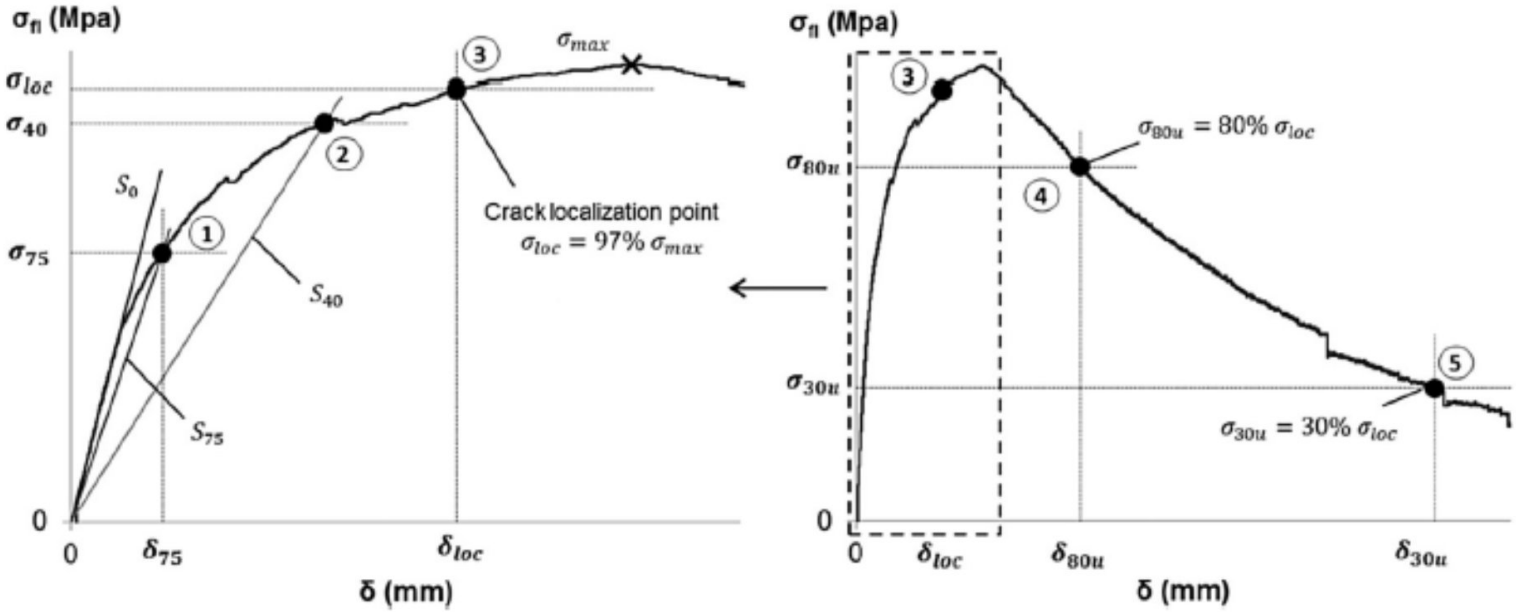

Fig. 4. The five proposed key points obtained from the $\sigma_{fl}-\delta$ curve.

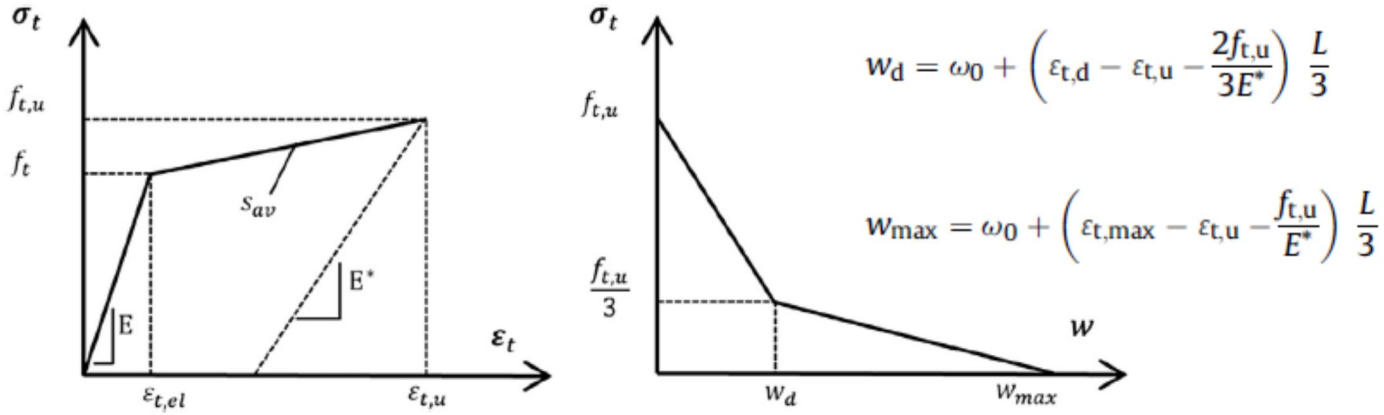

Fig. 5. The bilinear $\sigma-w$ relationship considered for UHPFRC behaviour.

Table 1
The simplified inverse analysis formulation to determine the stress–strain relationship from the five key points extracted from the $\sigma_{fl}-\delta$ experimental curve (Fig. 4).

	$L/h = 3$	$L/h = 4.5$
f_t	$\frac{\sigma_{75}}{1.63}\left(\frac{\sigma_{75}}{\sigma_{40}}\right)^{0.19}$	$\frac{\sigma_{75}}{1.59}\left(\frac{\sigma_{75}}{\sigma_{40}}\right)^{0.21}$
$\varepsilon_{t,u}$	$\frac{f_t}{E}\left(7.65\frac{\delta_{loc}}{\delta_{75}}-10.53\right)$	$\frac{f_t}{E}\left(6.65\frac{\delta_{loc}}{\delta_{75}}-9.40\right)$
$f_{t,u}$	$\alpha^{-0.18}\left(2.46\frac{\sigma_{loc}}{\sigma_{75}}-1.76\right)f_t$	$\alpha^{-0.17}\left(2.24\frac{\sigma_{loc}}{\sigma_{75}}-1.55\right)f_t$
$\varepsilon_{t,d}$	$\gamma^{-0.37}\alpha^{0.88}\left(3.00\frac{\delta_{80u}}{\delta_{loc}}-1.80\right)\frac{f_t}{E}$	$\gamma^{-0.38}\alpha^{0.89}\left(2.82\frac{\delta_{80u}}{\delta_{loc}}-1.68\right)\frac{f_t}{E}$
$\varepsilon_{t,max}$	$2.81\beta^{-0.76}\gamma^{-0.19}\alpha^{1.42}\left(\frac{\delta_{80u}}{\delta_{loc}}\right)^{1.85}\frac{f_t}{E}$	$2.17\beta^{-0.76}\gamma^{-0.26}\alpha^{1.48}\left(\frac{\delta_{80u}}{\delta_{loc}}\right)^{1.86}\frac{f_t}{E}$

A simplified five-point inverse analysis method to determine the tensile properties of UHPFRC from unnotched four-point bending tests

Juan Ángel López [a, *], Pedro Serna [a], Juan Navarro-Gregori [a], Hugo Coll [b]

[a] *Universitat Politècnica de València, Spain*
[b] *Research & Development Concretes S.L. Spain*

UN-NOTCHED BEAMS

Test set-up

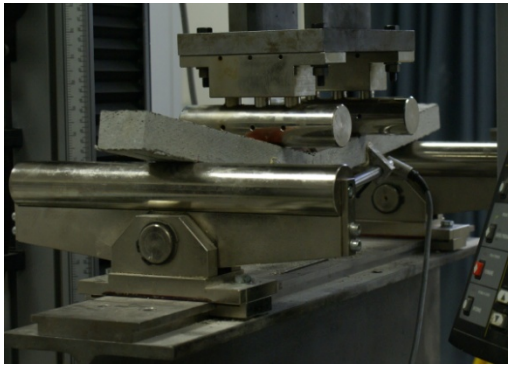

Specimens geometry

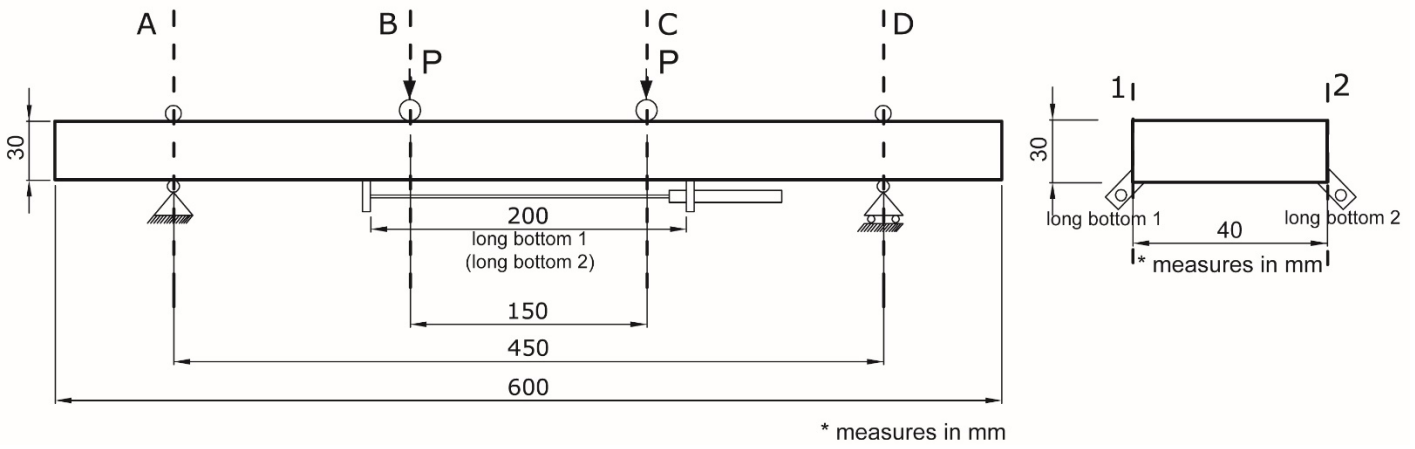

STATIC FIELD: BENDING TESTS

Un-notched specimens

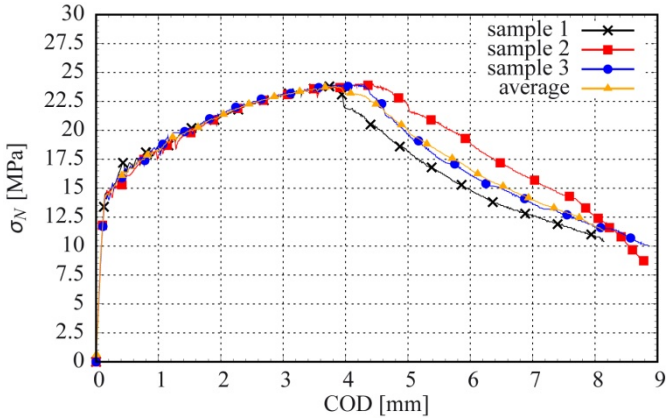

same material

- different cast procedure
- different specimen (sizes and notch)

EN14651 specimens

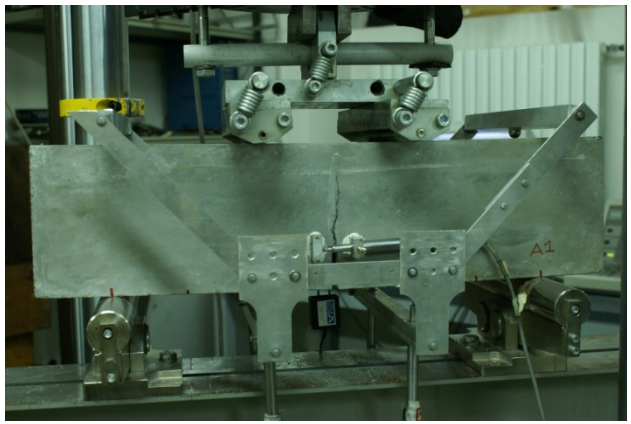

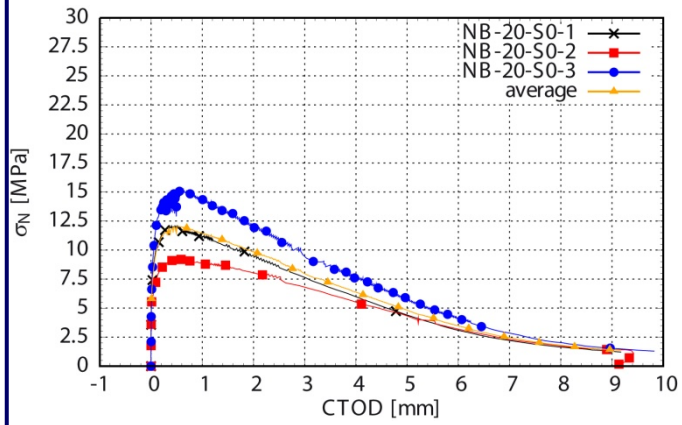

Model Code 2020: Performance classification

The strength interval is defined by f_{R1k} values in [MPa]:
1.0, 1.5, 2.0, 2.5, 3.0, 4.0, 5.0, 6.0, 7.0, 8.0, **10.0, 12.0, 14.0**
and a letter *(a, b, c, d, e)* corresponding to residual strength ratios:

a	if $0.5 < f_{R3k}/f_{R1k} \leq 0.7$
b	if $0.7 \leq f_{R3k}/f_{R1k} \leq 0.9$
c	if $0.9 \leq f_{R3k}/f_{R1k} \leq 1.1$
d	if $1.1 \leq f_{R3k}/f_{R1k} \leq 1.3$
e	if $1.3 \leq f_{R3k}/f_{R1k}$

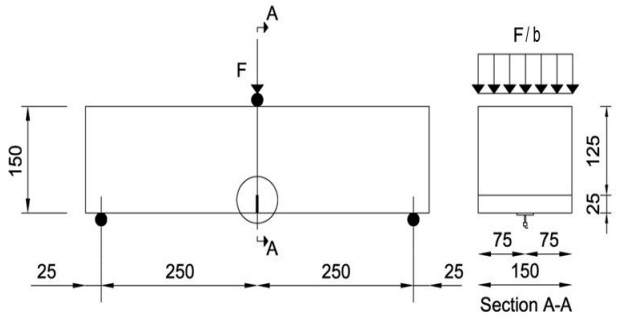

EN 14651

$$f_{R,j} = \frac{3F_j l}{2bh_{sp}^2}$$

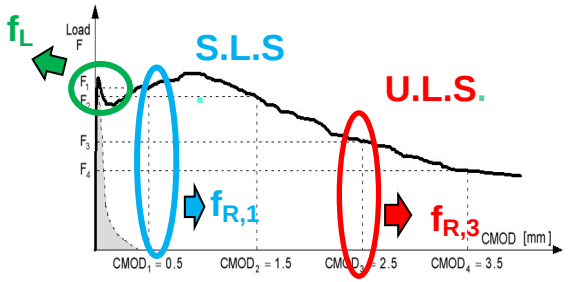

Constitutive laws (LoA III) in MC 2020

CASE (I)

$f_{Fts} \leq 0.8\, f_{ctm}$

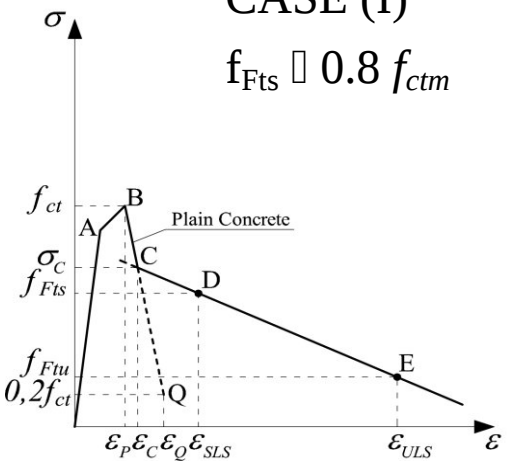

CASE (III)

$f_{Fts} > f_{ctm}$

$\varepsilon_P < 1\%$

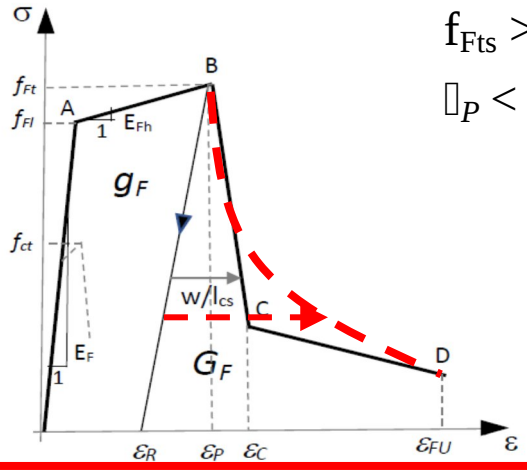

CASE (II)

$f_{Fts} > 0.8\, f_{ctm}$

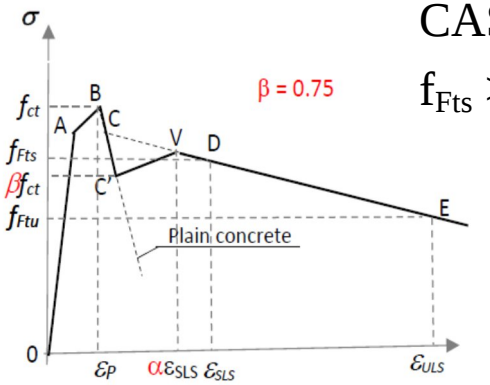

CASE (IV)

$f_{Fts} > f_{ctm}$

$\varepsilon_P > 1\%$

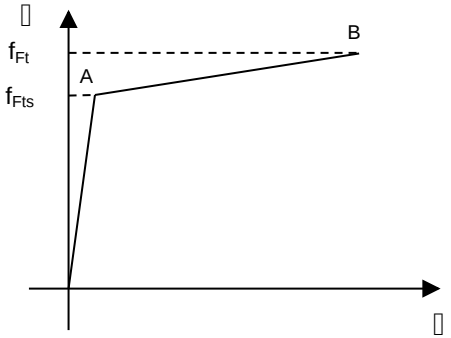

Reference UHPFRC material

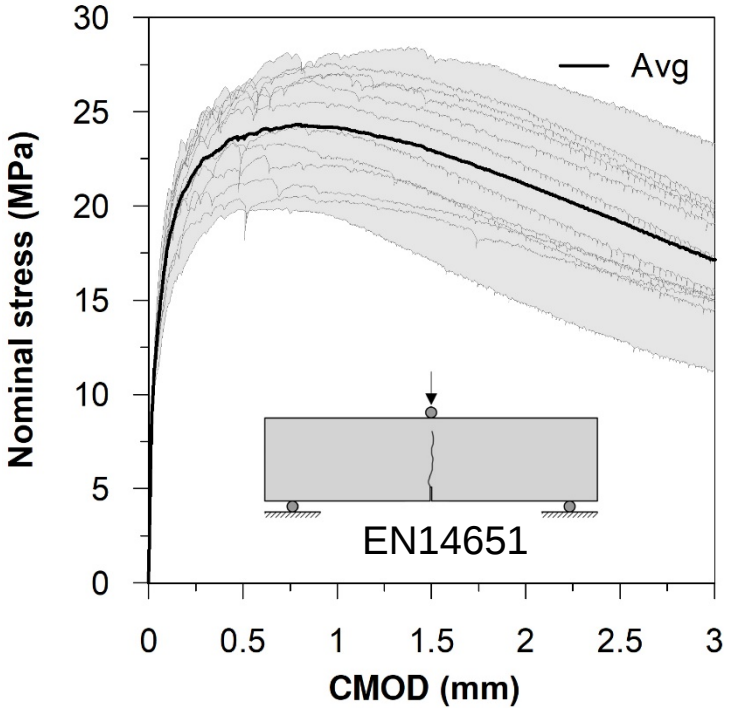

Thixotropic UHPFRC

Ingredient	Dosage
Premix powder	2105.3 kg
Water	153.7 l
Superplasticizer	31.6 kg
Fibers	263.2 kg

OL 13/.20, AR 65

V_f = 3.3%

	f_{ctfl} (MPa)	f_{R1} (MPa)	f_{R2} (MPa)	f_{R3} (MPa)	f_{R4} (MPa)
Avg	13.56	23.68	22.96	19.17	15.17
CV%	9%	10%	15%	19%	20%
k (log-n)	11.43	19.23	17.04	13.12	10.2

19a FRC class

$f_{cm,cube}$ = 143.7 MPa C130 class

Compressive behavior assumed linear elastic

G. Zani, M. di Prisco, Identification of Uniaxial Tensile Laws for UHPFRC Modelling, FRC2023: Fiber Reinforced Concrete: from Design to Structural Application, Joint ACI-fib-RILEM International Workshop | Arizona State University, 18th - 20th September 2023, Tempe, USA

Parametric study

Mechanical properties of the reference material

Parameter	Value
Elastic modulus E_F	45 GPa
Cracking tensile strength f_{Fl}	8 MPa
Peak tensile strength f_{Ft}	9 MPa
Strain at peak tensile strength ε_P	0.38%
Residual strength f_{R1m}	23.68 MPa
Residual strength f_{R3m}	19.17 MPa

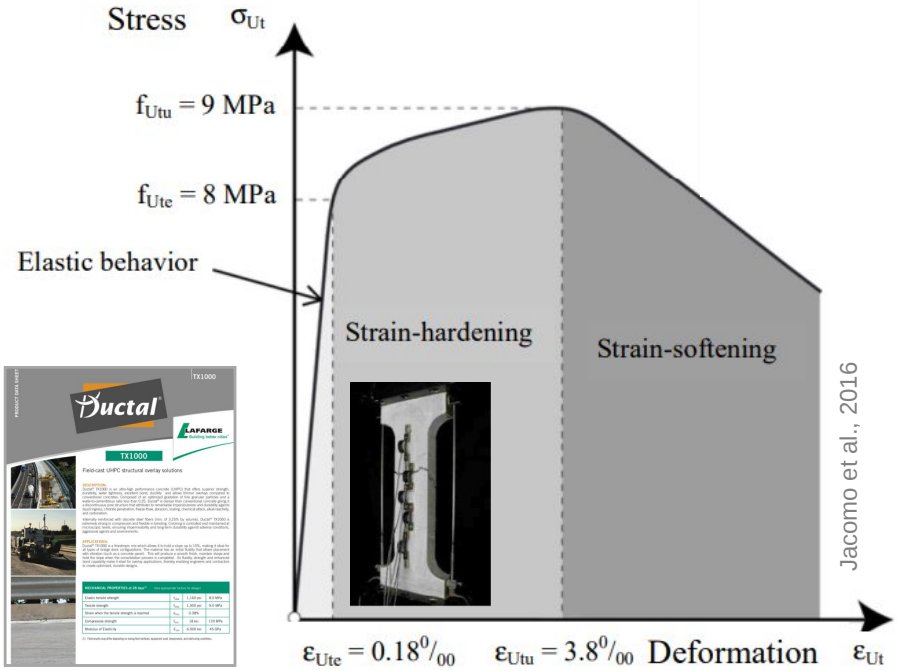

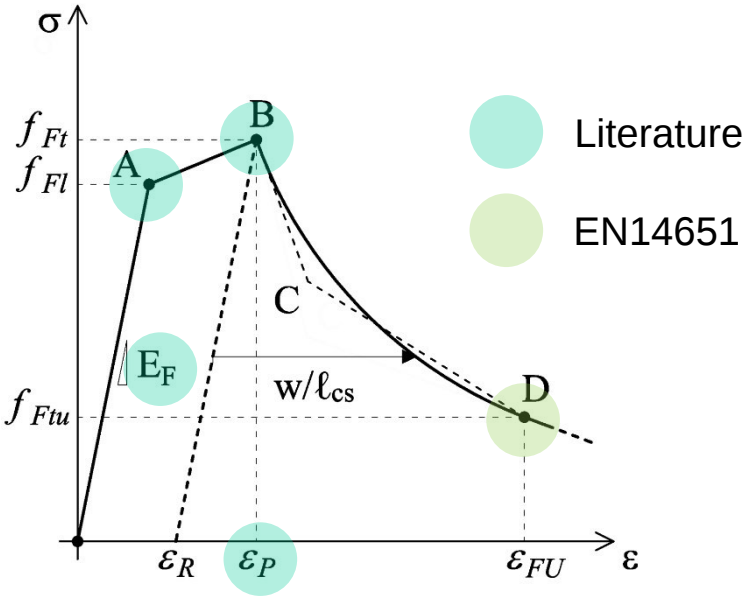

G. Zani, M. di Prisco, Identification of Uniaxial Tensile Laws for UHPFRC Modelling, FRC2023: Fiber Reinforced Concrete: from Design to Structural Application, Joint ACI-fib-RILEM International Workshop | Arizona State University, 18th - 20th September 2023, Tempe, USA

Recommendations introduced in the *fib* MC2020

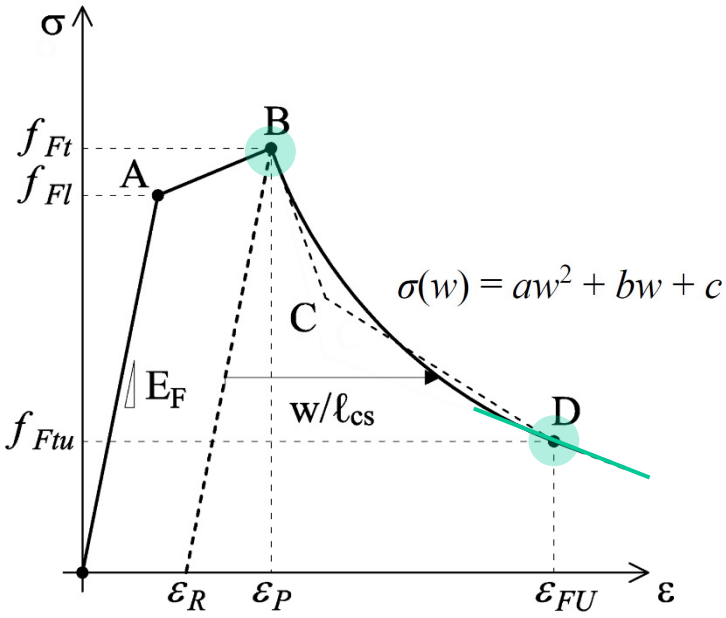

$$\varepsilon_D = \varepsilon_{FU} = 2.5\text{mm}/l_{cs}$$

$$w_D = 2.5 \text{ mm} - l_{cs}\varepsilon_R$$

$$f_{Fts} = 0.37 \cdot f_{R1k}$$

$$f_{Ftu} = f_{Fts} - \frac{w_D - \text{CMOD}_1}{\text{CMOD}_3 - \text{CMOD}_1}\left(f_{Fts} - 0.57 \cdot f_{R3k} + 0.26 \cdot f_{R1k}\right)$$

where the constants a, b, c can be determined imposing the passage for B and D

$w = 0 \quad \sigma = f_{Ft}; \qquad w = w_D \quad \sigma = f_{Ftu}$

and the condition that:

$$\frac{d\sigma}{dw} = \frac{-f_{Ftu}}{\left(\frac{l_f}{2} - w_D\right)} \quad \text{for } w = w_D \qquad (18.4\text{-}20)$$

$$a = \frac{f_{Ft}}{w_D^2} - \frac{\frac{l_f}{2} f_{Ftu}}{w_D^2\left(\frac{l_f}{2} - w_D\right)}$$

$$b = -2a \cdot w_D - \frac{f_{Ftu}}{\left(\frac{l_f}{2} - w_D\right)}$$

$$c = f_{Ft}$$

G. Zani, M. di Prisco, Identification of Uniaxial Tensile Laws for UHPFRC Modelling, FRC2023: Fiber Reinforced Concrete: from Design to Structural Application, Joint ACI-fib-RILEM International Workshop | Arizona State University, 18th - 20th September 2023, Tempe, USA

Parametric study

Plane-section parametric analyses: ±1 MPa on the peak stress f_{Ft}

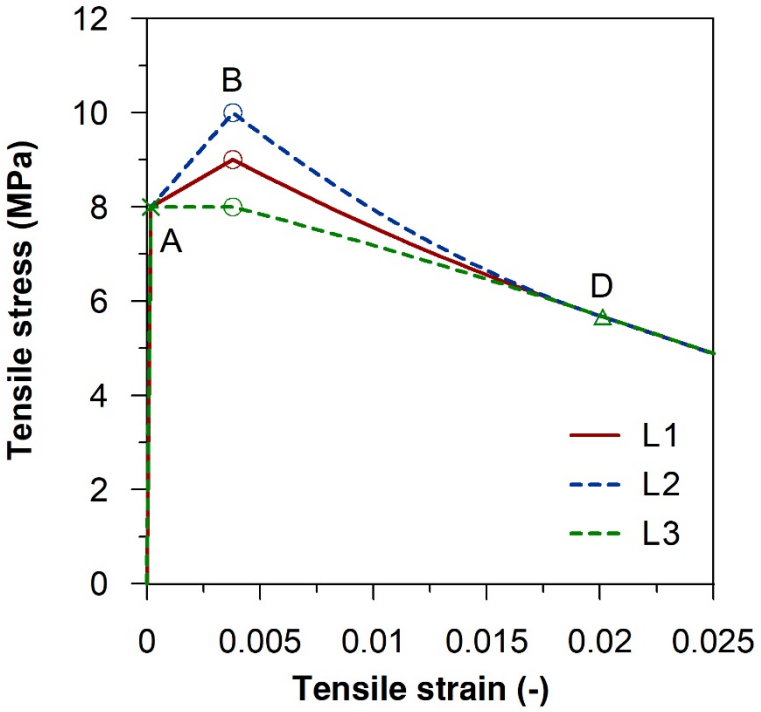

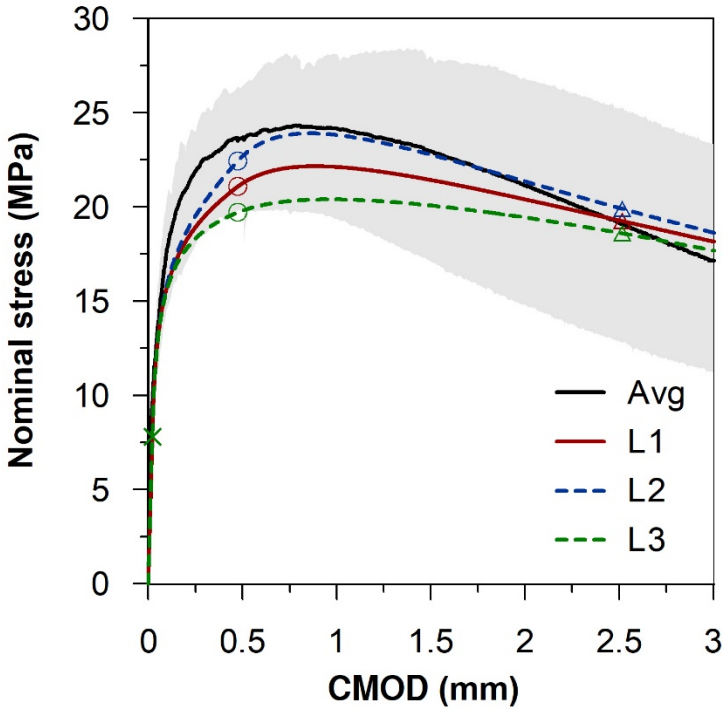

G. Zani, M. di Prisco, Identification of Uniaxial Tensile Laws for UHPFRC Modelling, FRC2023: Fiber Reinforced Concrete: from Design to Structural Application, Joint ACI-fib-RILEM International Workshop | Arizona State University, 18th - 20th September 2023, Tempe, USA

Parametric study

Plane-section parametric analyses: ±1 MPa on the first cracking strength f_{Fl}

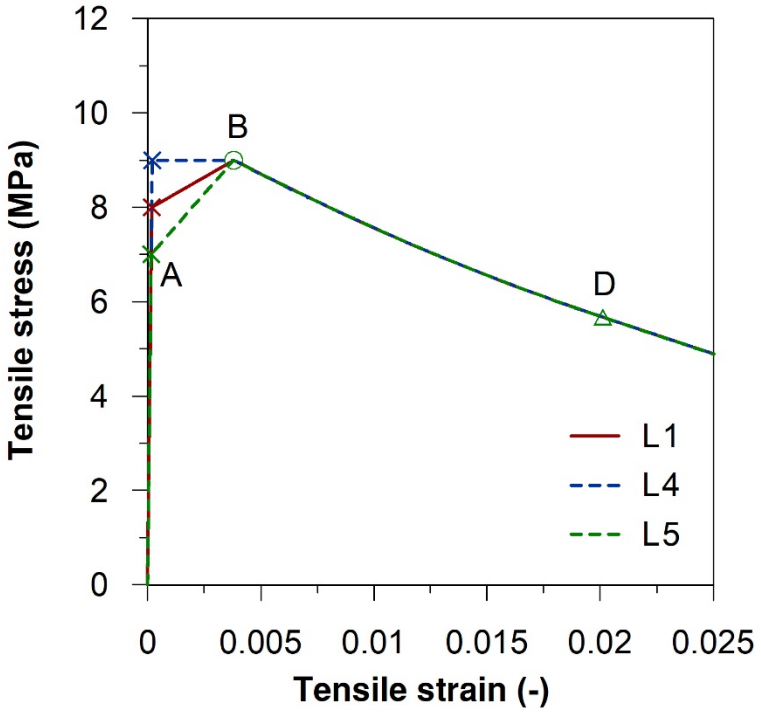

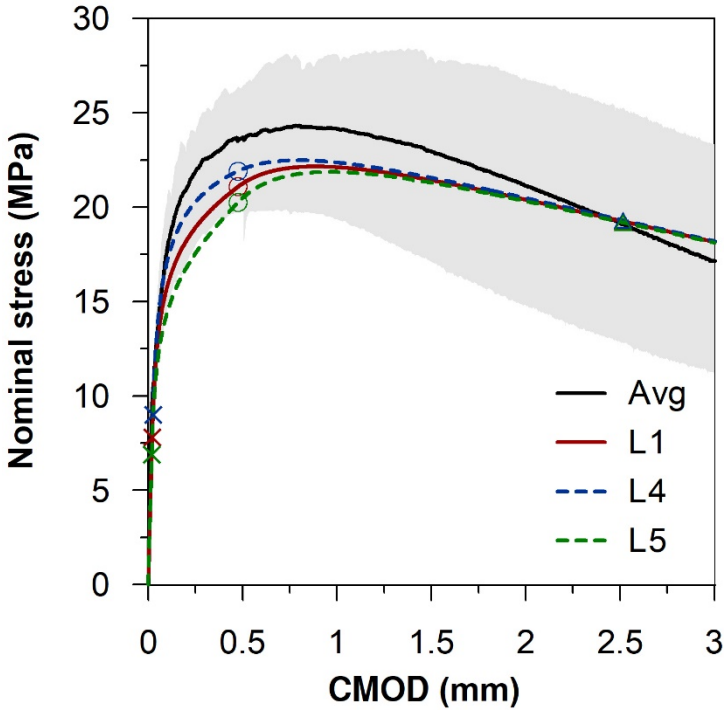

G. Zani, M. di Prisco, Identification of Uniaxial Tensile Laws for UHPFRC Modelling, FRC2023: Fiber Reinforced Concrete: from Design to Structural Application, Joint ACI-fib-RILEM International Workshop | Arizona State University, 18th - 20th September 2023, Tempe, USA

Parametric study

Plane-section parametric analyses: change in the peak strain ε_P (0.20%, 0.38%, 0.60%)

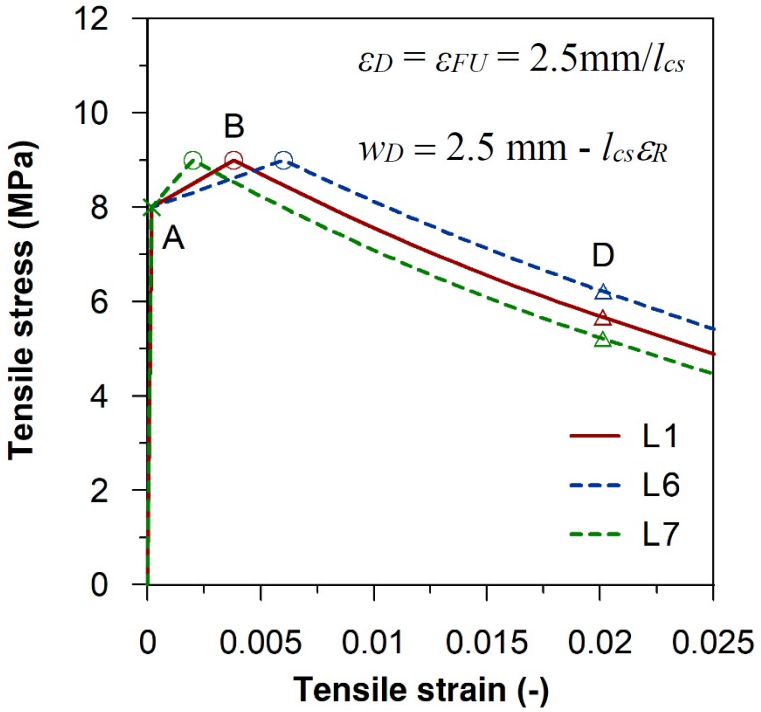

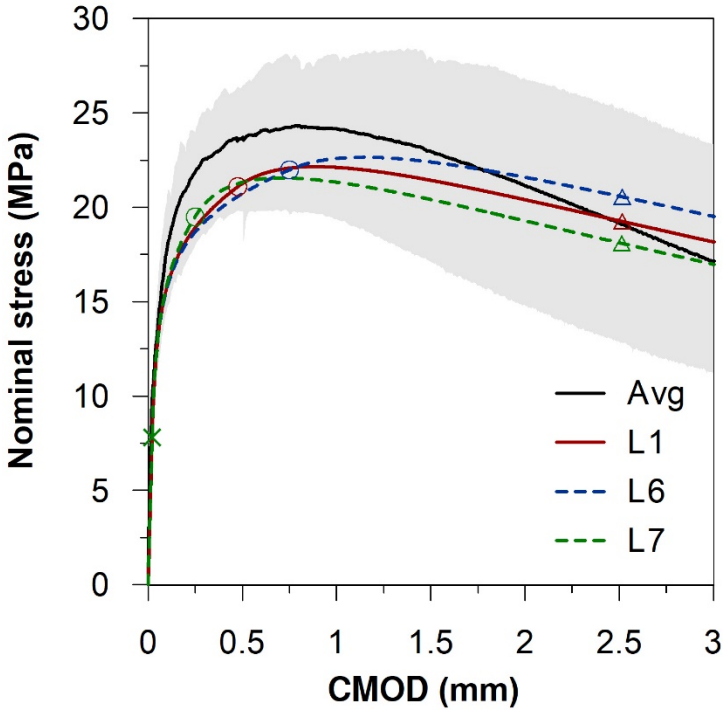

G. Zani, M. di Prisco, Identification of Uniaxial Tensile Laws for UHPFRC Modelling, FRC2023: Fiber Reinforced Concrete: from Design to Structural Application, Joint ACI-fib-RILEM International Workshop | Arizona State University, 18th - 20th September 2023, Tempe, USA

Parametric study

Plane-section parametric analyses: ±1 MPa on both f_{Fl} and f_{Ft} strengths

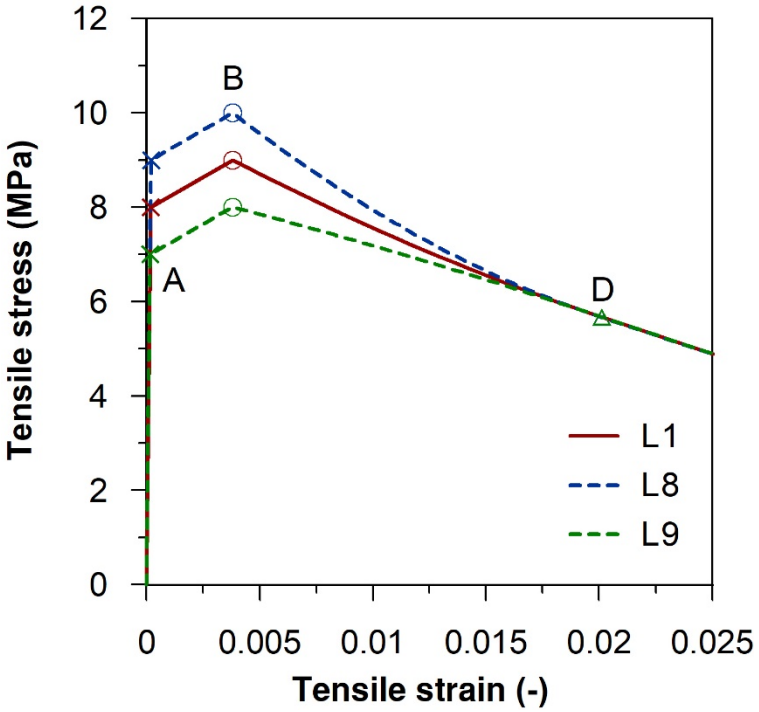

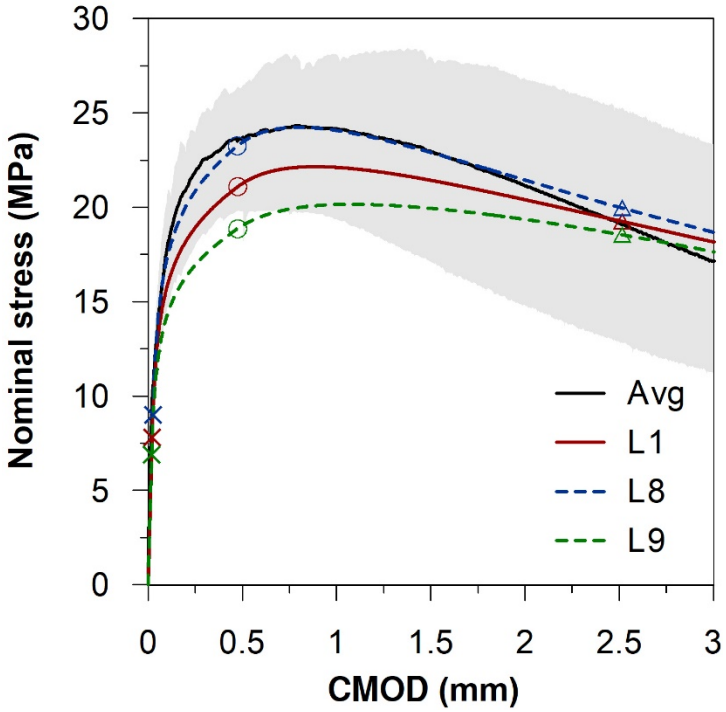

G. Zani, M. di Prisco, Identification of Uniaxial Tensile Laws for UHPFRC Modelling, FRC2023: Fiber Reinforced Concrete: from Design to Structural Application, Joint ACI-fib-RILEM International Workshop | Arizona State University, 18th - 20th September 2023, Tempe, USA

Back-calculation procedure

Is it possible to fully identify the uniaxial tensile behavior from notched beam data?

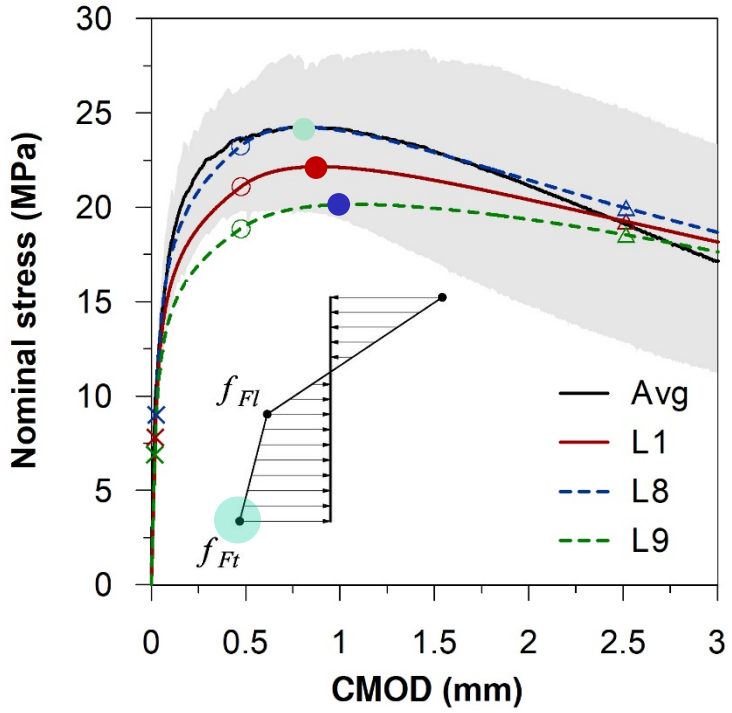

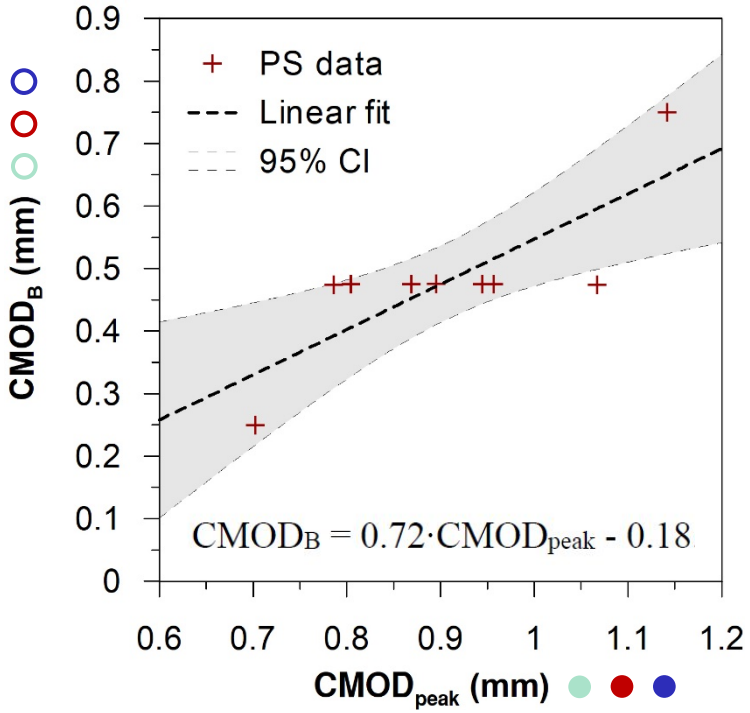

G. Zani, M. di Prisco, Identification of Uniaxial Tensile Laws for UHPFRC Modelling, FRC2023: Fiber Reinforced Concrete: from Design to Structural Application, Joint ACI-fib-RILEM International Workshop | Arizona State University, 18th - 20th September 2023, Tempe, USA

Back-calculation procedure

Is it possible to fully identify the uniaxial tensile behavior from notched beam data?

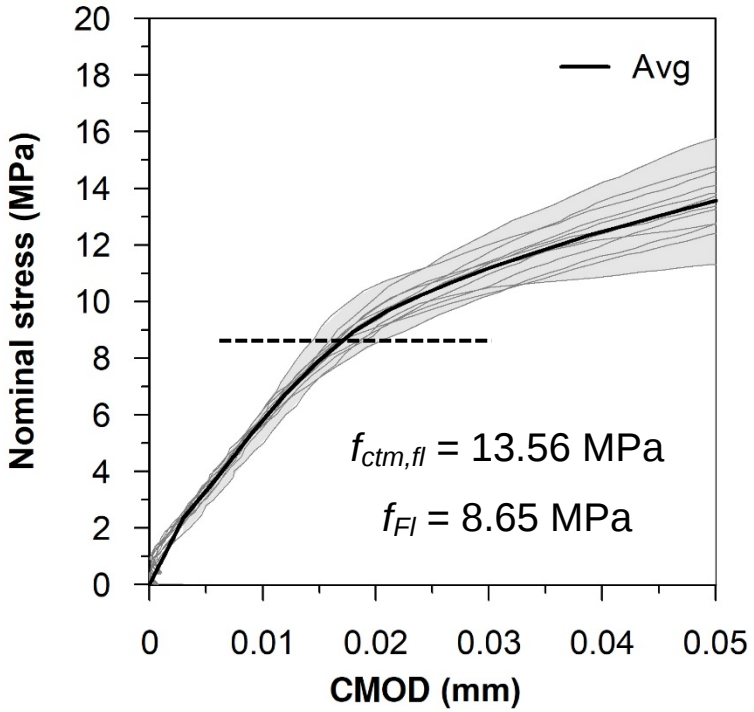

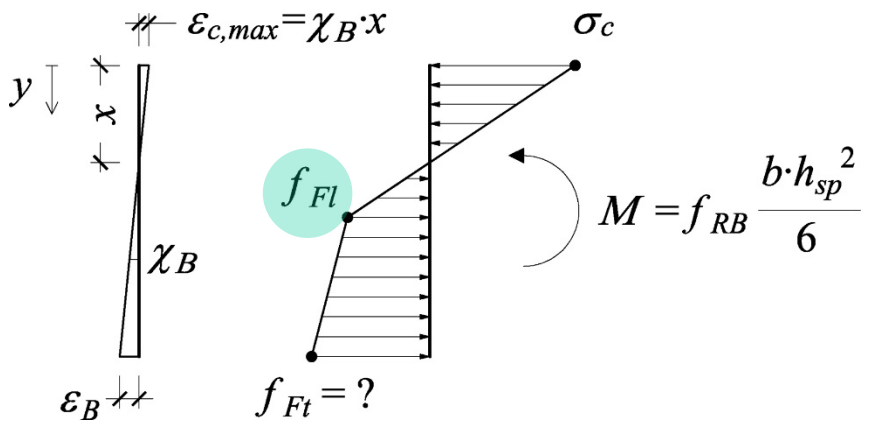

$$\alpha_{fl} = 0.06 \cdot h_{sp}^{0.7}/(1+0.06 \cdot h_{sp}^{0.7})$$

$$f_{Fl} = f_{ctm,fl} \cdot \alpha_{fl}.$$

- No notch effect
- 0.06 (NSC)

G. Zani, M. di Prisco, Identification of Uniaxial Tensile Laws for UHPFRC Modelling, FRC2023: Fiber Reinforced Concrete: from Design to Structural Application, Joint ACI-fib-RILEM International Workshop | Arizona State University, 18th - 20th September 2023, Tempe, USA

Back-calculation procedure

Is it possible to fully identify the uniaxial tensile behavior from notched beam data?

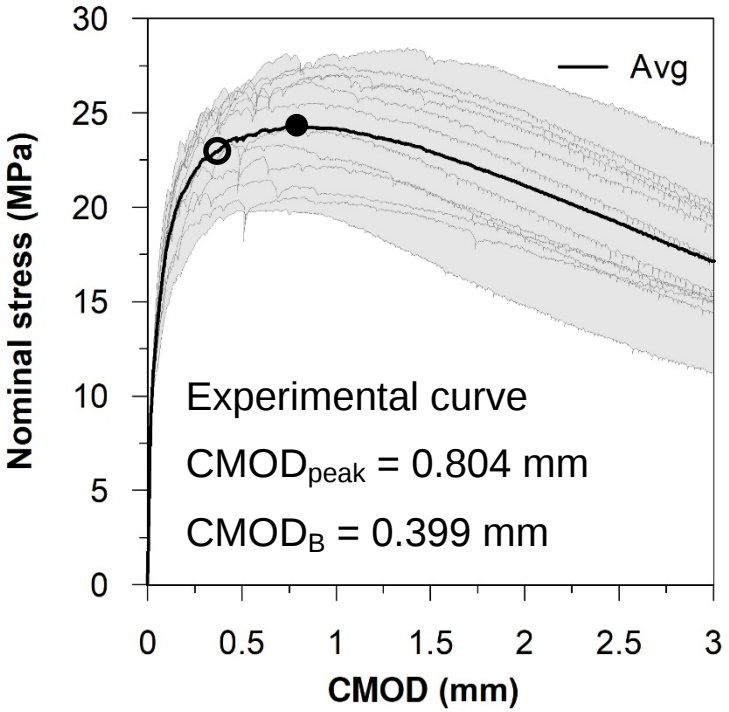

$$CMOD_B = 0.72 \cdot CMOD_{peak} - 0.18$$

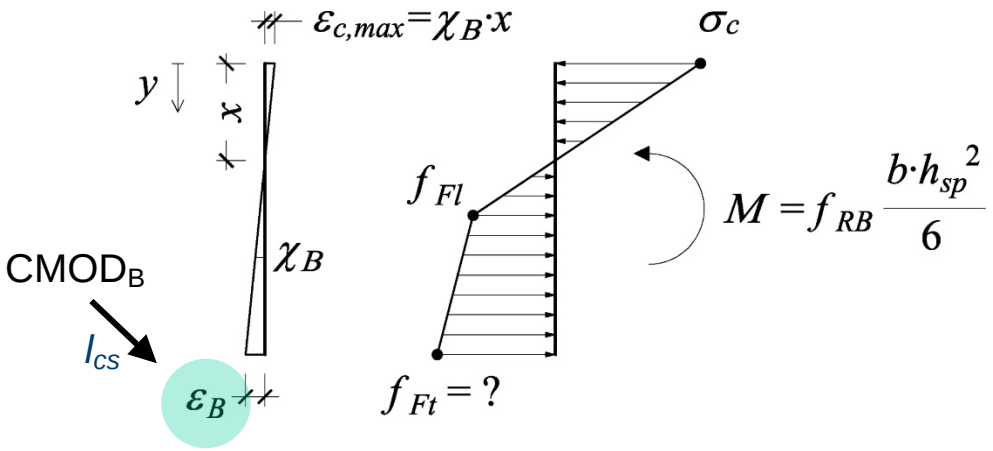

Numerically solved with a minimization algorithm

f_{Ft} = 10.52 MPa

G. Zani, M. di Prisco, Identification of Uniaxial Tensile Laws for UHPFRC Modelling, FRC2023: Fiber Reinforced Concrete: from Design to Structural Application, Joint ACI-fib-RILEM International Workshop | Arizona State University, 18th - 20th September 2023, Tempe, USA

Results

Simplified plane-section (PS) analyses

- Correct equilibrium at ULS
- Null stress at $l_f/4$ in place of $l_f/2$

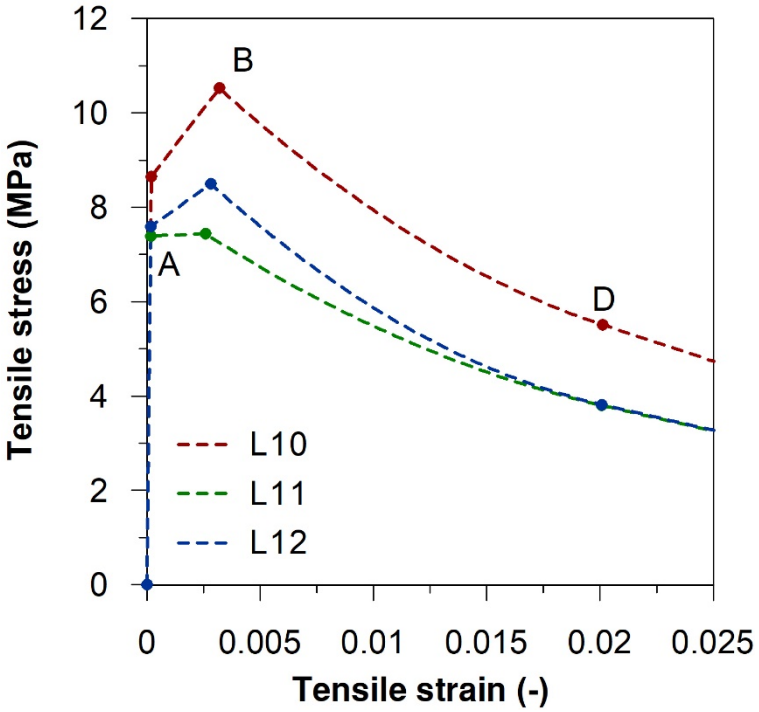

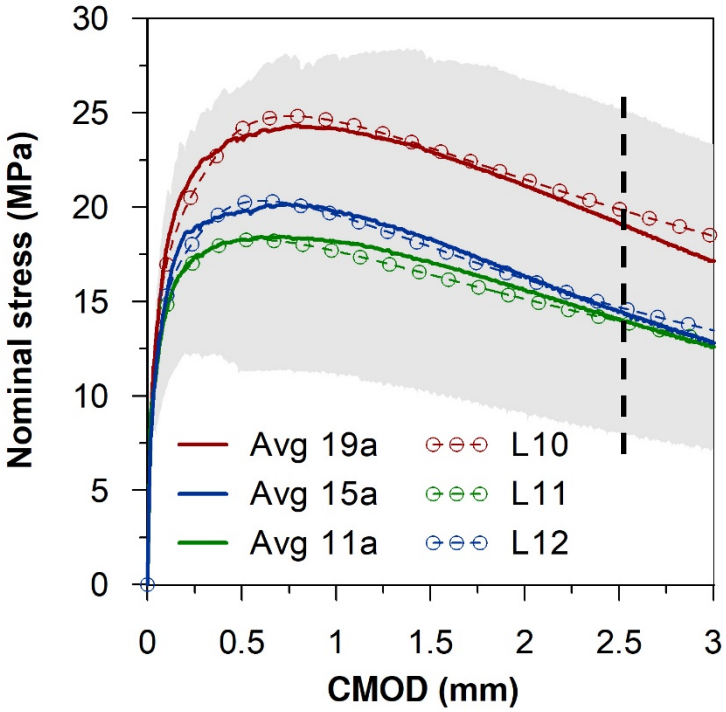

G. Zani, M. di Prisco, Identification of Uniaxial Tensile Laws for UHPFRC Modelling, FRC2023: Fiber Reinforced Concrete: from Design to Structural Application, Joint ACI-fib-RILEM International Workshop | Arizona State University, 18th - 20th September 2023, Tempe, USA

Material specification

Component	Content
Cement I 52.5	600 kg/m^3
Sand $0 \div 2$ mm	977 kg/m^3
Water	212.7 l/m^3
Superplasticizer	33 l/m^3
Slag	500 kg/m^3
Steel fibers	100 kg/m^3

w/b=0.19 and SP/c=5.5%

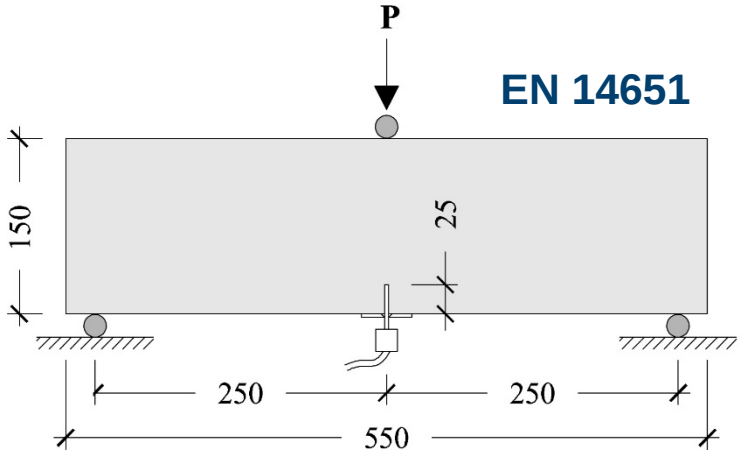

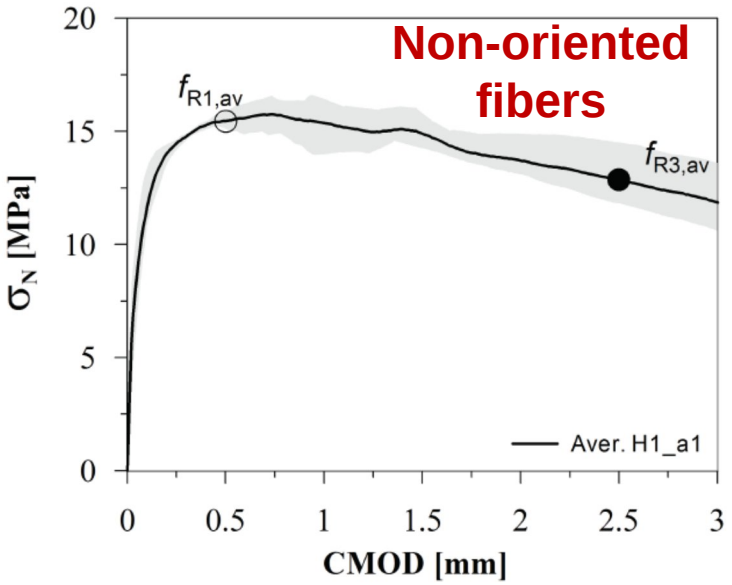

1.2% by volume of straight high-carbon steel microfibers

l_f =13 mm, d_f =0.20 mm, aspect ratio = 65

14a class fiber-reinforced composite **C120** grade concrete

Tensile behavior and size effect phenomena

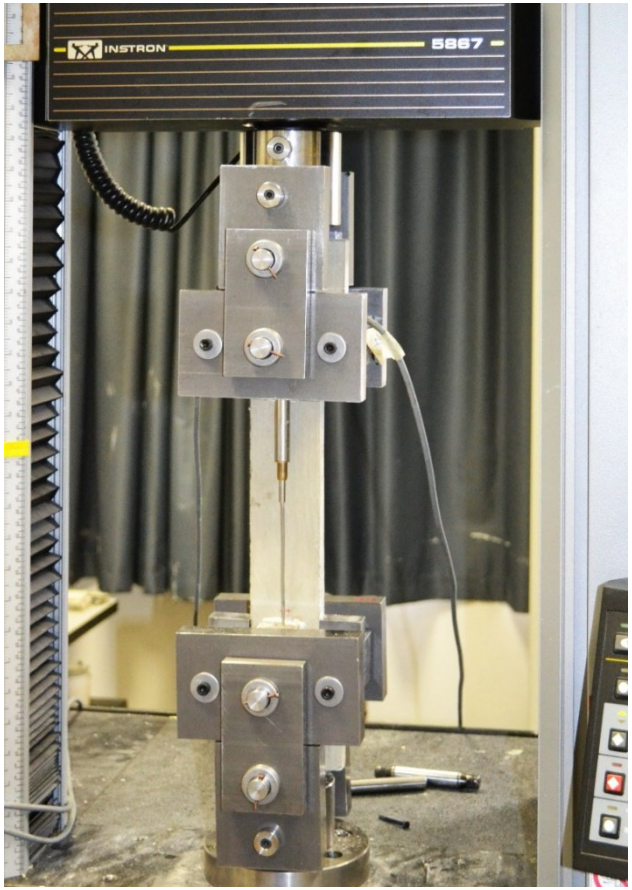

Rotating-end apparatus

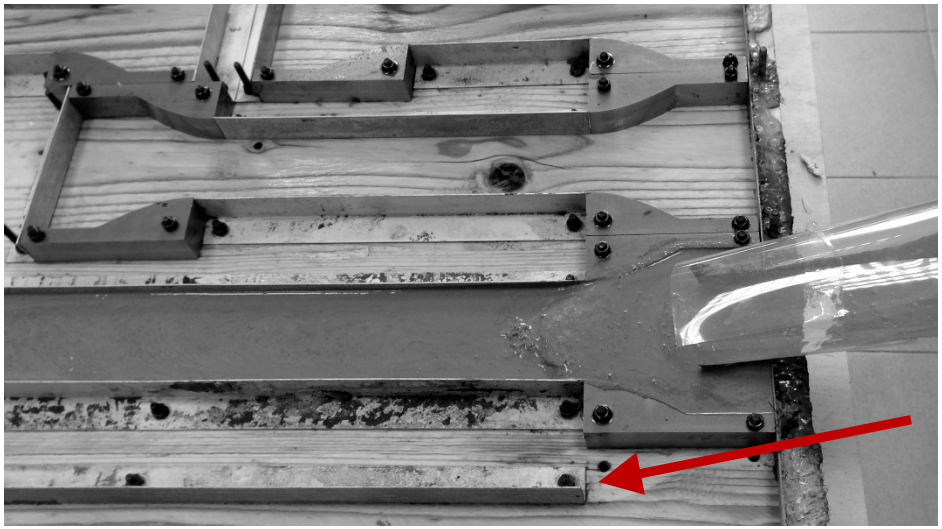

Four gage lenths l_0 (three nominally identical specimens)

20 mm

80 mm

200 mm

440 mm

G. Zani, M. Colombo, M. di Prisco, size effect of HPFRCC in uniaxial tension, AFGC-ACI-fib-RILEM Int. Symposium on Ultra-High Performance Fibre-Reinforced Concrete, UHPFRC 2017 – October 2-4, 2017, Montpellier, France

Tensile behavior and size effect phenomena

Set	$\sigma_{N,peak,av}$ [MPa] (std)	$(COD/\ell_0)_{peak,av}$ [-] (std)
A	6.30 (0.47)	$3.70 \cdot 10^{-3}$ ($5.89 \cdot 10^{-3}$)
B	7.08 (0.46)	$1.89 \cdot 10^{-3}$ ($1.52 \cdot 10^{-3}$)
C	6.15 (0.39)	$6.55 \cdot 10^{-4}$ ($7.75 \cdot 10^{-4}$)
D	4.65 (1.17)	$9.50 \cdot 10^{-4}$ ($7.56 \cdot 10^{-4}$)

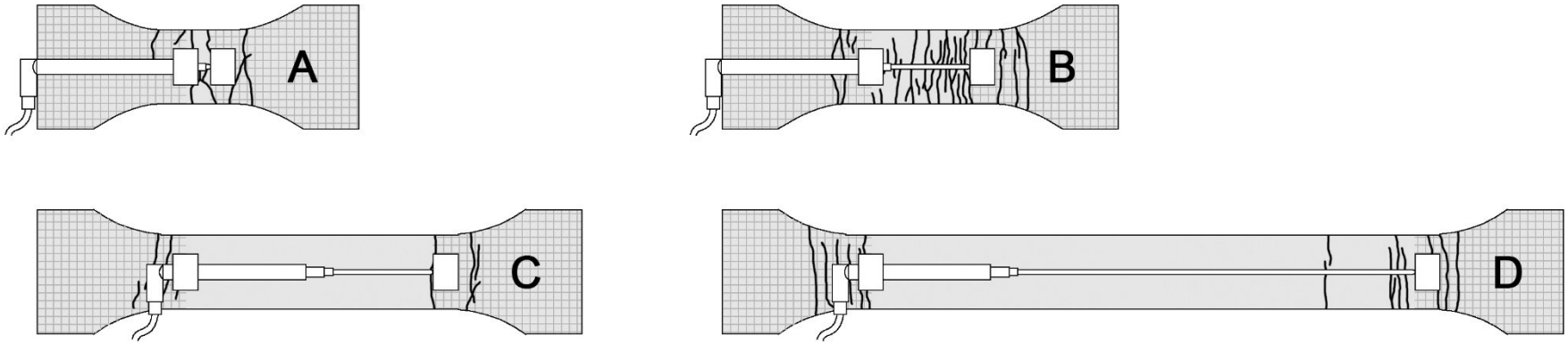

G. Zani, M. Colombo, M. di Prisco, size effect of HPFRCC in uniaxial tension, AFGC-ACI-fib-RILEM Int. Symposium on Ultra-High Performance Fibre-Reinforced Concrete, UHPFRC 2017 – October 2-4, 2017, Montpellier, France

Tensile behavior and size effect phenomena

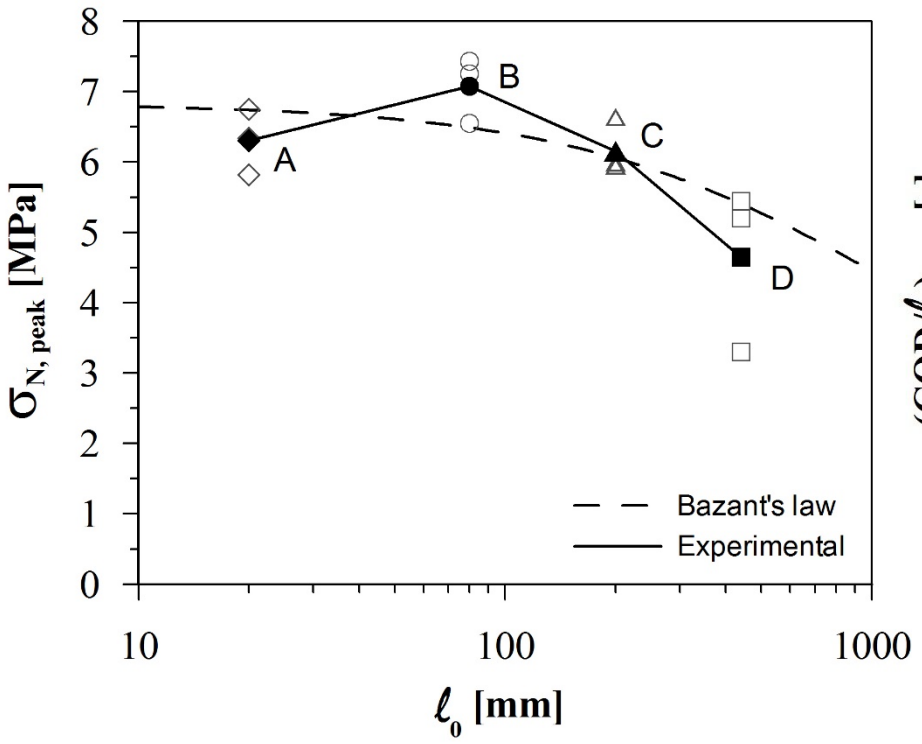

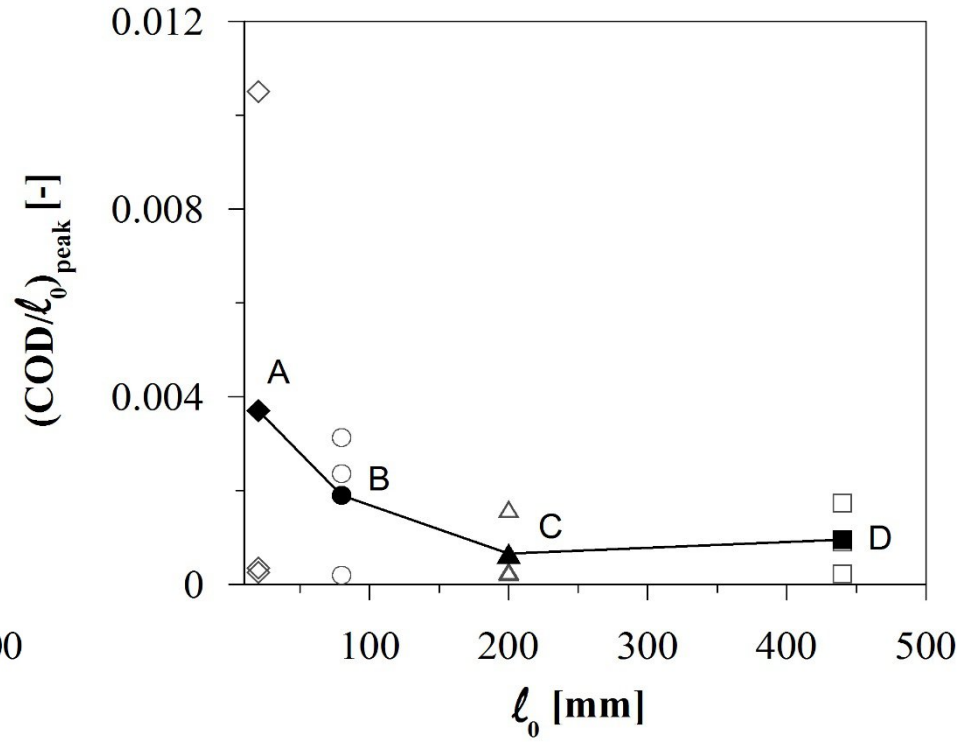

Solid-hatched marks = average responses

G. Zani, M. Colombo, M. di Prisco, size effect of HPFRCC in uniaxial tension, AFGC-ACI-fib-RILEM Int. Symposium on Ultra-High Performance Fibre-Reinforced Concrete, UHPFRC 2017 – October 2-4, 2017, Montpellier, France

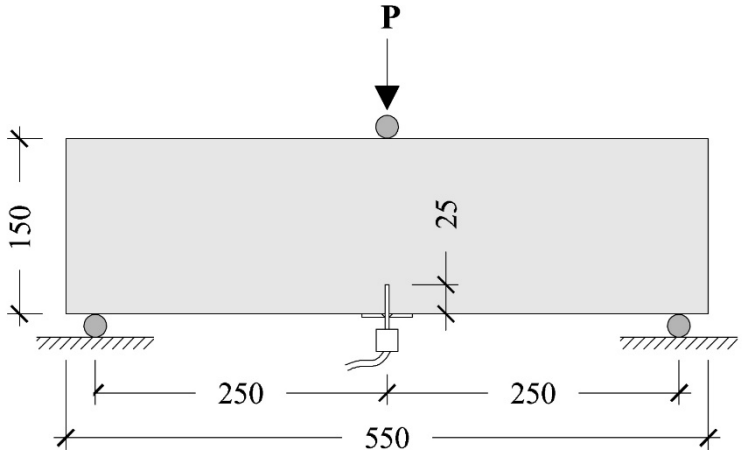

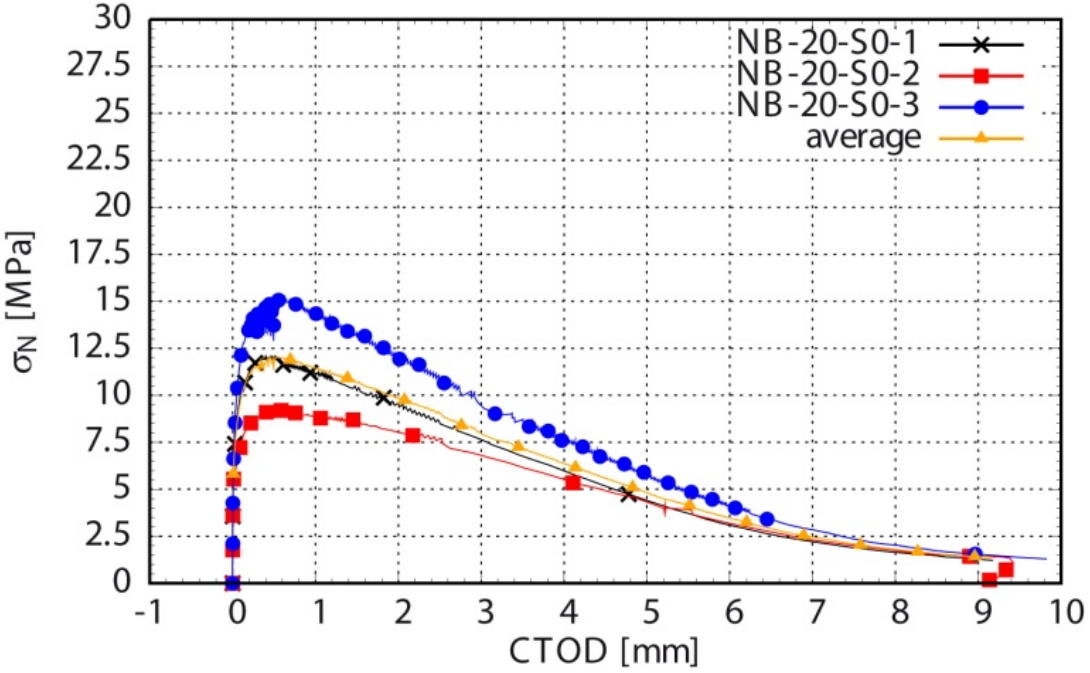

Caverzan, A., Colombo, M., di Prisco, M., Rivolta, B., High performance steel fibre reinforced concrete: residual behaviour at high temperature, (2015) Materials and Structures, 48 (10), pp. 3317-3329.

HIGH TEMPERATURE BEHAVIOUR

Component	Dosage (kg/m^3)
Cement type I 52.5	600
Slag	500
Water	200
Super Plasticizer	33 (l/m^3)
Sand 0-2 mm	983
Steel fibres (l_f =13 mm; d_f=0.16 mm)	100

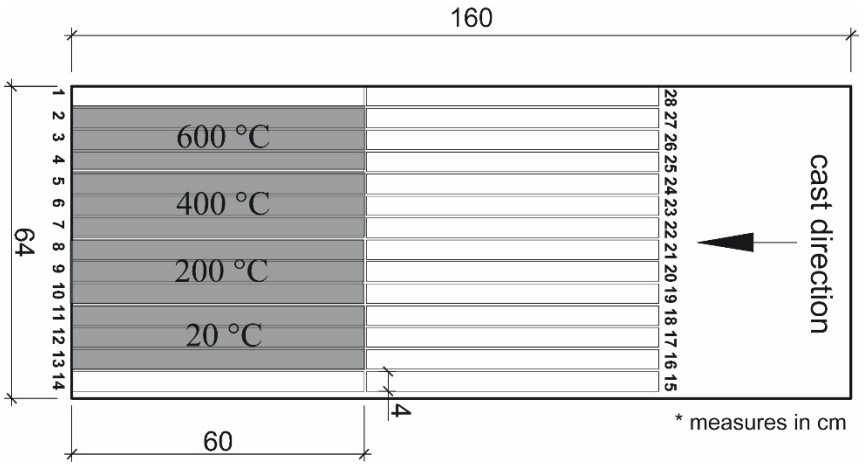

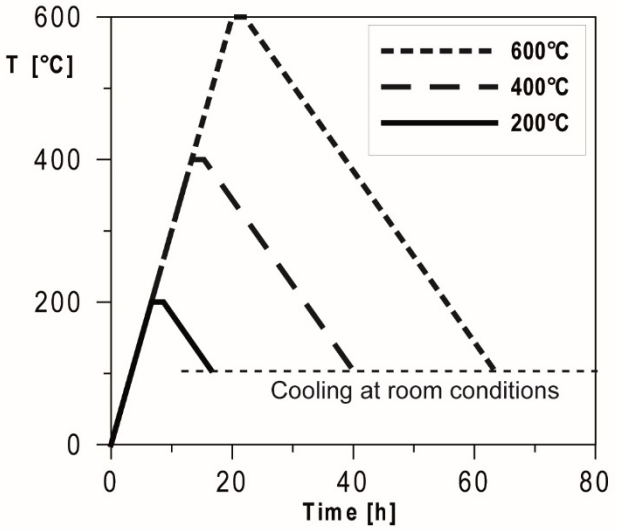

Caverzan, A., Colombo, M., di Prisco, M., Rivolta, B., High performance steel fibre reinforced concrete: residual behaviour at high temperature, (2015) Materials and Structures, 48 (10), pp. 3317-3329.

UN-NOTCHED BEAMS

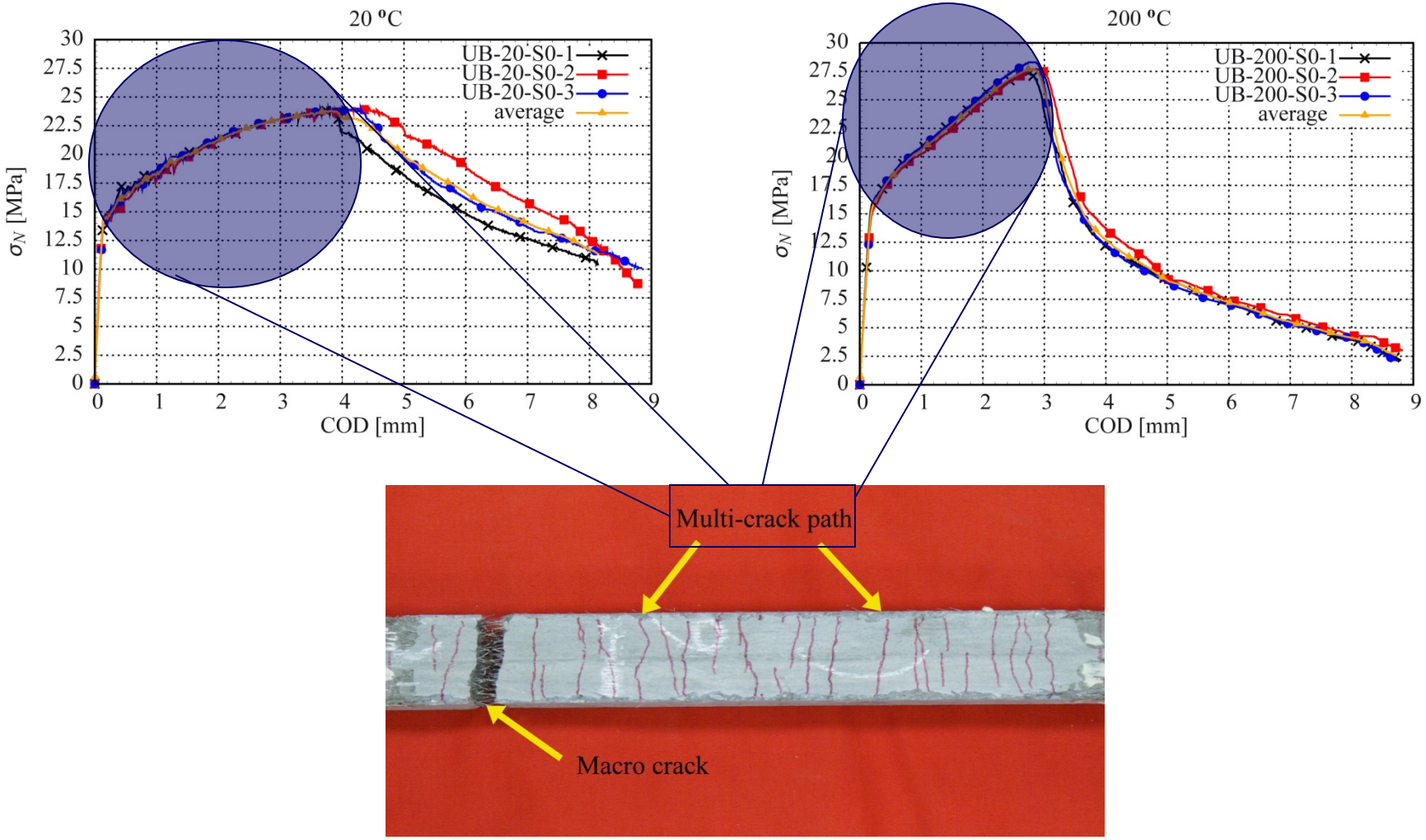

Caverzan, A., Colombo, M., di Prisco, M., Rivolta, B., High performance steel fibre reinforced concrete: residual behaviour at high temperature, (2015) Materials and Structures, 48 (10), pp. 3317-3329.

UN-NOTCHED BEAMS

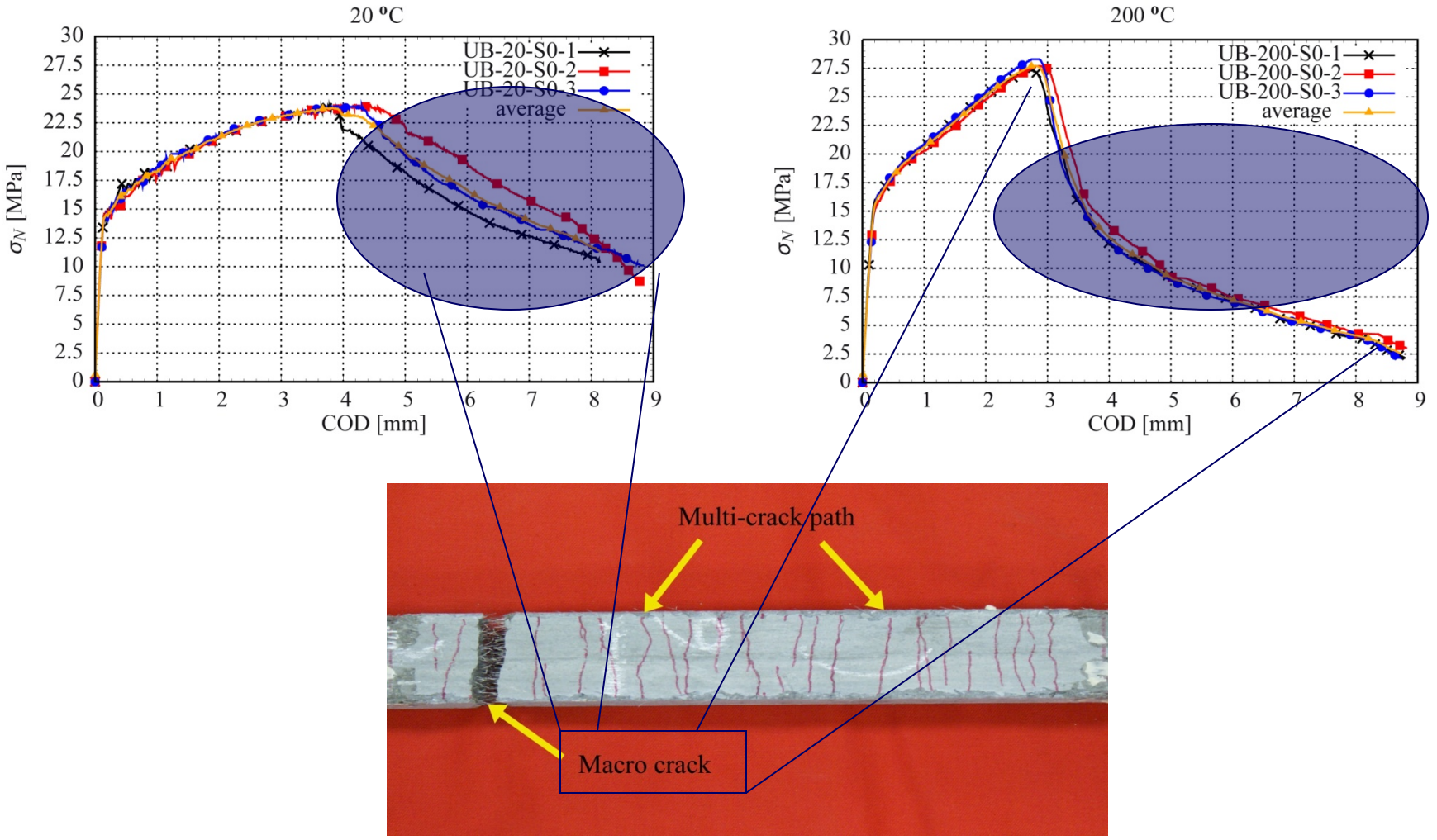

Caverzan, A., Colombo, M., di Prisco, M., Rivolta, B., High performance steel fibre reinforced concrete: residual behaviour at high temperature, (2015) Materials and Structures, 48 (10), pp. 3317-3329.

UN-NOTCHED BEAMS

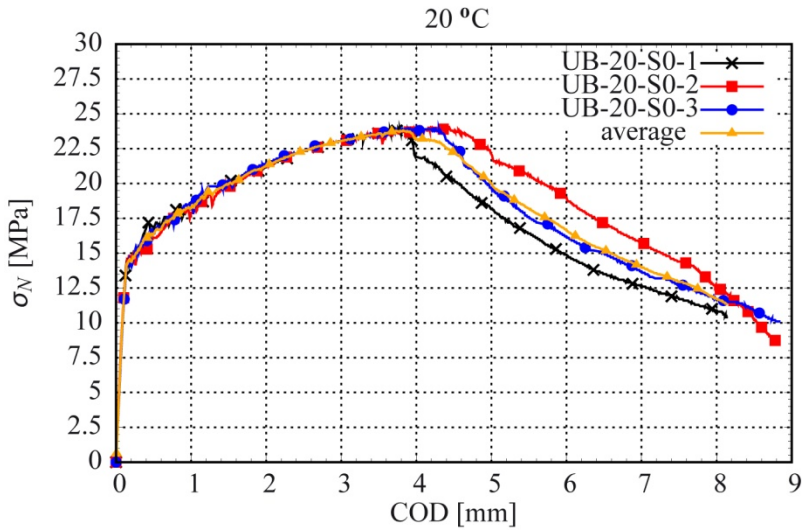

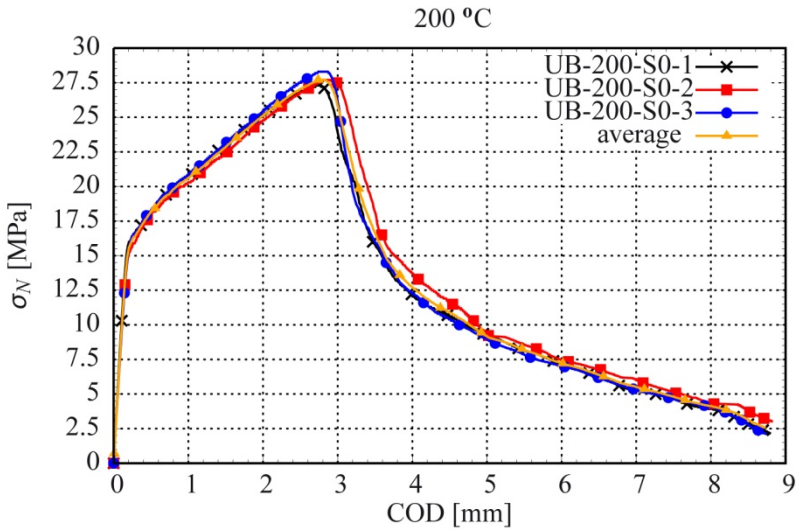

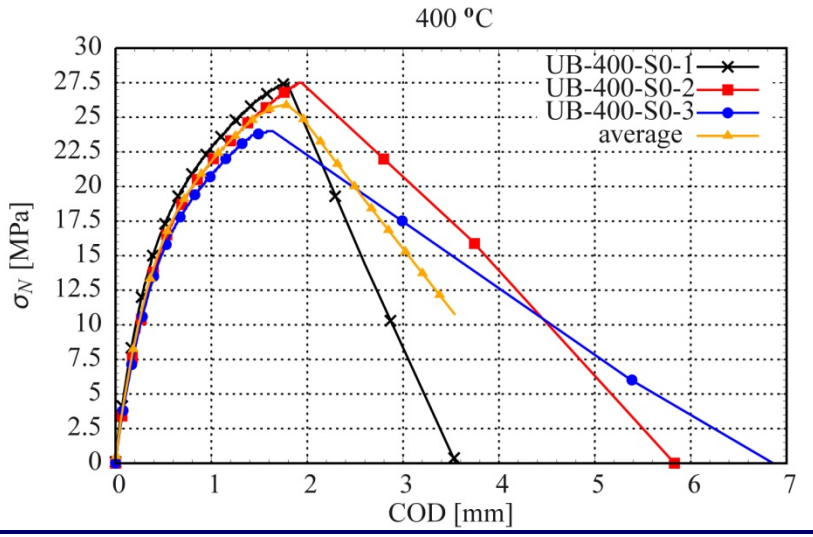

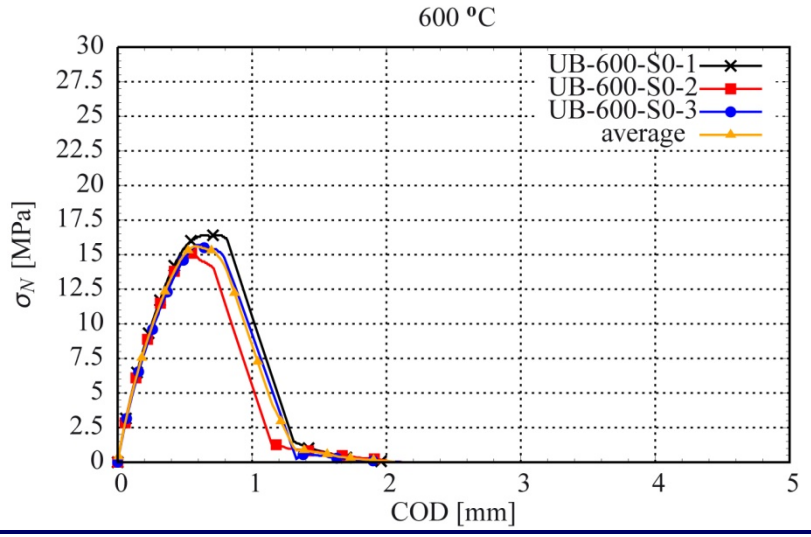

Caverzan, A., Colombo, M., di Prisco, M., Rivolta, B., High performance steel fibre reinforced concrete: residual behaviour at high temperature, (2015) Materials and Structures, 48 (10), pp. 3317-3329.

by G. Jen and C.P. Ostertag, 2016

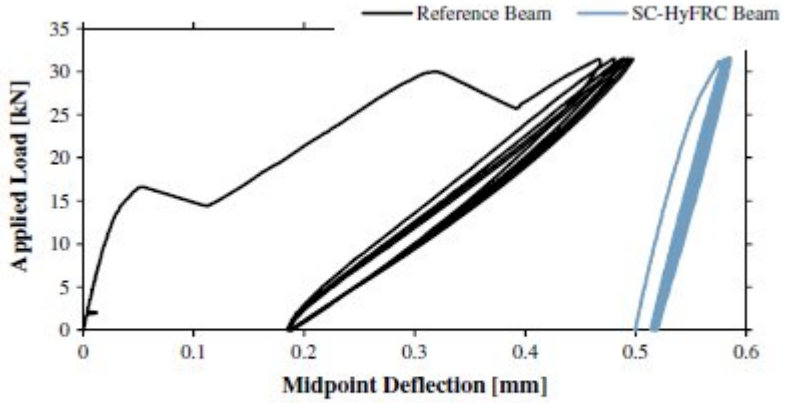

Fig. 2. Load–deflection responses of reference and SC-HyFRC beams to cyclic flexural loading.

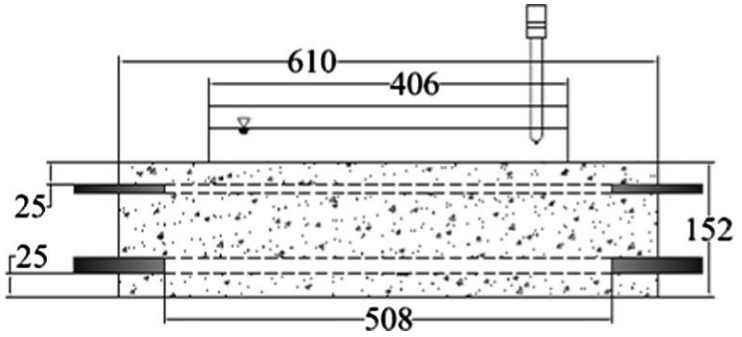

Table 1
Concrete mix proportions (kg/m^3).

	Portland cement	Class F fly ash	Water	Fine aggregate	Coarse aggregate	PVA fiber	Steel fiber
Reference[1]	397	131	237	1006	497	–	–
SC-HyFRC[1]	397	131	237	1044	418	2.6	102

[1] Chemical admixtures, superplasticizer and viscosity modifying admixture, added to achieve flowable behavior.

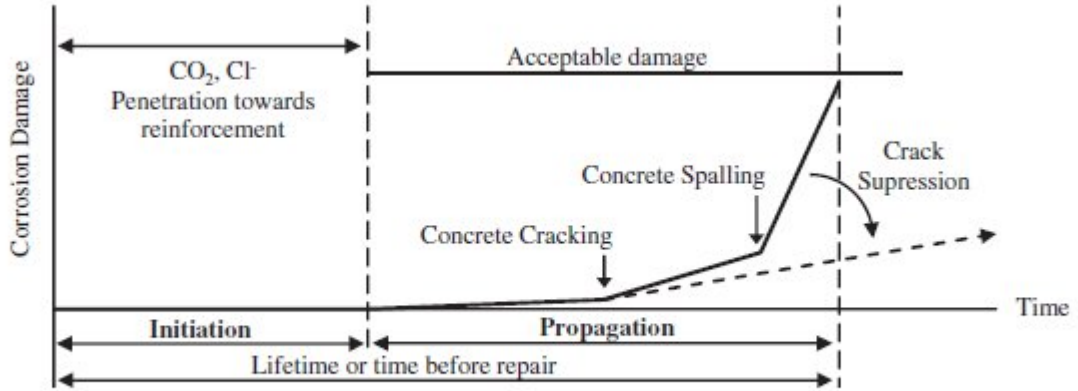

Fig. 9. Corrosion damage model of *fib* Model Code (2006) for undamaged concrete beams, with suggested crack suppression influence shown in dashed line.

New solutions for sustainable roofing

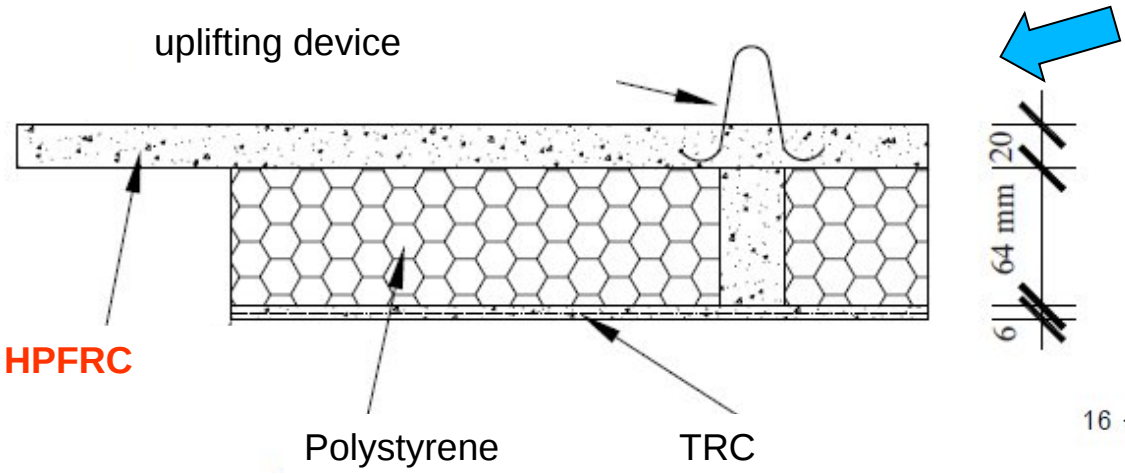

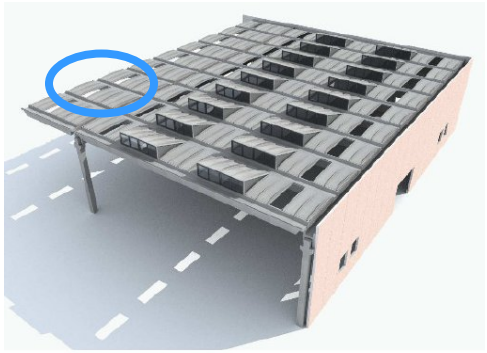

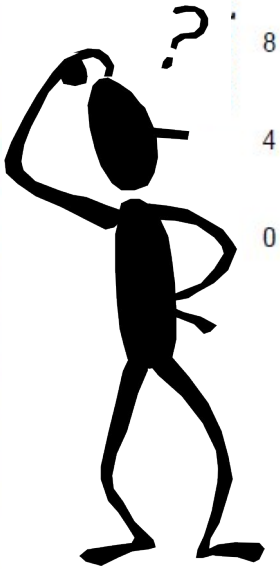

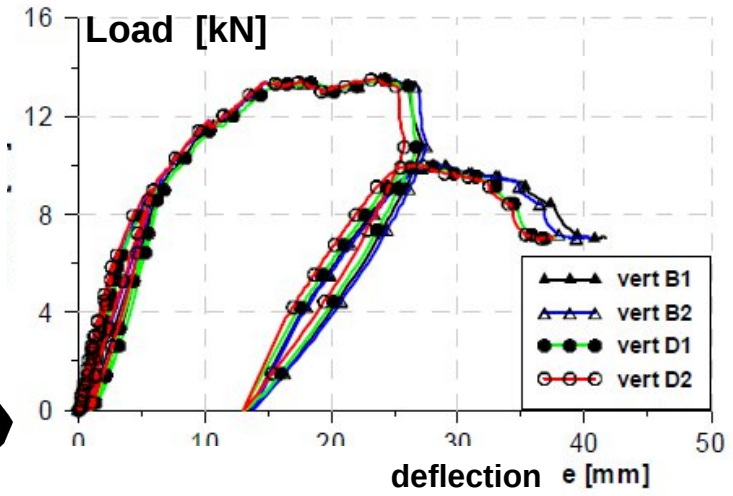

CASE STUDY: ROOFING ELEMENT

Roof systems are in important component of the building envelope, since they are specifically designed to separate the living spaces from the natural environment. They should ensure:

- adequate mechanical performances;
- energy efficiency;
- sound insulation;
- durability;
- aesthetics.

HOW CAN WE MEET THE REQUIREMENTS OF THE REVISED NATIONAL CODES?

A retrofitting strategy that might be successfully applied to several precast structures in northern Italy is represented by the substitution of the unsafe tertiary roofing elements with innovative multilayer panels characterized by lightness and remarkable structural performances.

S.IN.E.RG.I.E ATTI.V.E.

SISTEMA INTEGRATO SOSTENIBILE ENERGETICAMENTE ATTIVO PER IL RINNOVO DEGLI EDIFICI INDUSTRIALI ATTRAVERSO COPERTURE COMPOSITE

UNIONE EUROPEA

Ministero dell'Istruzione dell'Università e della Ricerca

RegioneLombardia

FOR COMPETITIVITÀ 2007-2013

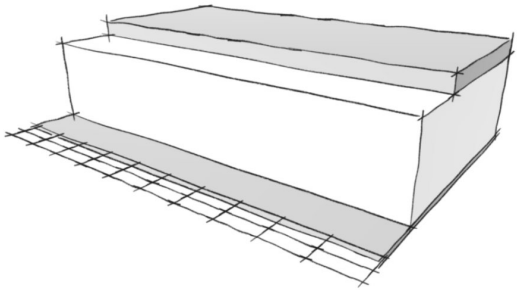

HPFRC + INSULATING CORE + TRC

- self-weight reduction to solve seismic requirements;
- fire safety improvement;
- environmental sustainability, relying both on the improvement of the thermal performances and on the design of Building-Integrated Photovoltaics (BIPV) and the use of recycled fibres;
- global cost reduction: no need of waterproofing layer

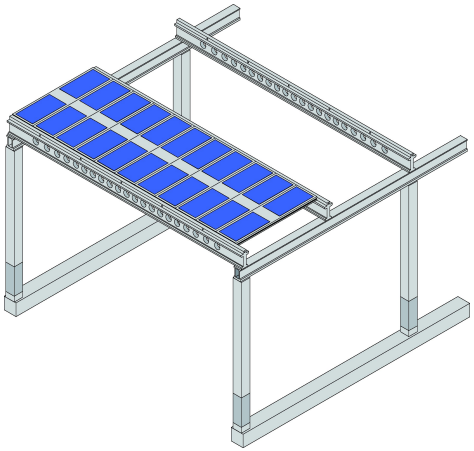

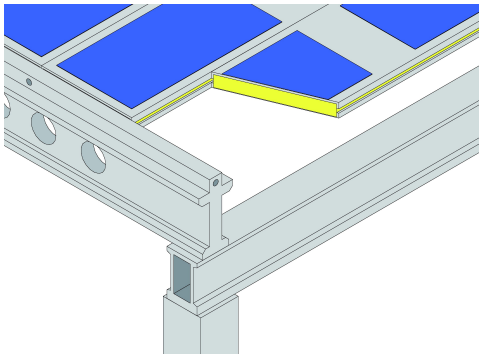

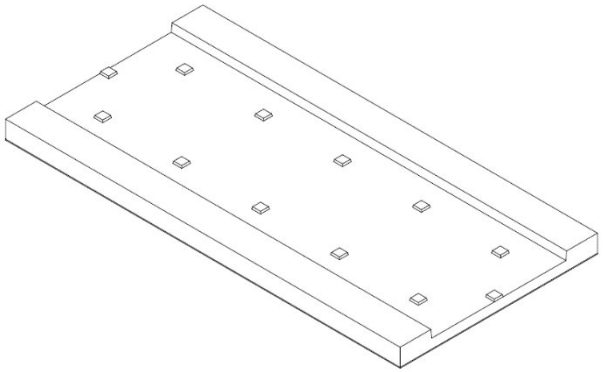

The proposal

2.5 m wide and 5 m long secondary prefabricated elements.
Main features: **lightness** (self-weight of about 1.2 kN/m^2); remarkable **thermal insulation** (U = 0.42 W/m^{2}K), **waterproof quality**, **ease of assembly**, **fire safety** (> R30) and effective **integration of photovoltaic systems**.

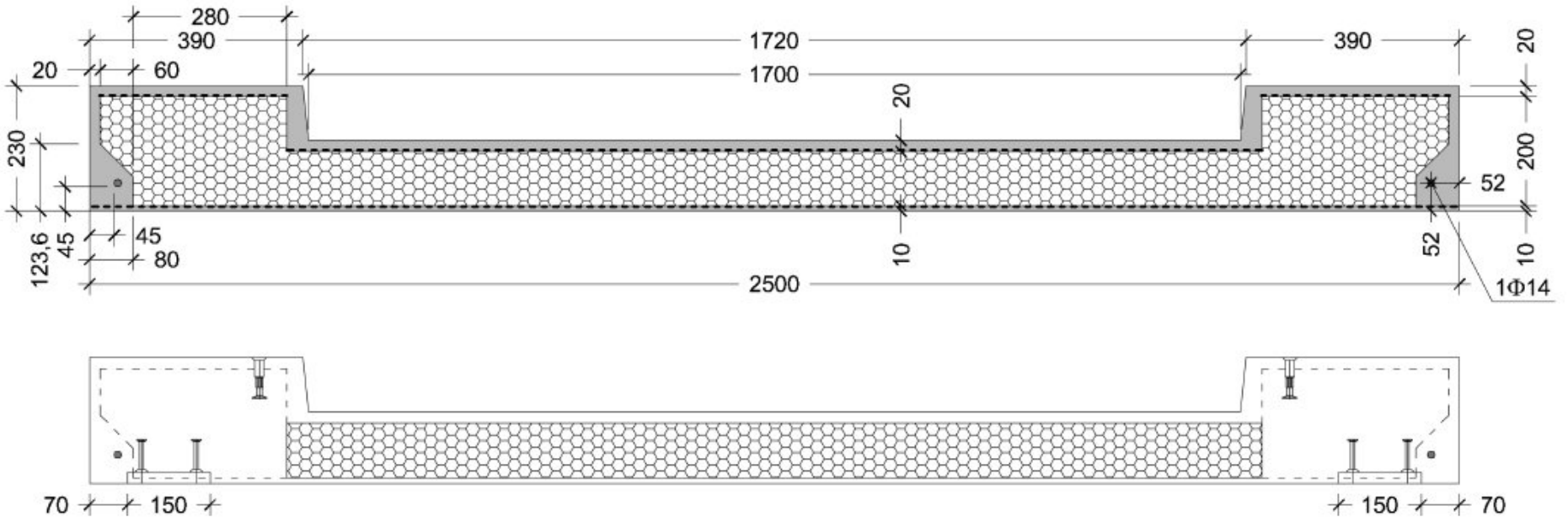

Transverse sections of the proposed composite panel (mid and end section)

No.	Failure mode		
A	tension failure of the reinforcement	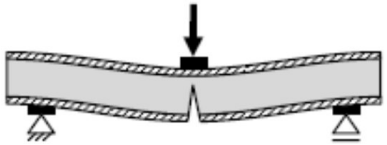	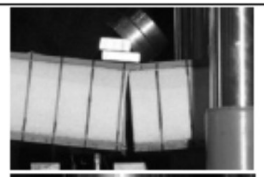
B	compression failure of the core at the point of load application	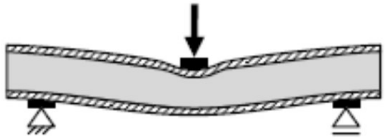	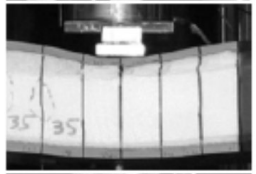
C	local bending failure of the upper facing	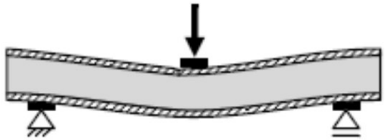	
D	local shear failure of the upper facing	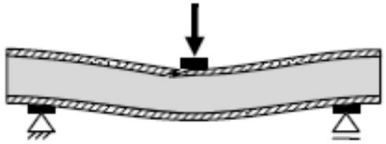	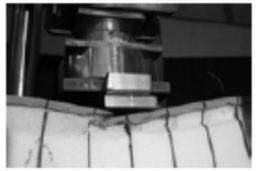
E	shear failure of the core and delamination of core and facings	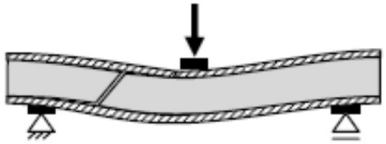	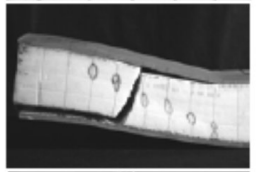
F	longitudinal shear failure of the bond between the core and the upper facing (at one or both ends)	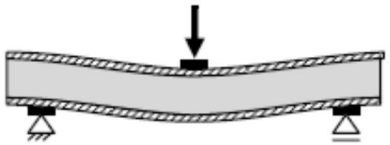	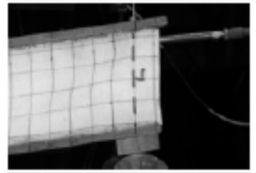
G	compression failure of the core at the supports (at one or both ends)	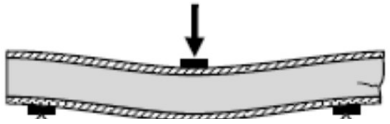	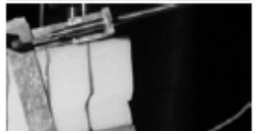

Cement-based composites

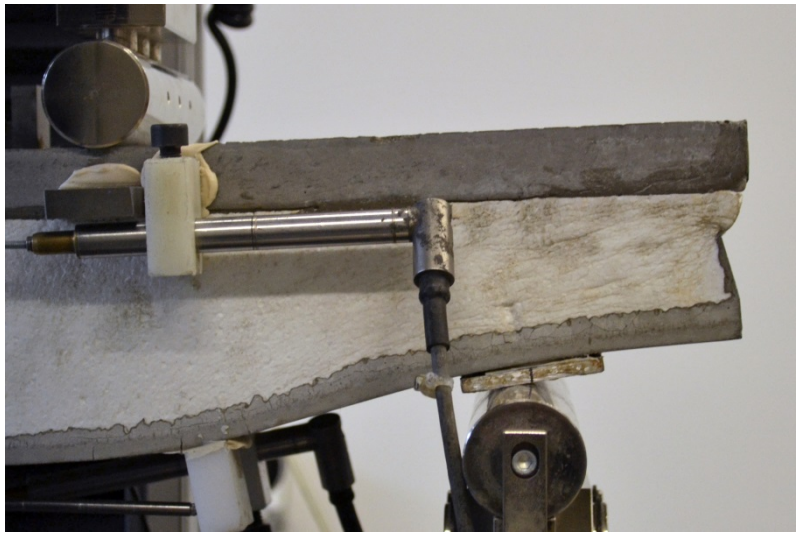

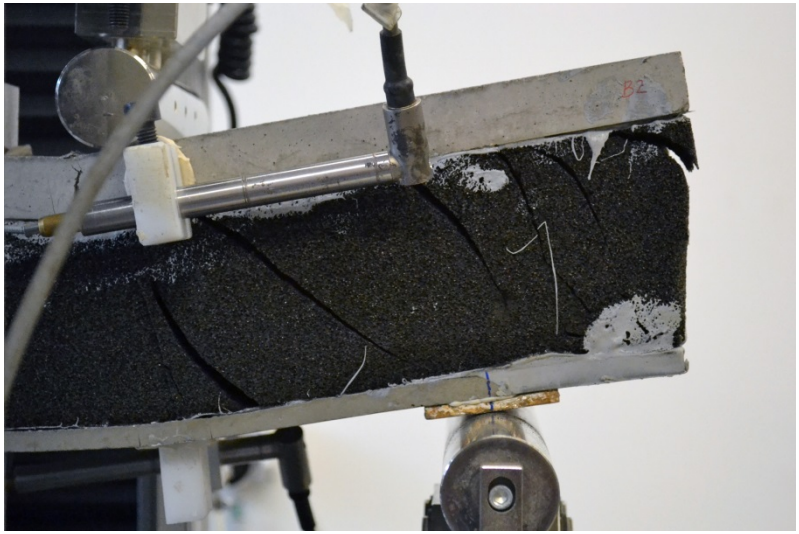

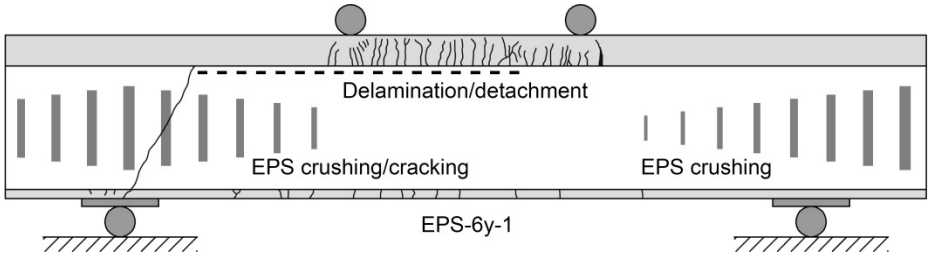

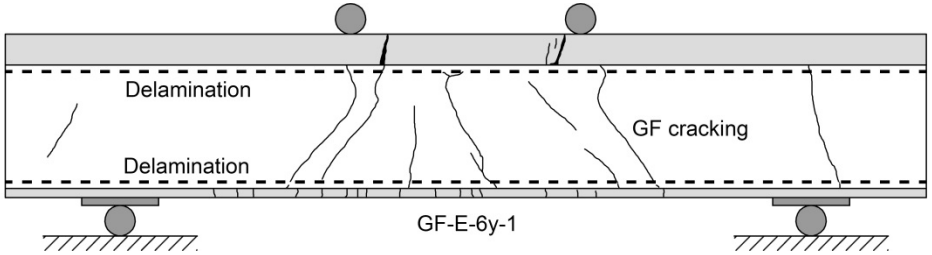

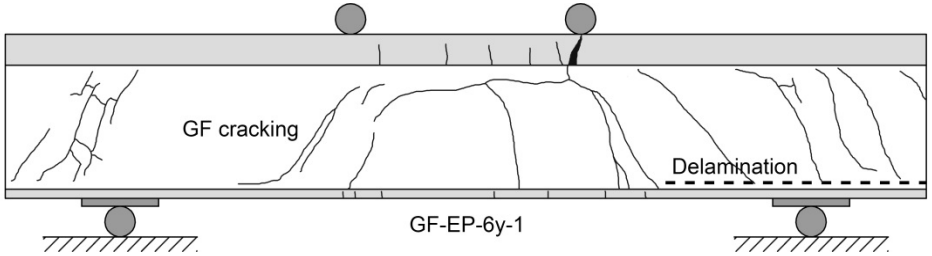

Mechanical characteristics of polystyrene

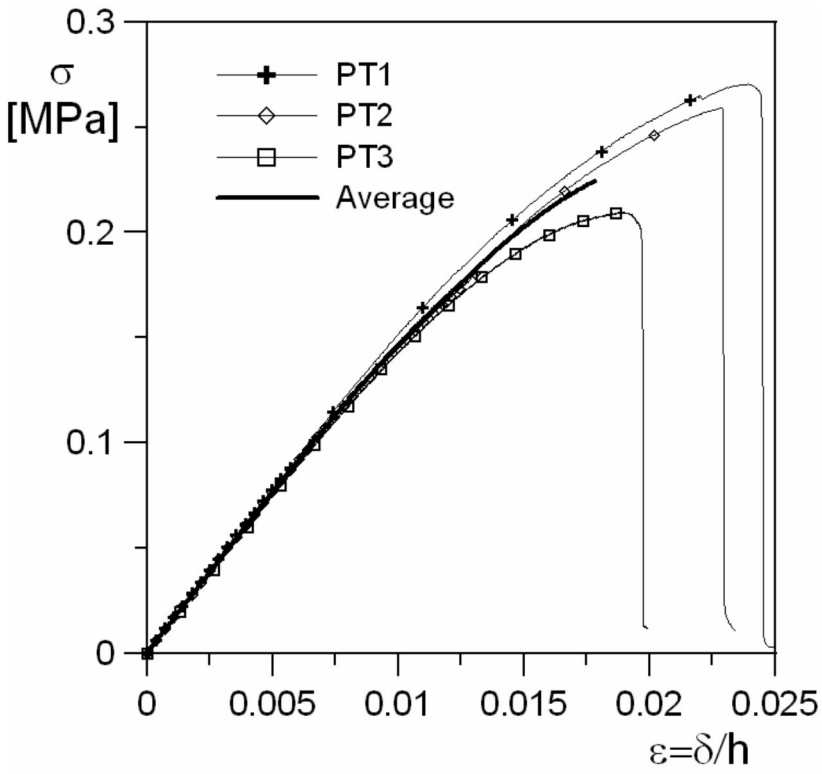

Uniaxial tension

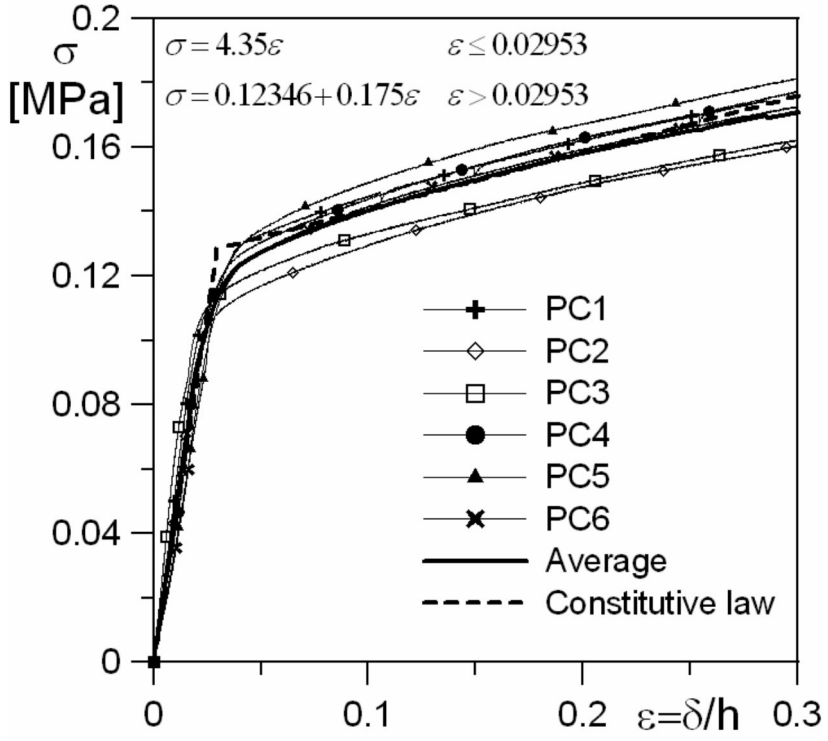

Uniaxial compression

EPS 100

Longitudinal bending tests - setup

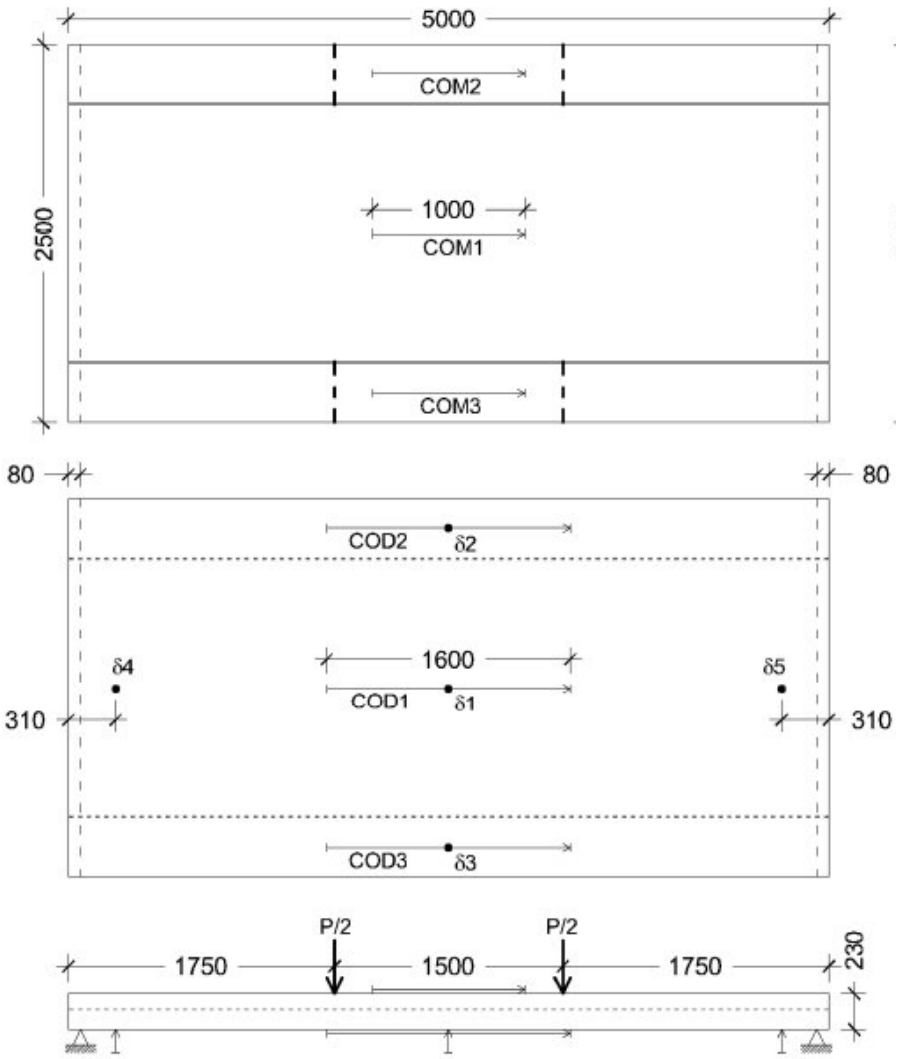

Longitudinal bending tests

- **Remarkable strength and ductility levels:** peak loads were about **3.5 to 4 times higher** than the one associated to the Ultimate Limit State (ULS).
- Test number 2 was halted right after the widening of some shear cracks, originally developed on an HPFRCC web, probably due to a poor control of the wall thickness and an uneven distribution of the fibrous reinforcement.

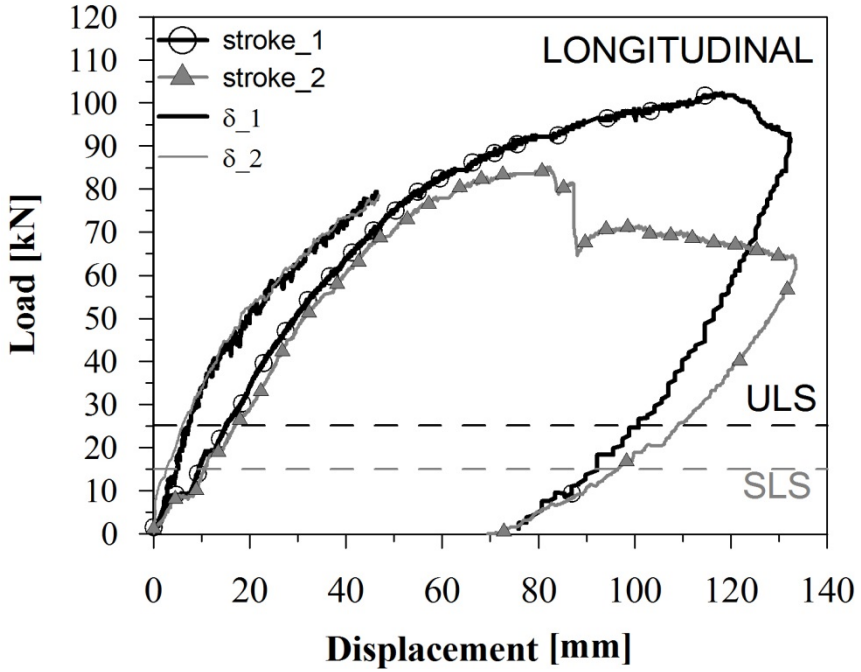

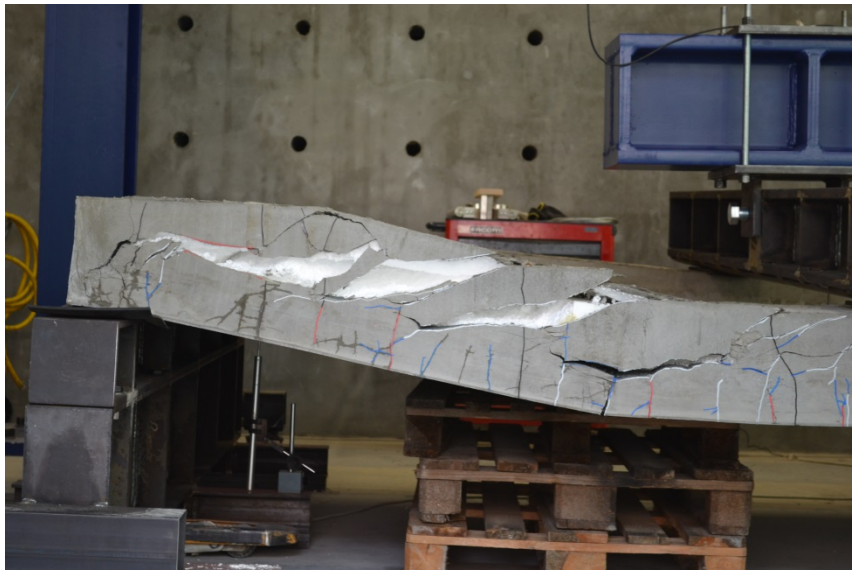

Transverse bending tests - setup

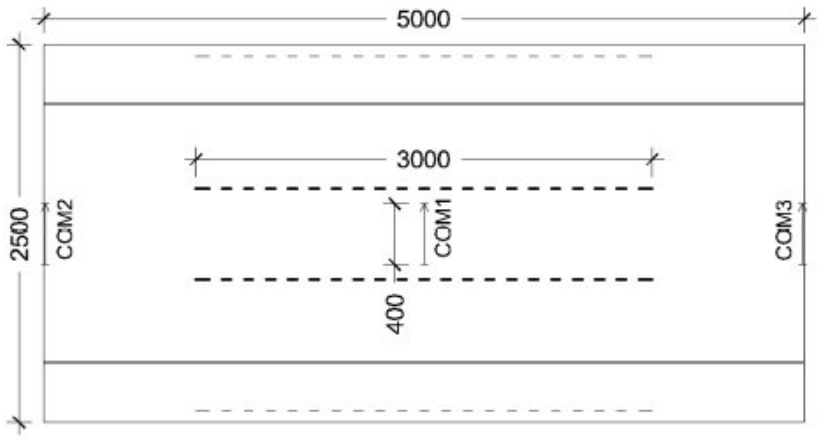

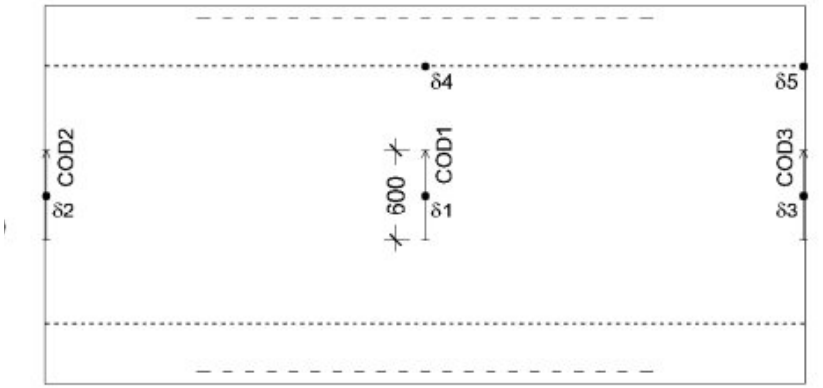

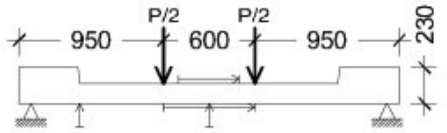

Transverse bending tests

- ✓ Ultimate loads about **4 to 4.5 times higher** than the ULS design one.
- ✓ Peak load of test number 1 corresponded to the localization of a flexural crack,
- ✓ Test number 2 an early failure occurred due to the delamination of the TRC bottom layer (caused by the introduction of an alternative production procedure).

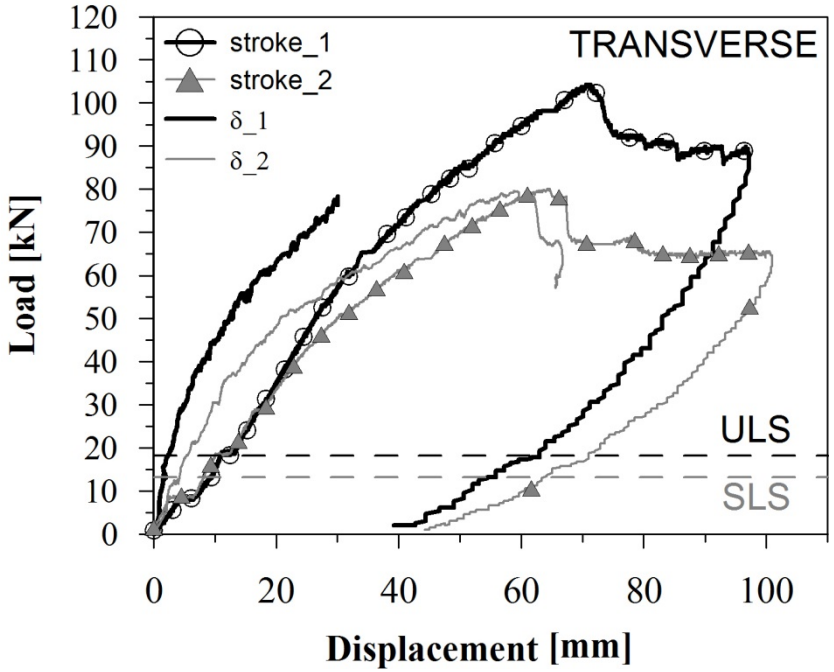

Cement-based composites

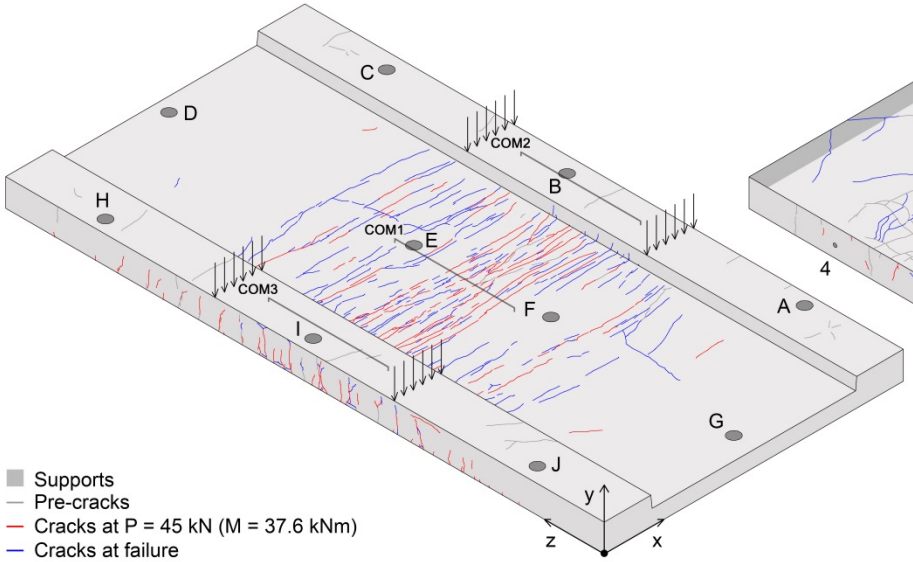

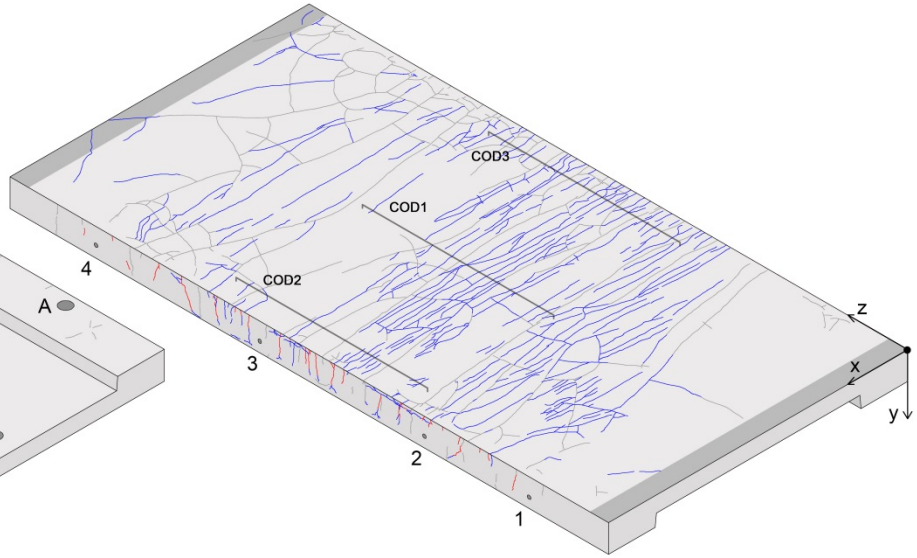

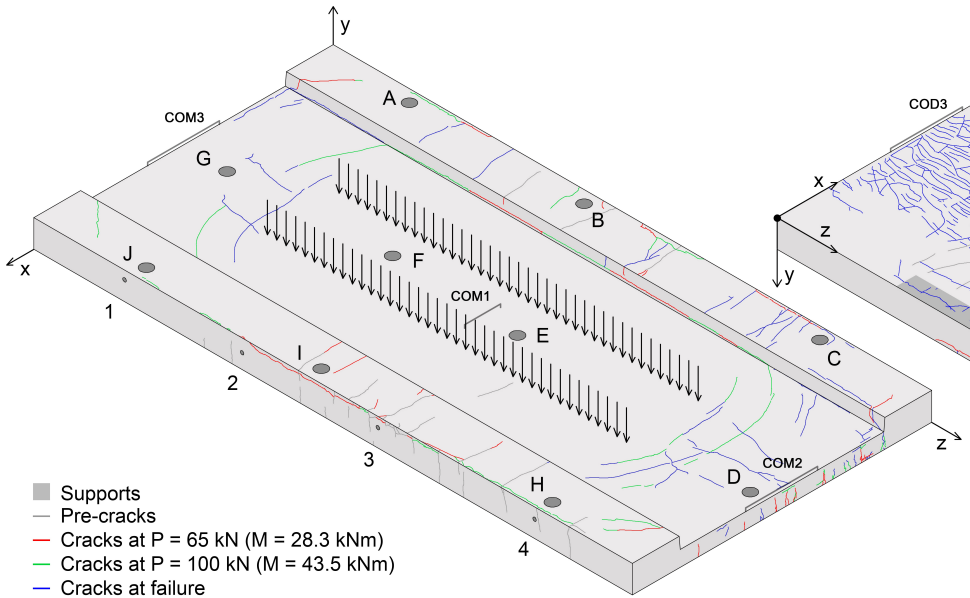

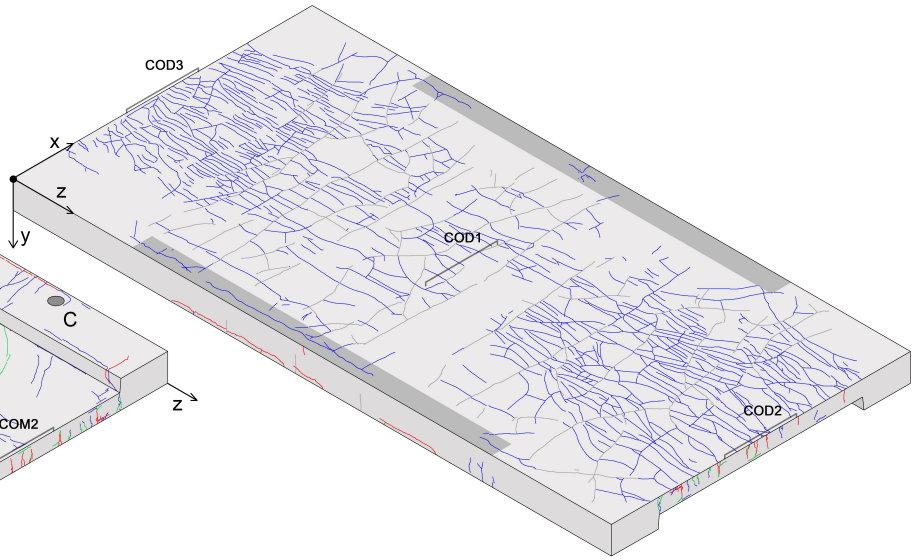

Constitutive laws for the cement-based materials

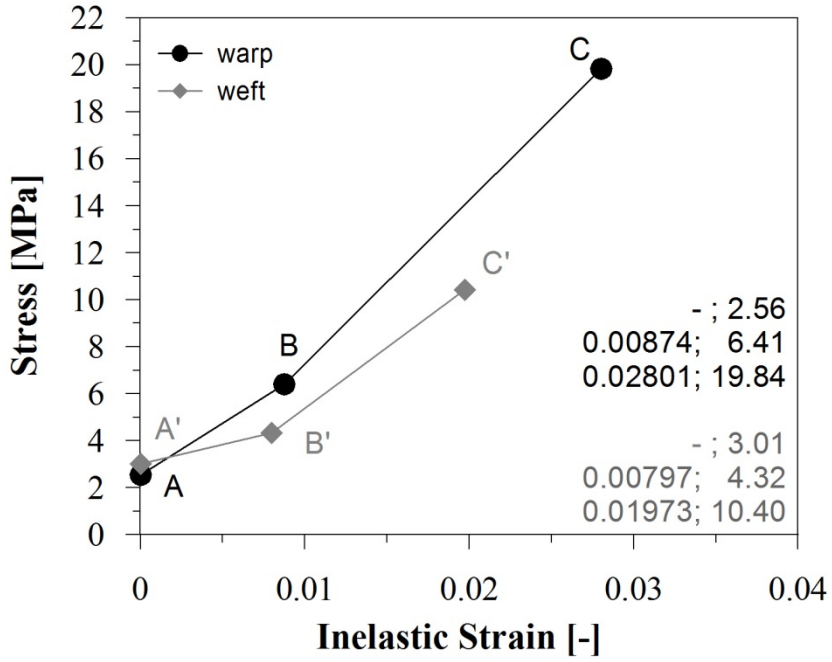

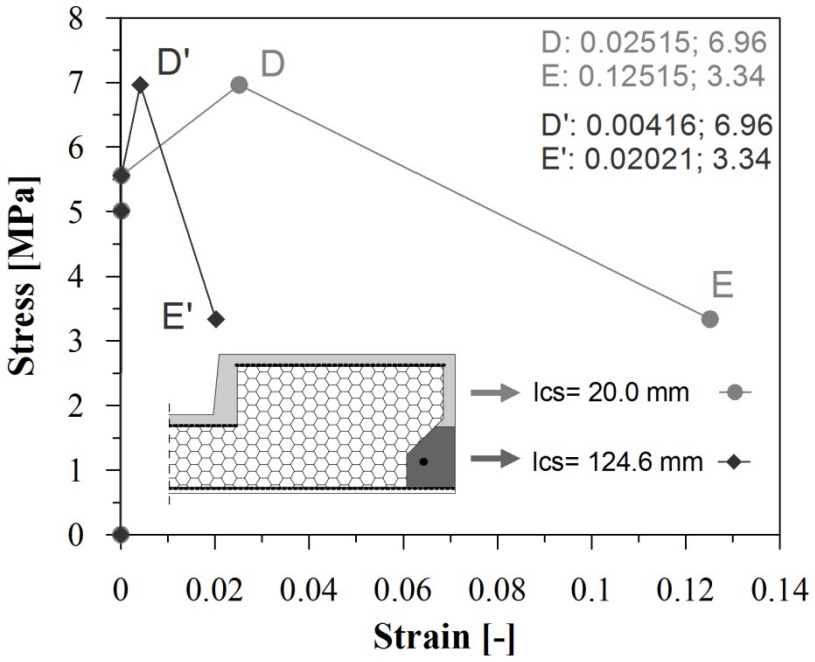

TRC and HPFRCC piecewise-linear constitutive laws

Zani,G., Rampini M.C., Colombo M., di Prisco M., (2019) Bending behaviour of cement-based multi-layered roof elements, Engineering Structures, 101-115

Table 7
Summary of the performed plane-section analyses. Peak curvatures of analyses ps1 and ps2 are omitted, being associated to failure mechanisms different from the ones observed on the full-scale panels.

Analysis	Intrados	Extrados	$\vartheta_{peak,PS}$ [1/mm]	$M_{peak,PS}$ [kNm]	$\frac{M_{peak,PS}}{M_{peak,LB1}}$	$\frac{M_{peak,PS}}{M_{peak,LB2}}$
ps1	–	plain concrete ($f_{ct} = 0$)	–	29.50	0.35	0.41
ps2	–	non-oriented, ℓ_{cs1} + non-oriented, ℓ_{cs2}	–	53.00	0.62	0.75
ps3	fabric	non-oriented, ℓ_{cs1} + non-oriented, ℓ_{cs2}	9.37e−5	109.00	1.28	1.53
ps4	fabric	non-oriented, ℓ_{cs1} + oriented, ℓ_{cs2}	9.47e−5	115.00	1.35	1.62
ps5	TRC	non-oriented, ℓ_{cs1} + non-oriented, ℓ_{cs2}	9.42e−5	110.00	1.29	1.55
ps6	TRC	non-oriented, ℓ_{cs1} + oriented, ℓ_{cs2}	9.52e−5	116.00	1.36	1.63

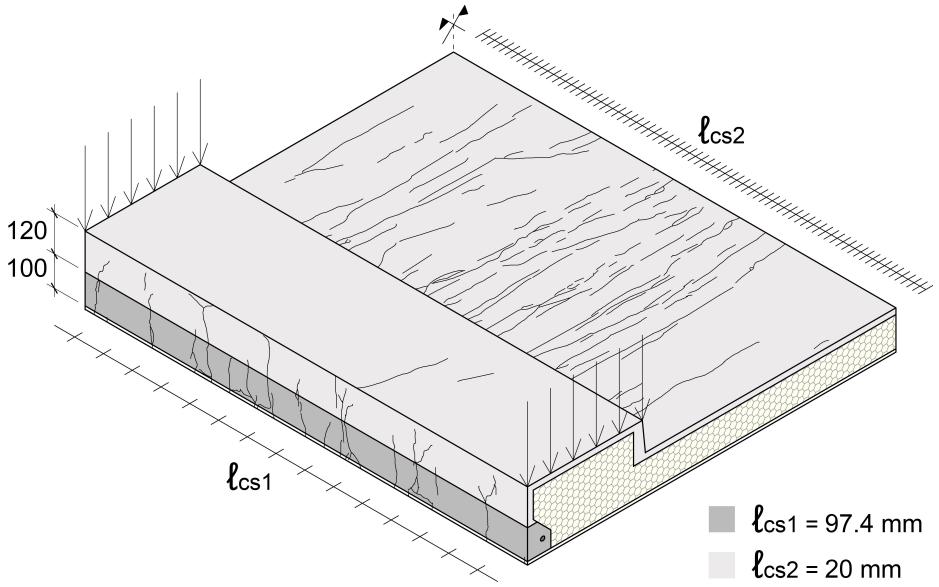

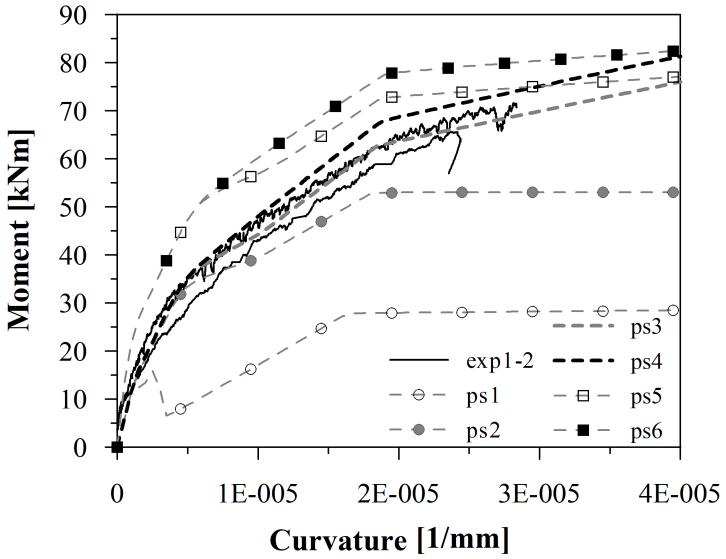

Cement-based composites

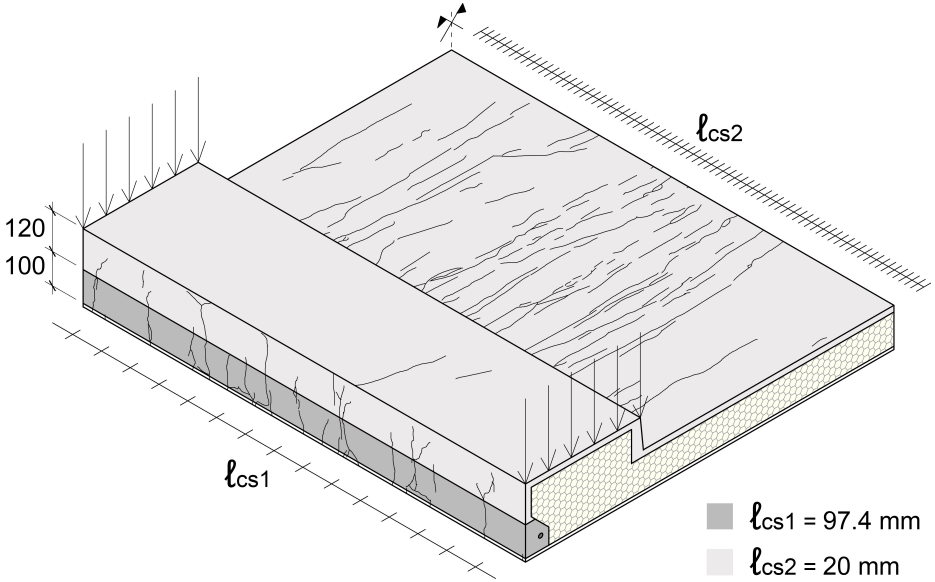

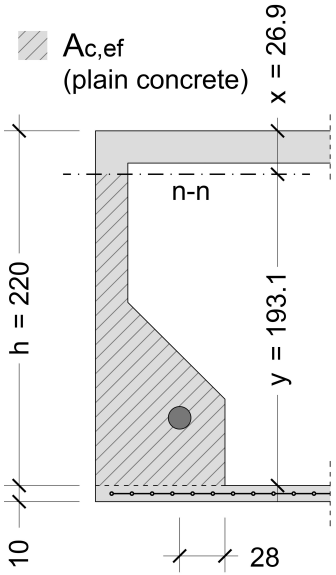

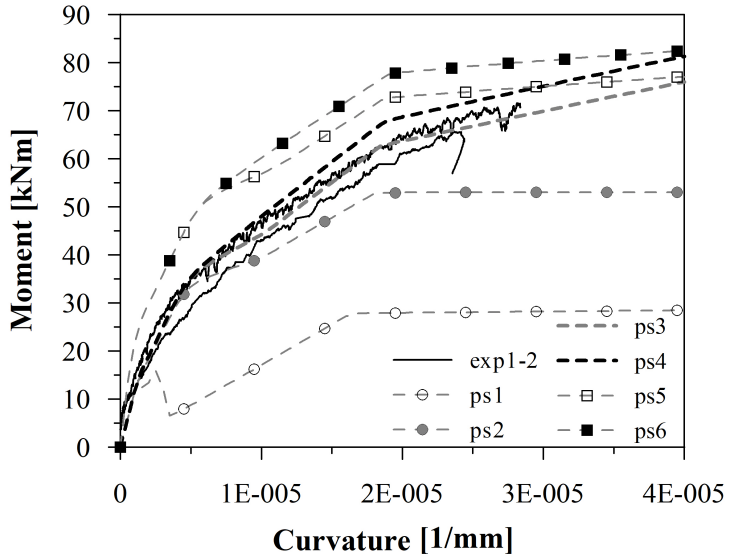

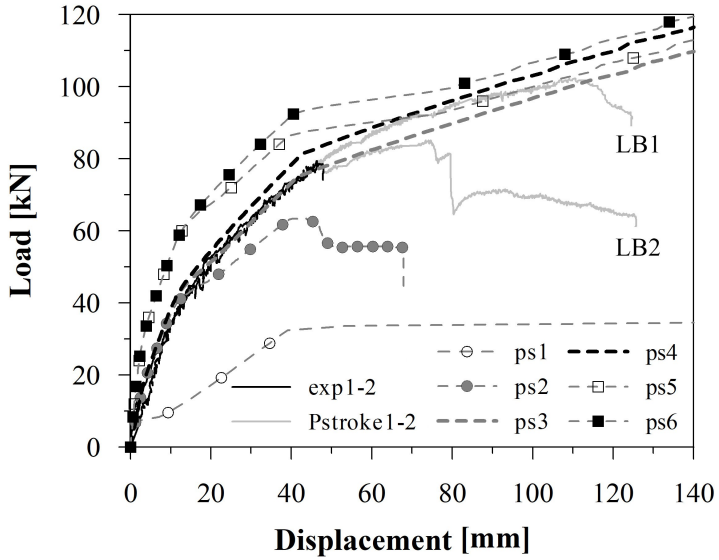

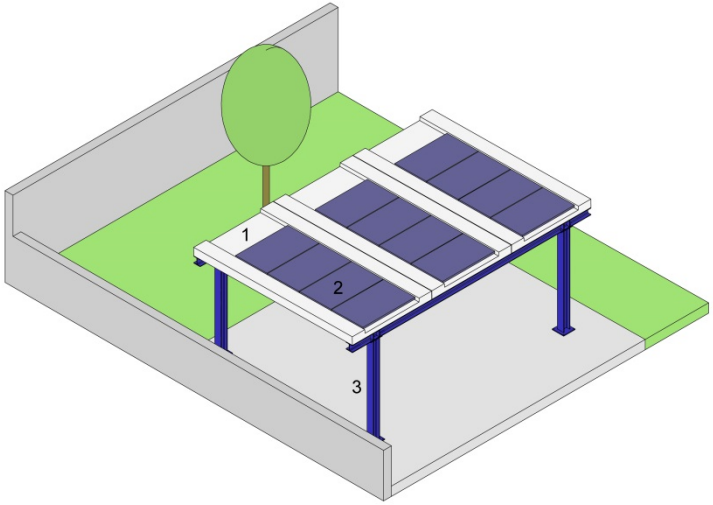

Lecco Campus

Unidirectional elevated slab: preliminary design

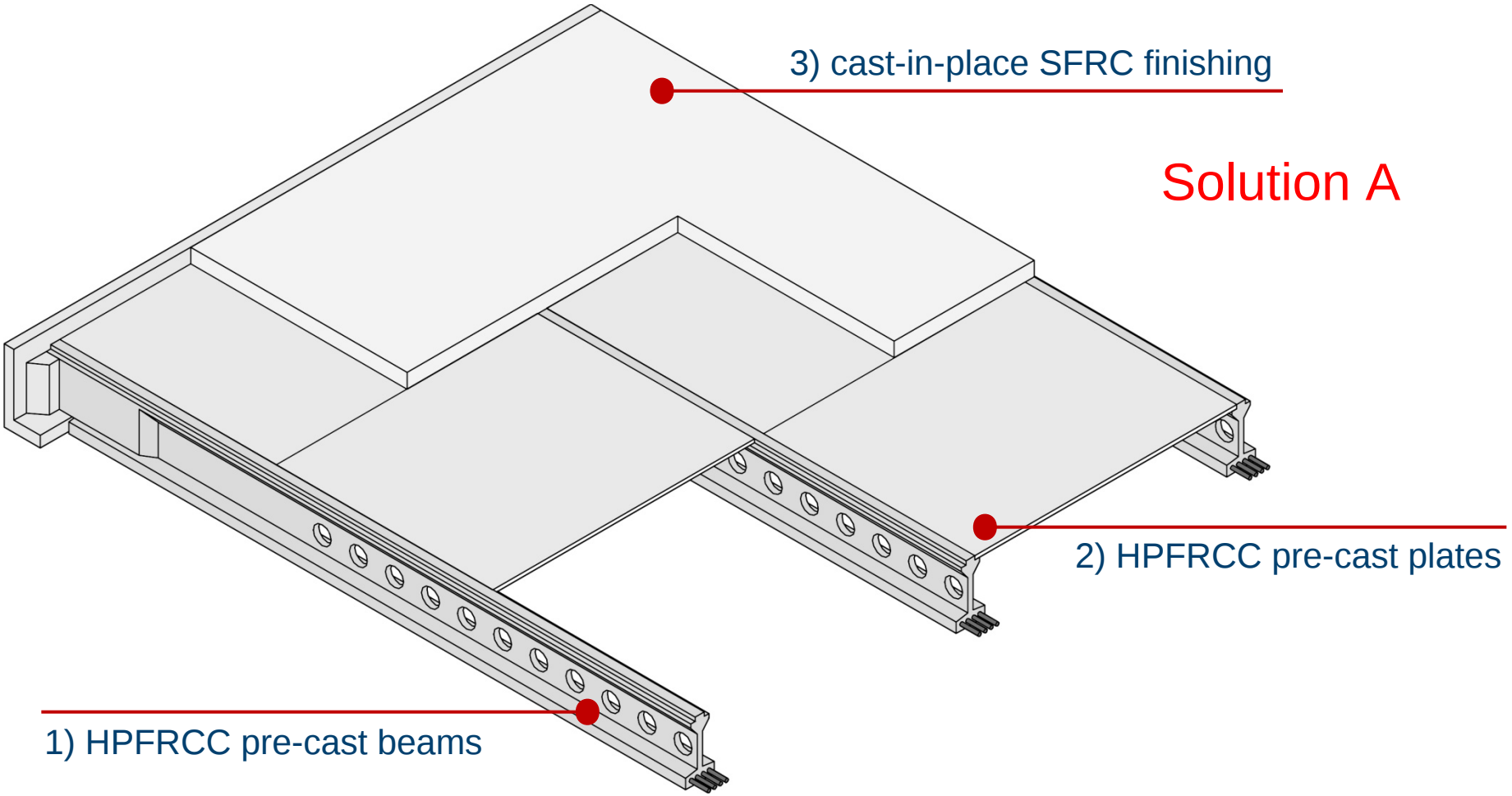

Bidirectional elevated slab: preliminary design

Live load: 4 kN/m^2
Slab spans: 7.5 m x 7.5 m

Solution B

HPFRCC pre-cast beams (shored up in the SFRC casting phase) + HPFRCC pre-cast plates (with integrated steel bars) + additional steel reinforcement + SFRC finishing casting

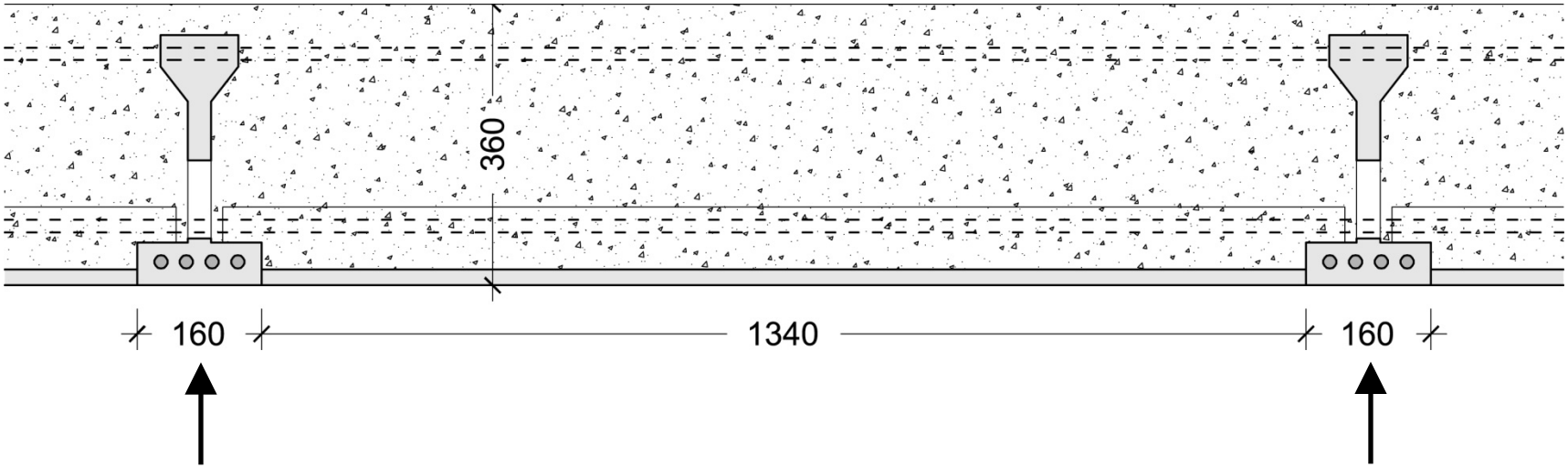

Engineering framework

Solution C

- Research project started in 2012 between Politecnico di Milano and Mangiavacchi Pedercini S.p.a. for the development of new design solutions for producing **light floors partially prefabricated**

POLITECNICO MILANO 1863

MANGIAVACCHI PEDERCINI SPA

HPFRCC beam: experimental investigation

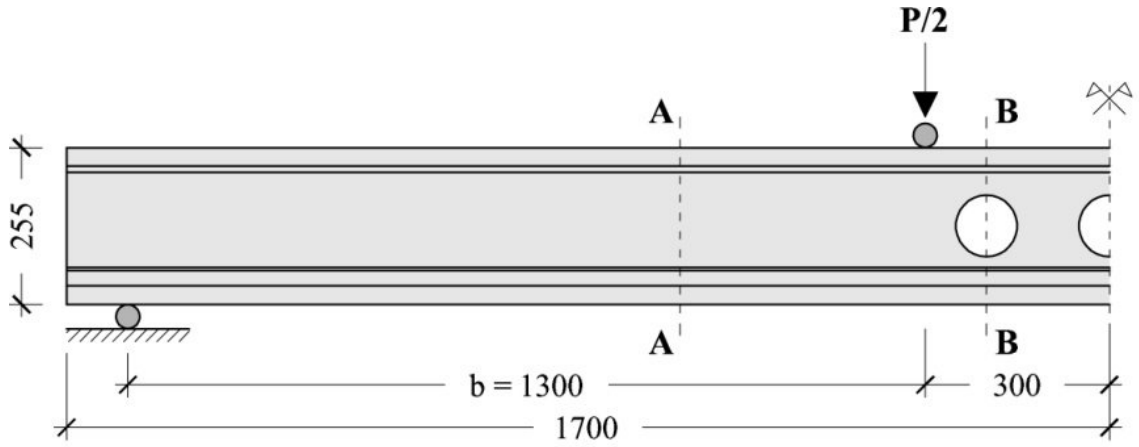

4PB tests on 3.4 m long beams

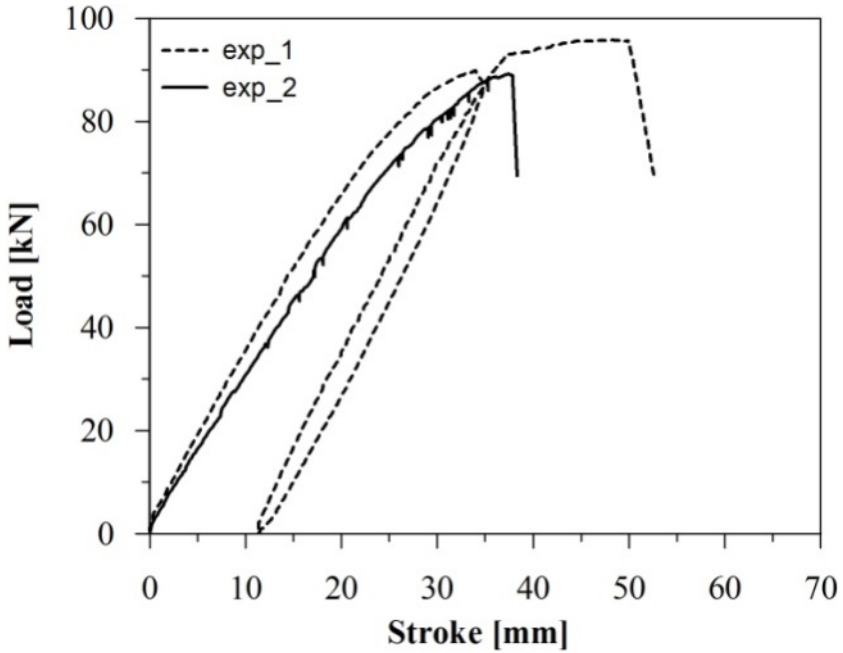

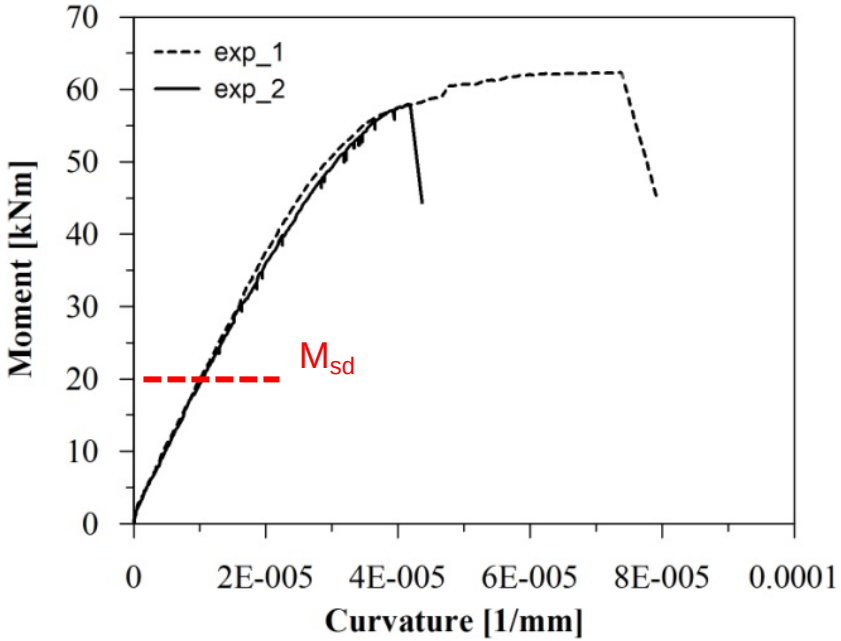

3P shear tests on 1 m long beams extracted from the ones tested in bending

without the holes in the web!

$$\chi_d = \chi_{sd} + f_{Ftud}/f_{cd} = 0.33 + 0.02 = 0.35$$

HPFRCC beam: resistance previsions

BENDING RESISTANCE: plane-section approach

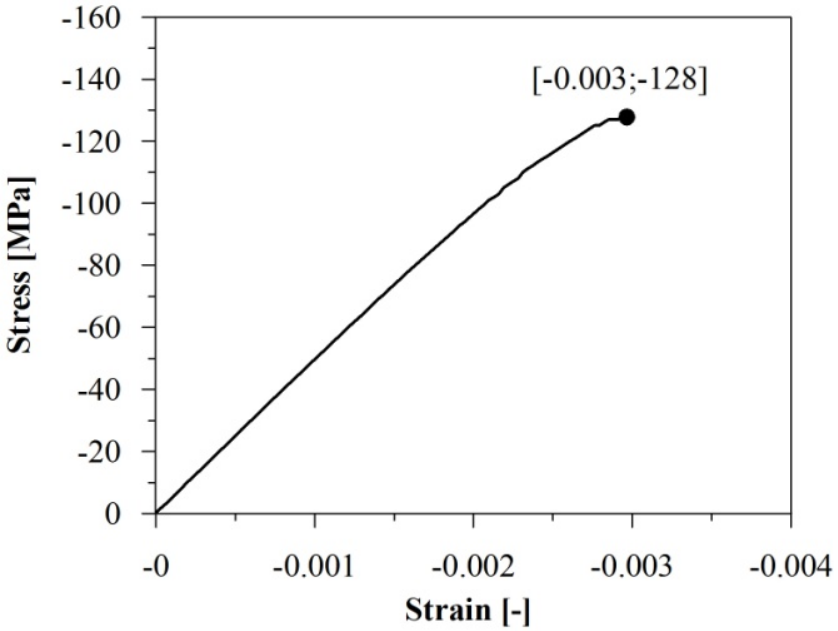

HPFRCC average law in compression

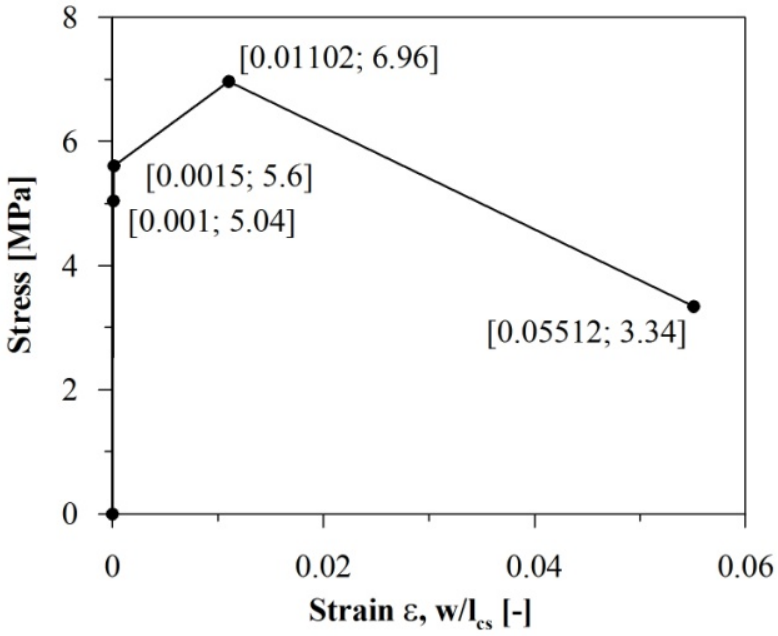

HPFRCC average law in tension

HPFRCC beam: resistance previsions

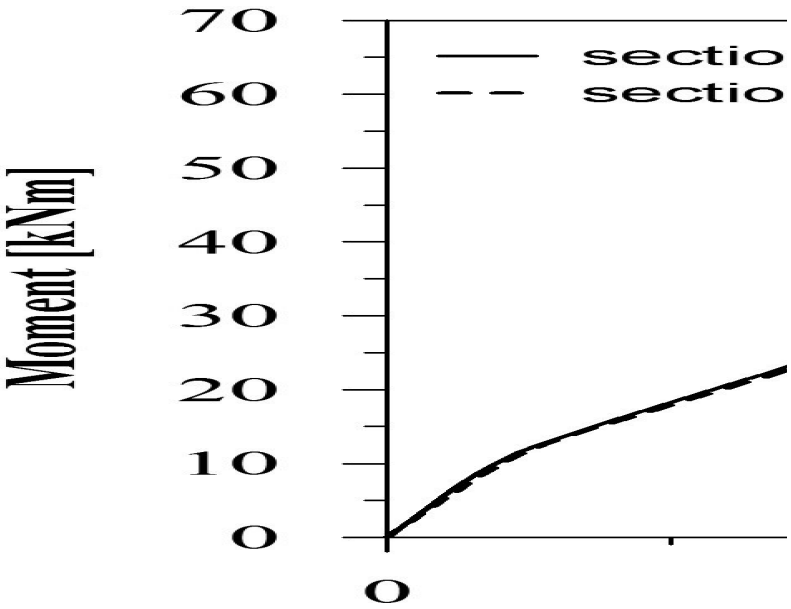

Ultimate bending moment
$M_{u,av}$ (B-B section): 64 kNm

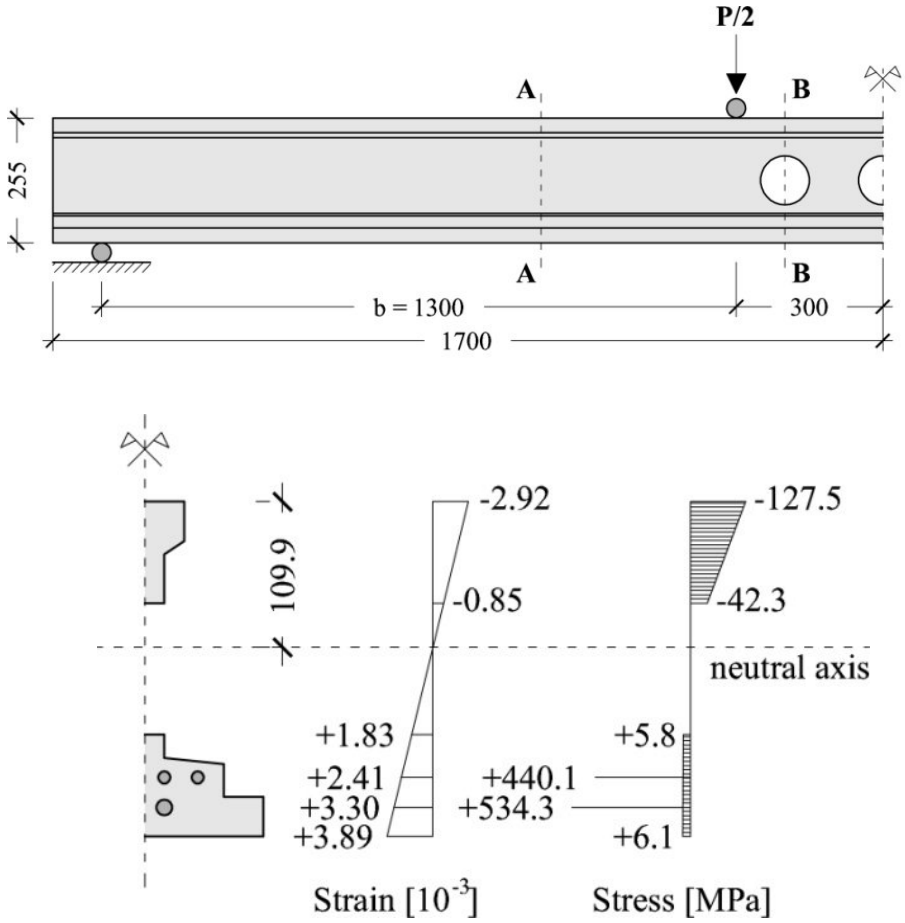

B-B ‘hole’ section
distributions at the response peak
(failure due to concrete compression)

HPFRCC beam: experimental investigation

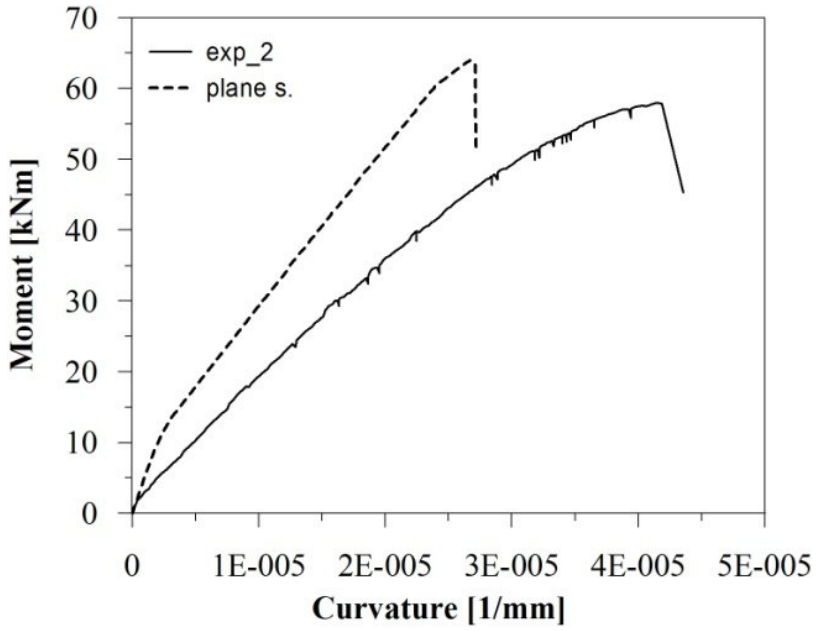

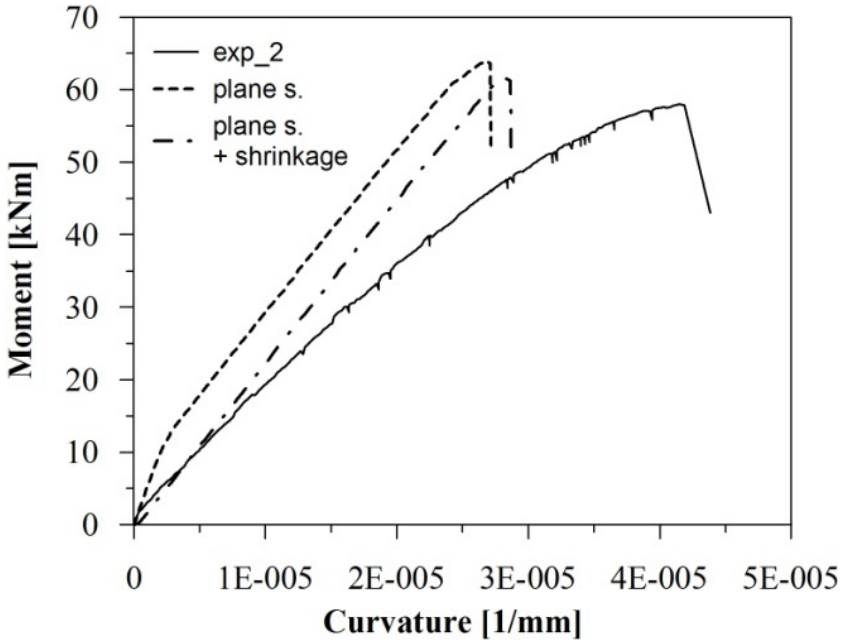

This model does not take into account shear deformability!

HPFRCC beam: resistance previsions

SHEAR RESISTANCE: Model Code 2010 formulation

$$V_{Rm} = \left\{0.18 \cdot k \cdot \left[100 \cdot \rho_l \cdot \left(1 + 7.5 \cdot \frac{f_{Ftu}}{f_{ct}}\right) \cdot f_{cm}\right]^{1/3}\right\} \cdot b_w \cdot d$$

f_{Ftum} (w = 1.5mm) = 5.15 MPa

Av. shear resistance

V_{Rm} = 48.1 kN

Specimen	P_{max} [kN]
1A	99.20
1B	77.68
2A	74.16
2B	66.47

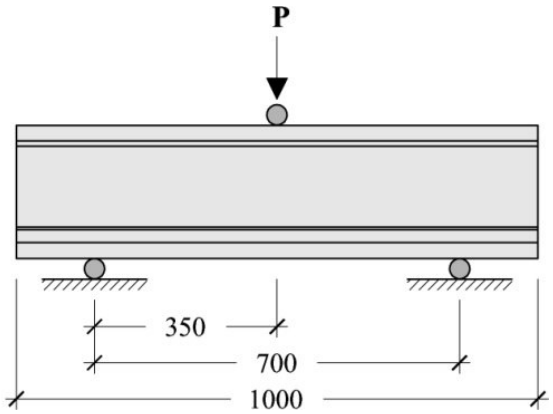

V_{sd} = 13.8 kN

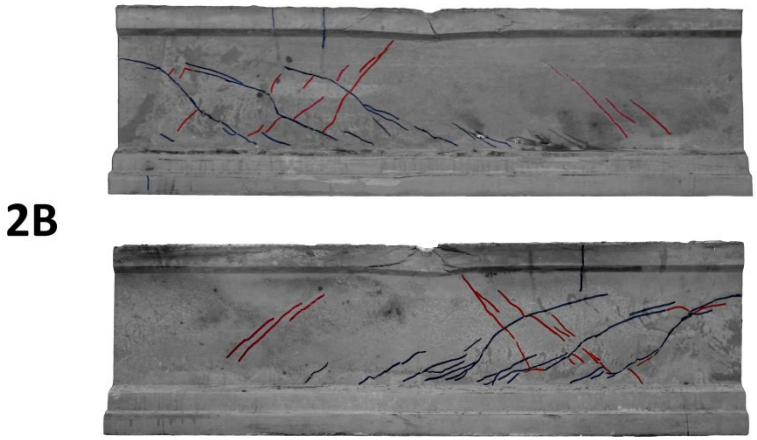

Disposable formwork evolution

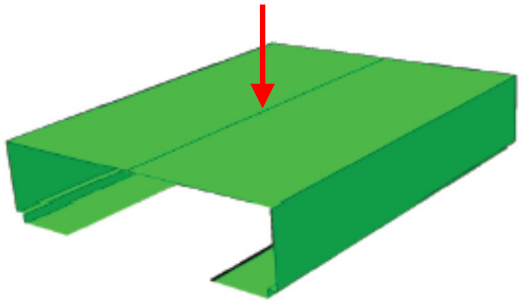

- too-high central deflections

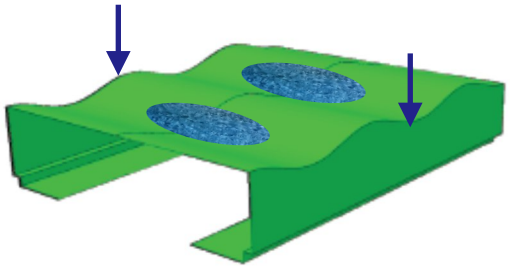

- water accumulations
- right angles between decking and joist web

- definitive geometry

TRC Characterization (6)

Bending tests (4PB) – comparisons and observations

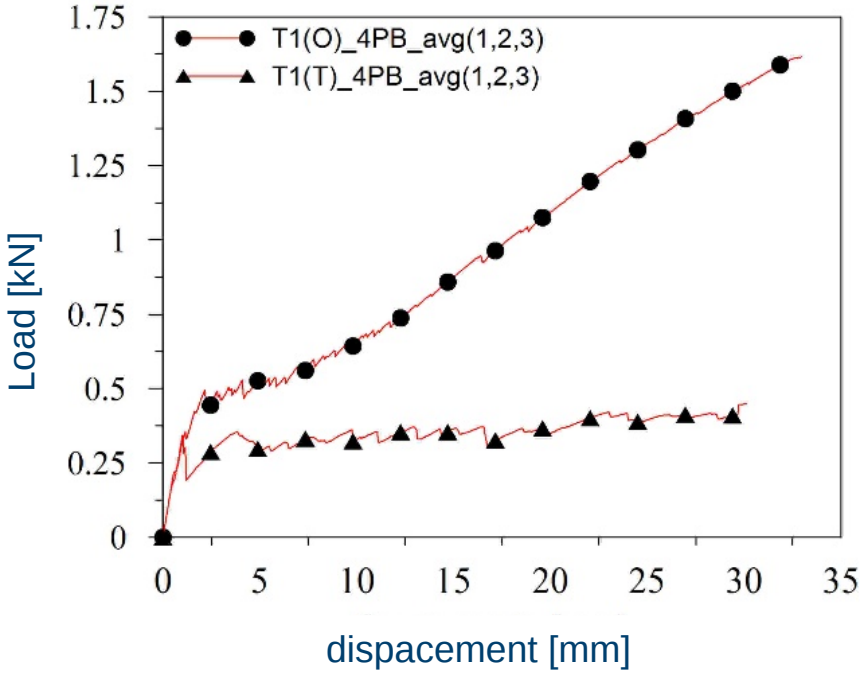

warp

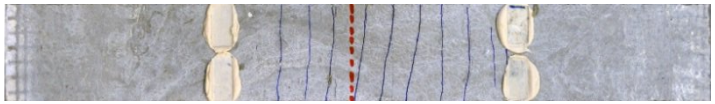

weft

Full-size tests (2)

Concentrated load applied to the centre (2)

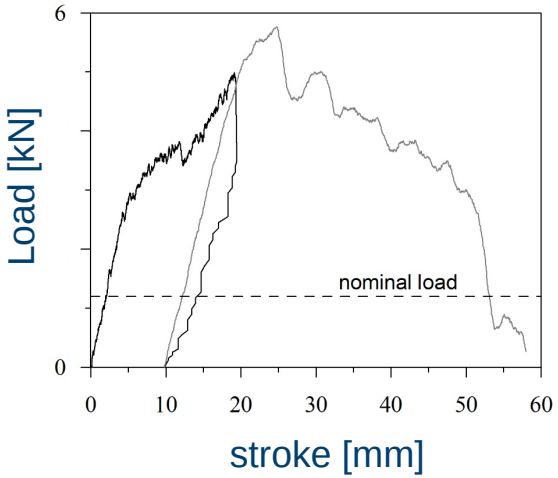

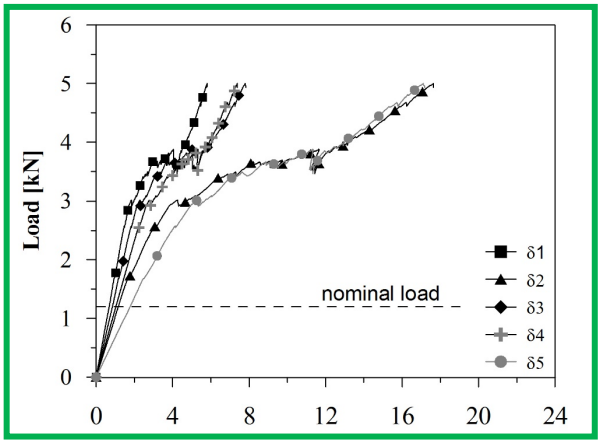

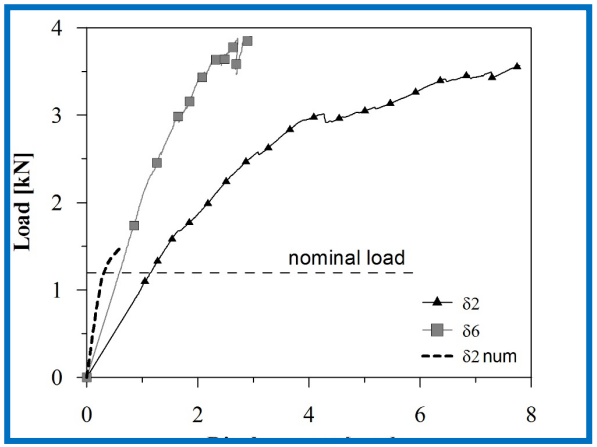

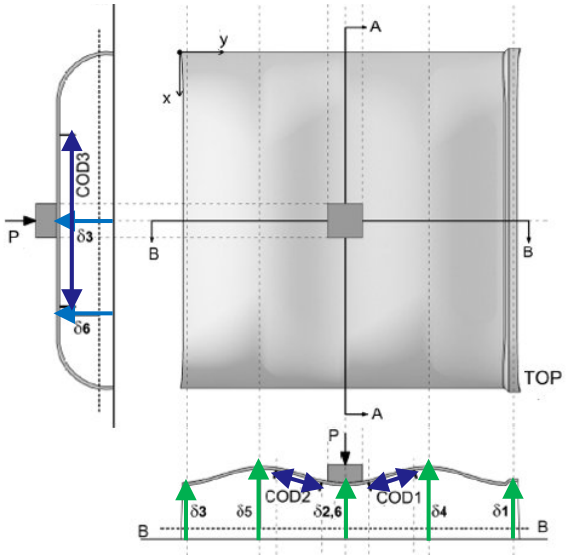

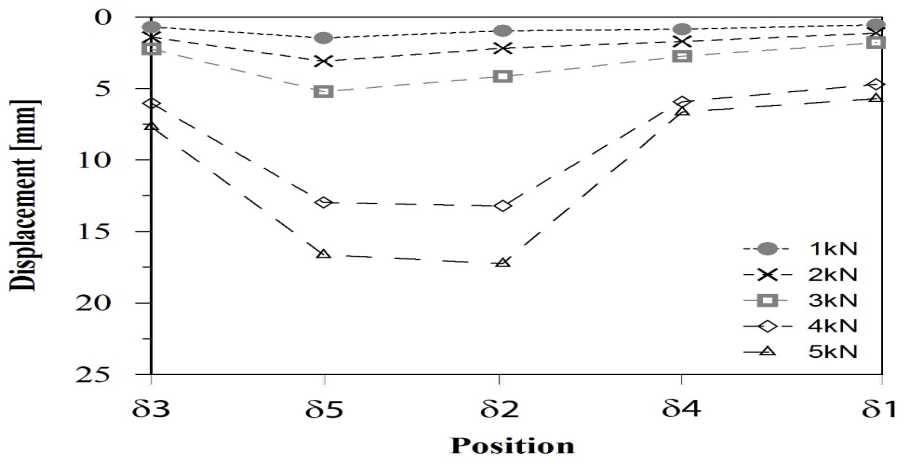

Full-size tests (5)

Concentrated load applied to the border (2)

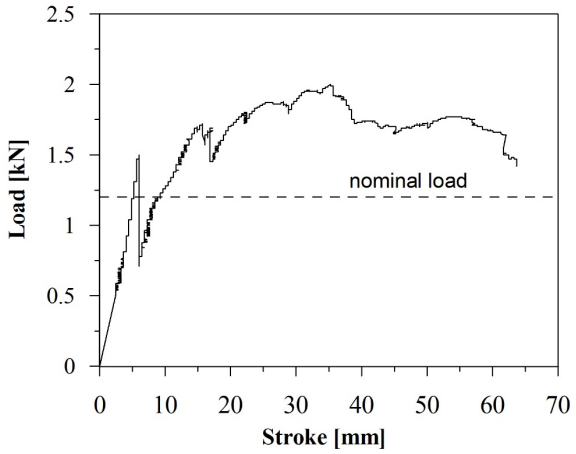

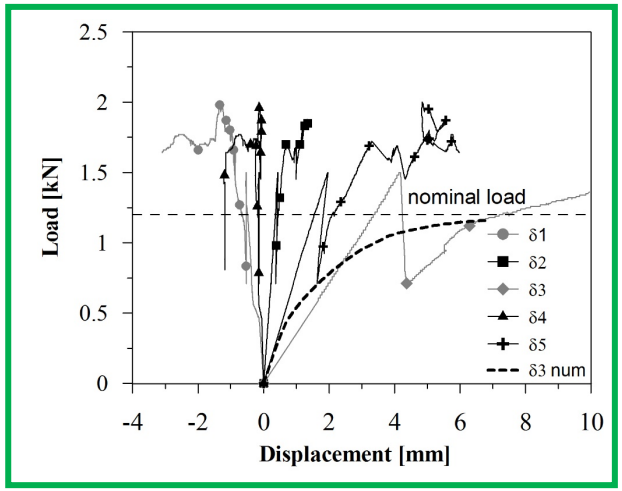

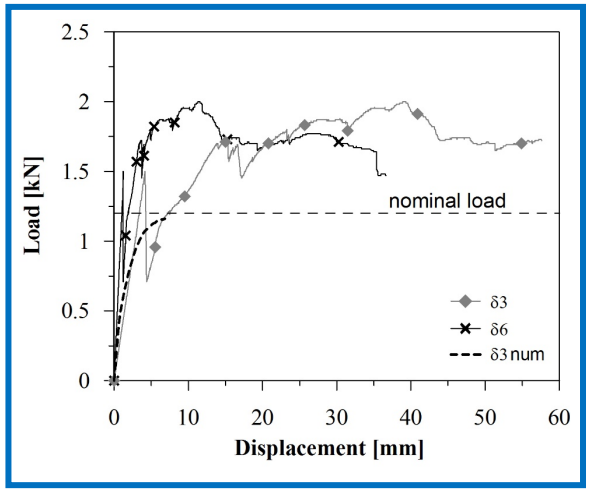

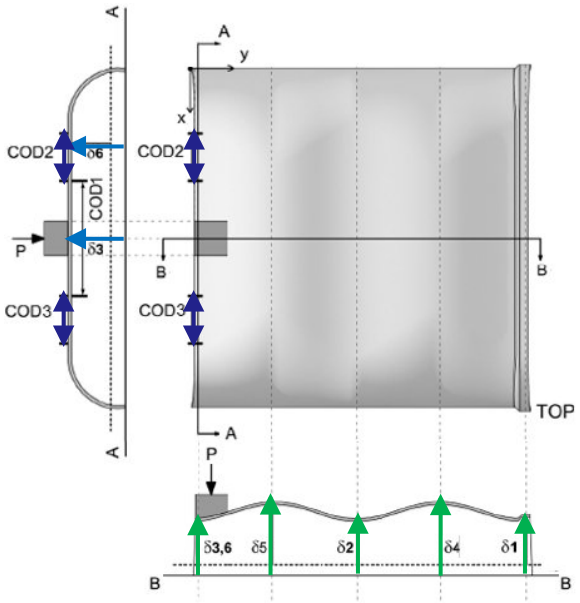

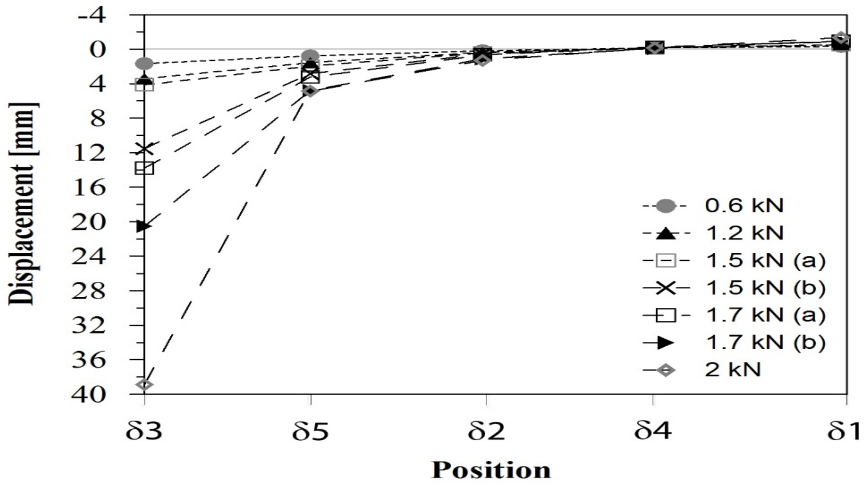

Tests end

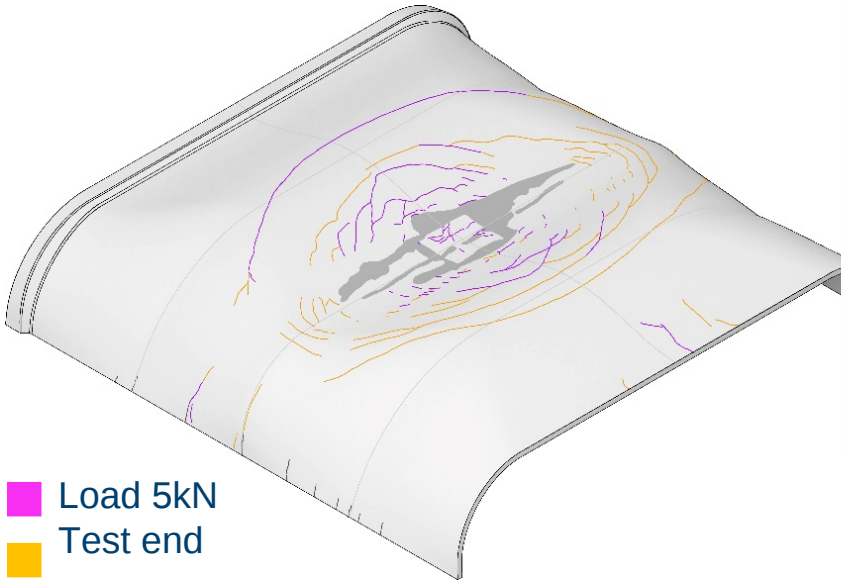

Load 5kN
Test end

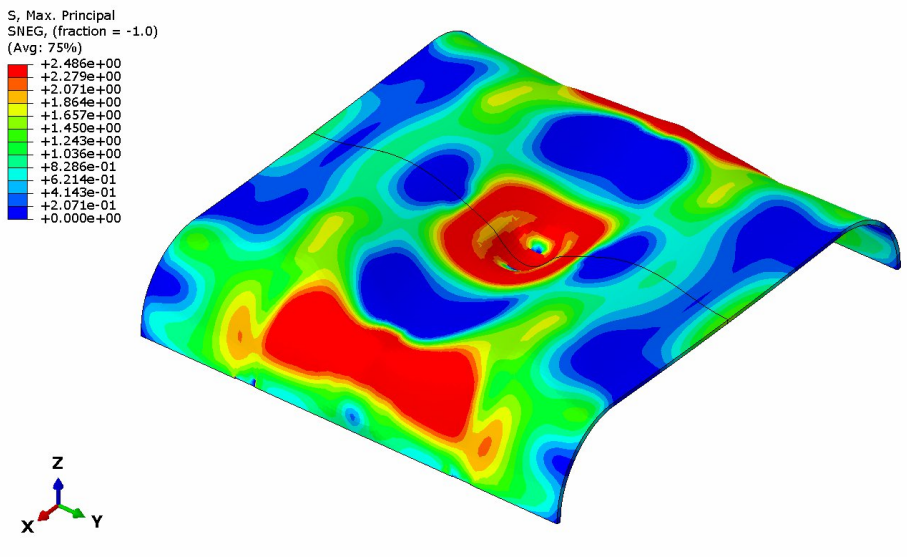

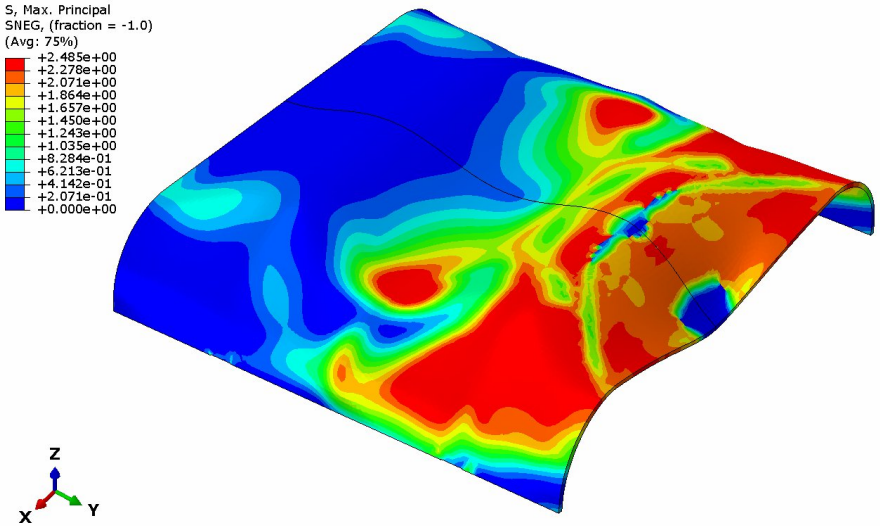

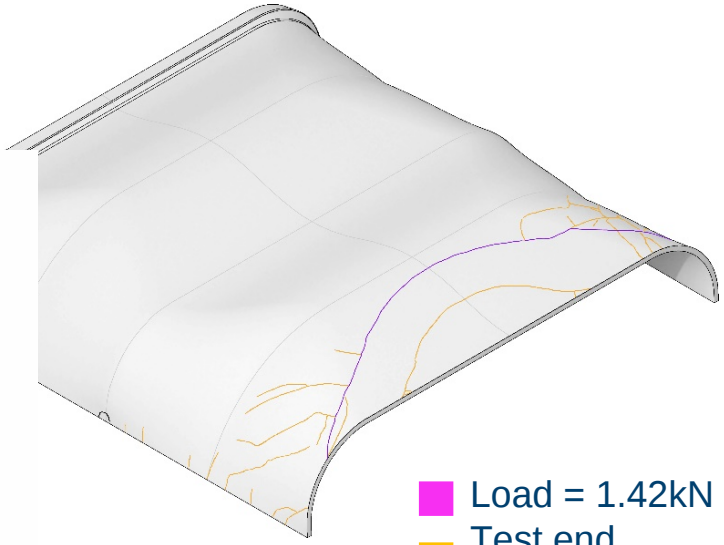

Load = 1.42kN
Test end

Characterization and optimization of FRCM composite systems

Effect of addition of dispersed short fibers (1% fraction volume)

Fibers:

- High Alkali resistance **PVA** fibers
  Φ 0.16-0.24 mm, l 18mm, aspect ratio 90
  yield strength 790-1160 MPa
- Straight high-carbon **steel** microfibers
  Φ 0.21mm, l 13mm, aspect ratio 62
  tensile strength 2750 MPa

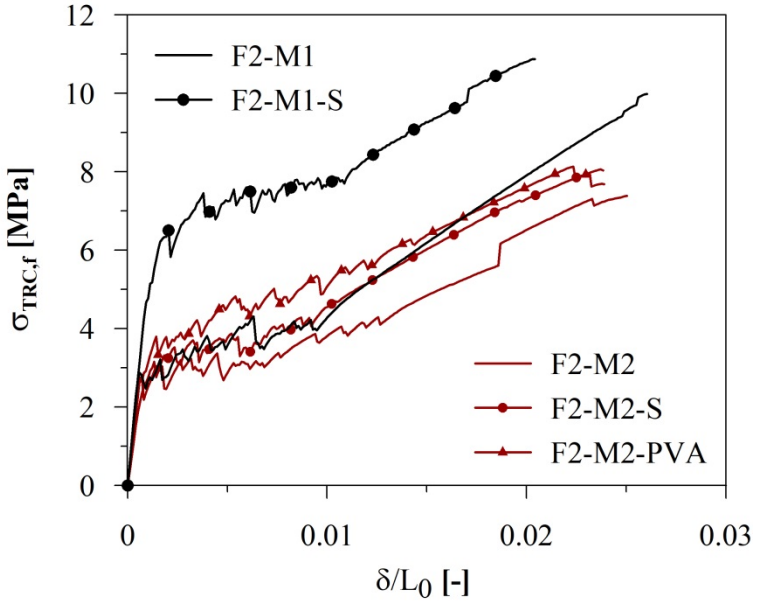

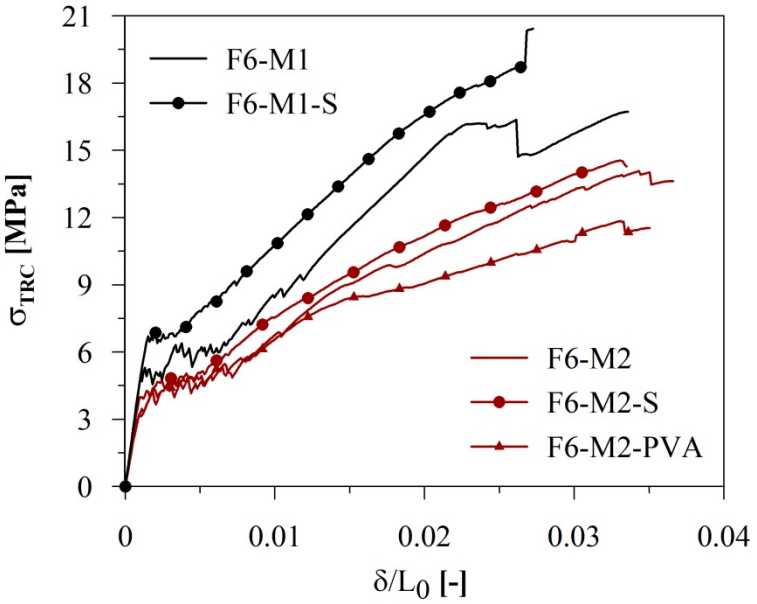

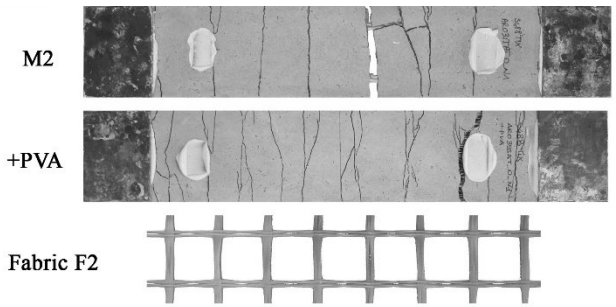

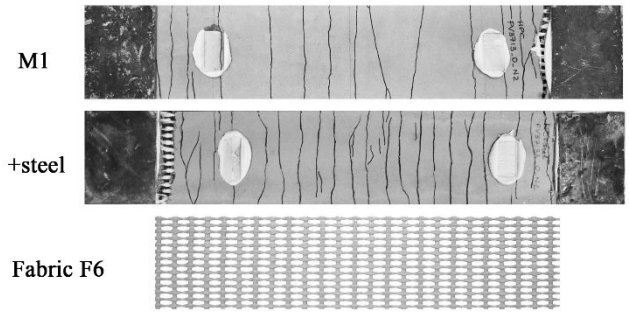

Bond-slip characterization: single lap shear tests

(30 specimens, 4 fabrics, 3 matrices, 2 types of fibers)

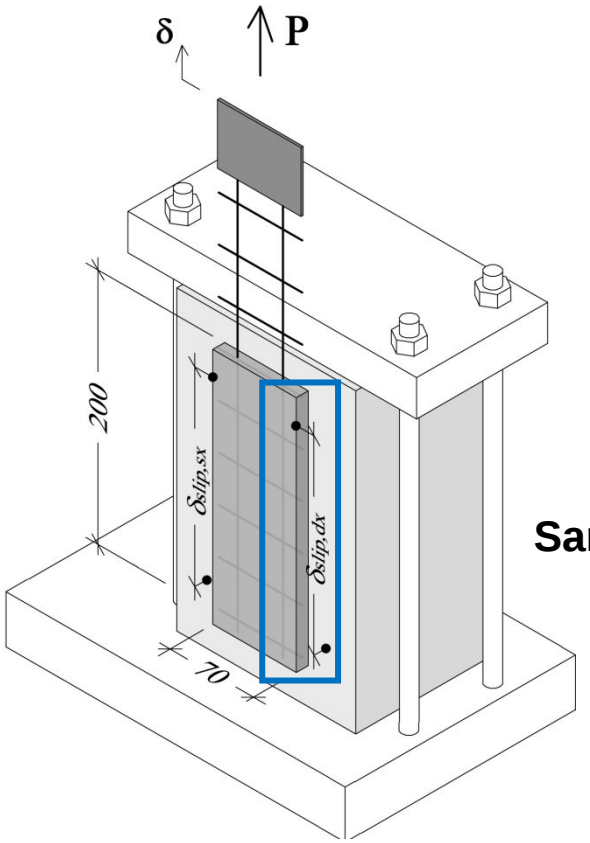

Concrete substrate:

- cement-based mortar;
- surface machining:
  - hydro-scarification **(A1)**
  - sandblasting **(A2)**

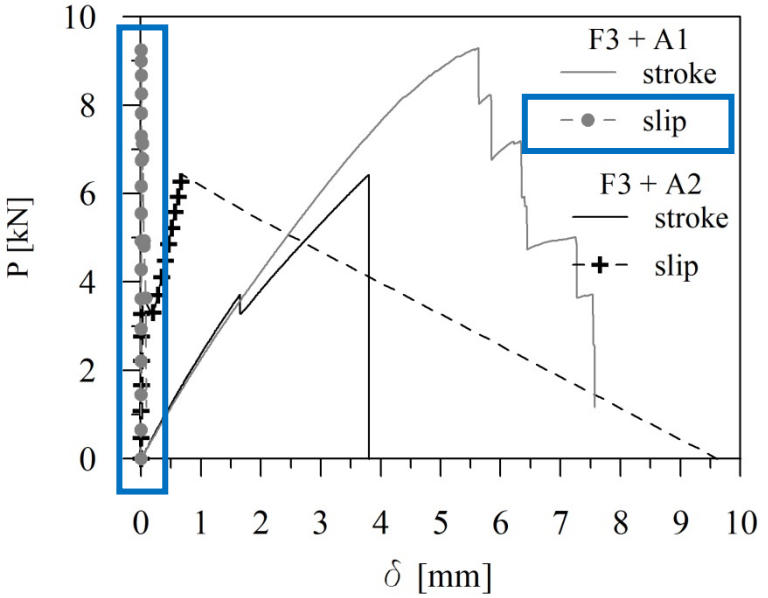

Sand-blasted substrate:

- cement-based mortar **(M2)**
- polimer-modified mortar **(M4)**

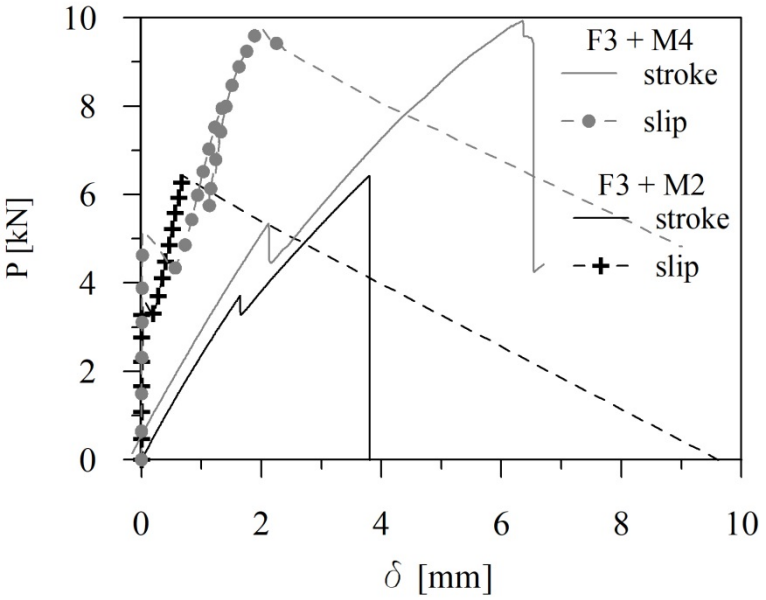

significant role of the roughness on the overall response

Bond-slip characterization: roughness analysis

Laser measurement setup

Positioning of the specimen

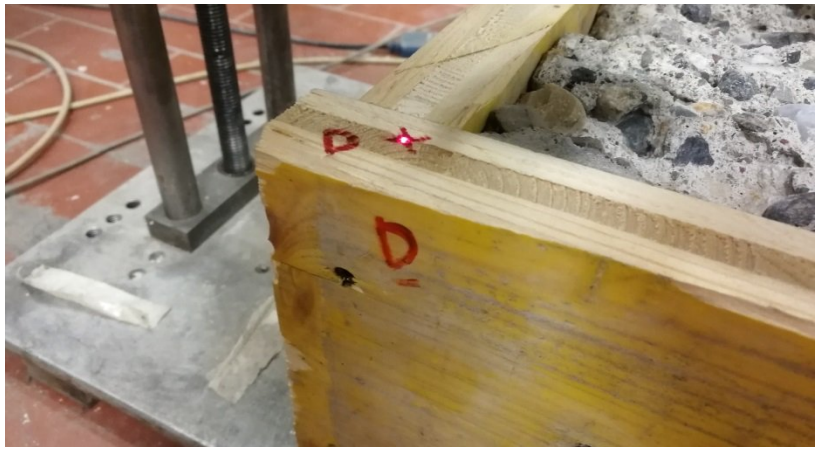

Specimen	Hydro-scarification pressure [atm]
1A-1B	200
2A-2B	500
3A-3B	1000
4A-4B	1500
5A-5B	2000**

Roughness measurements

Bond-slip characterization: roughness analysis

2B surface: 500 atm of water pressure

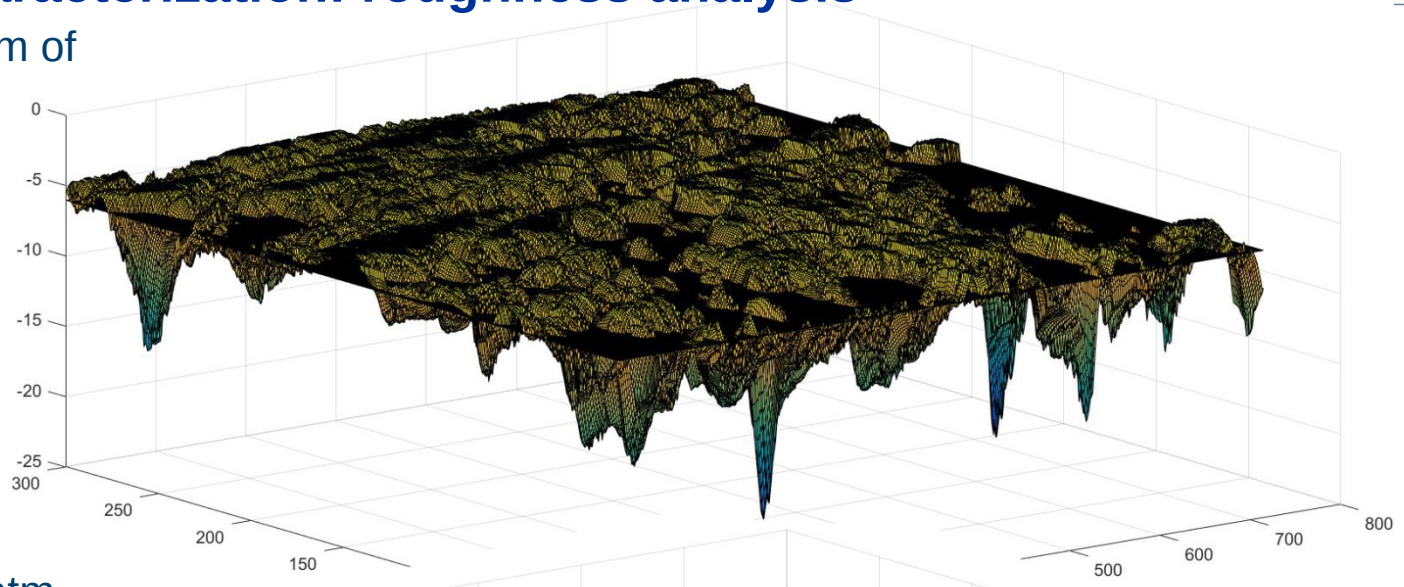

5A surface: 2000 atm water pressure

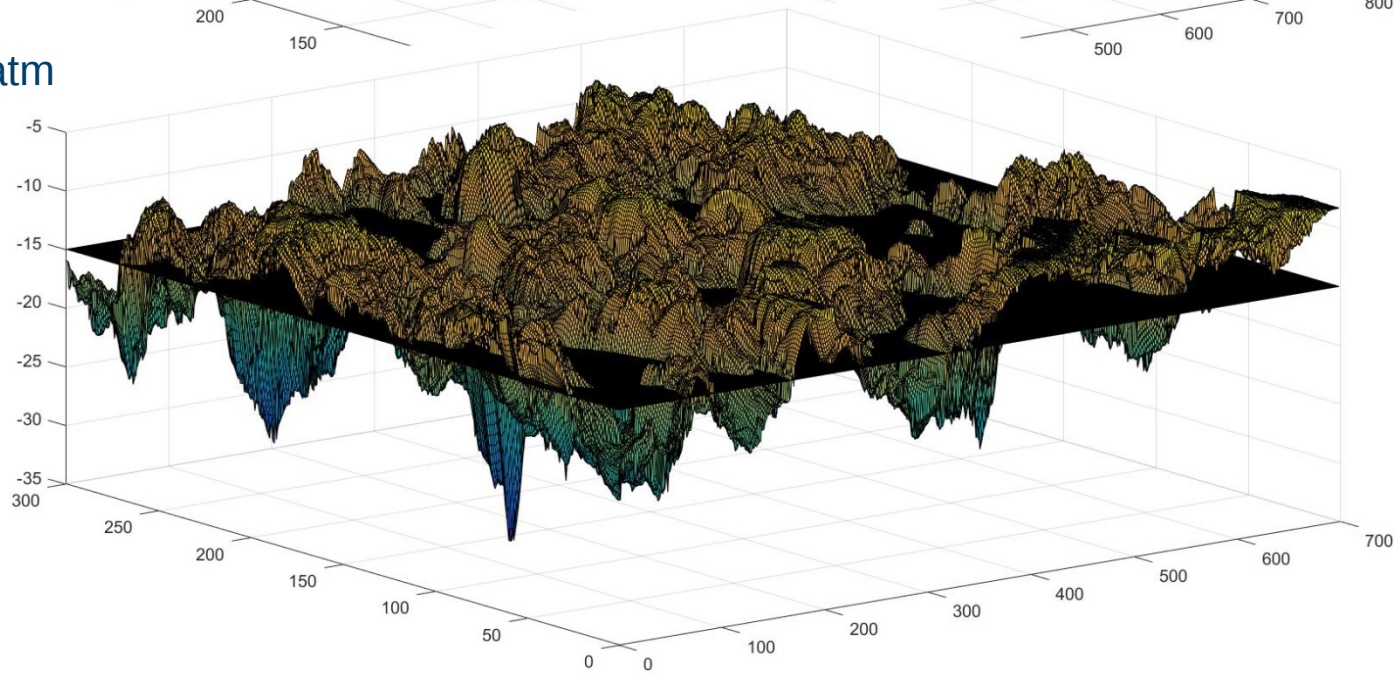

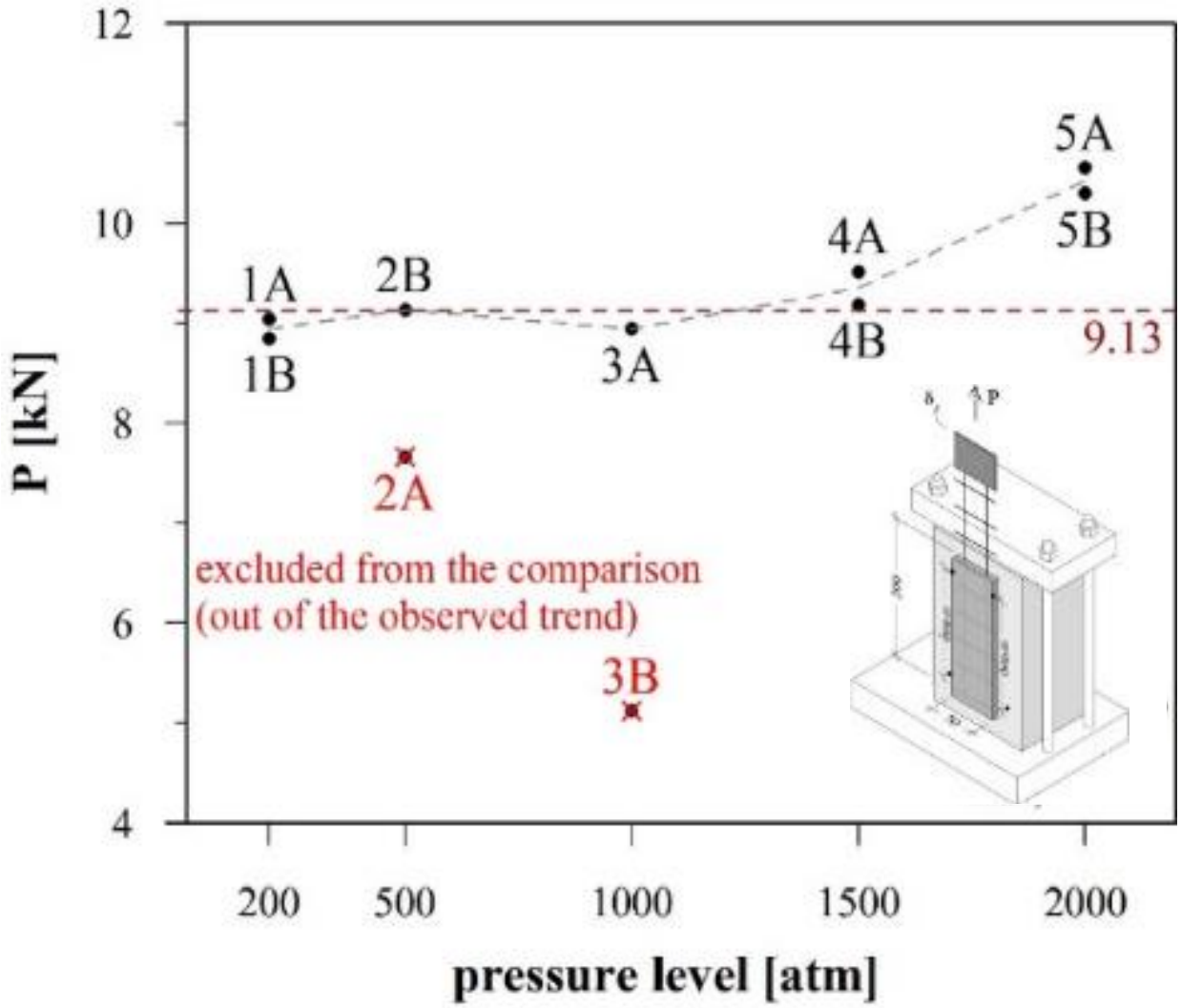
12
10
8
6
4
P [kN]
200
500
1000
1500
2000
pressure level [atm]
1A
1B
2B
2A
3A
3B
4A
4B
5A
5B
9.13
excluded from the comparison
(out of the observed trend)

DEWS technique

di Prisco et al. 2010

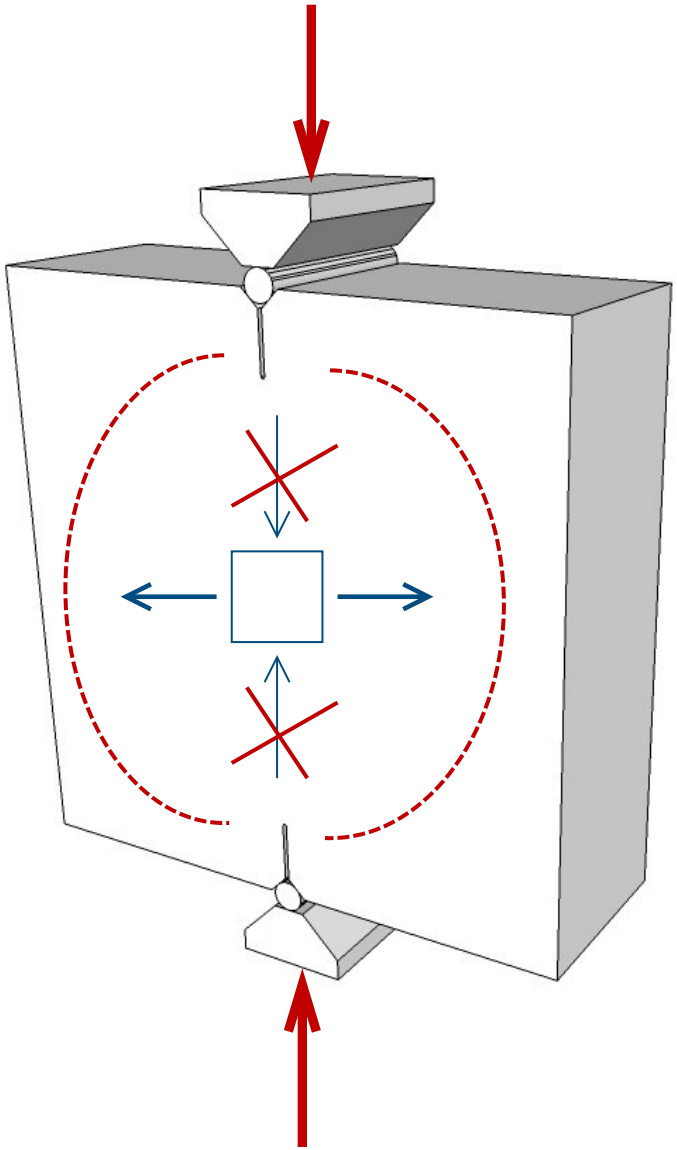

Specimen loaded in pure tension without any crosswise compressive stresses.

WEDGE SPLITTING TEST

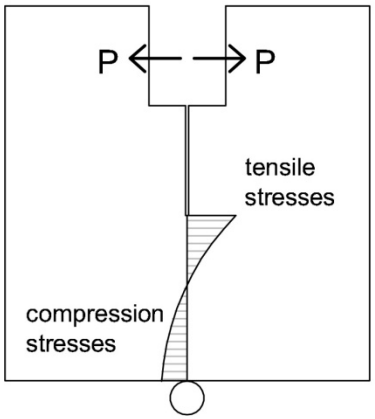

BRAZILIAN TEST

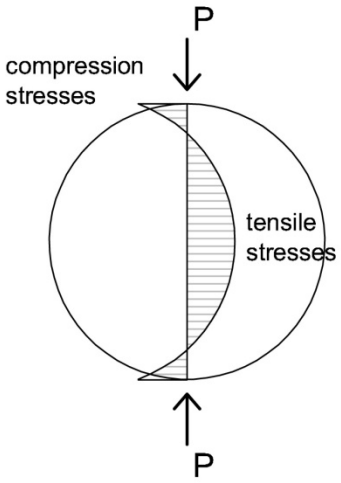

DEWS TEST

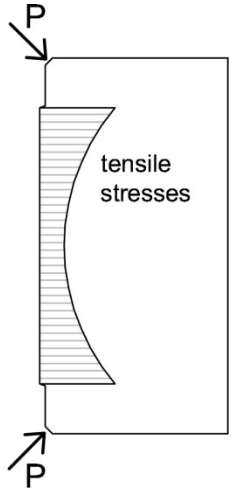

A. Magri, PhD thesis 2012

DEWS TEST

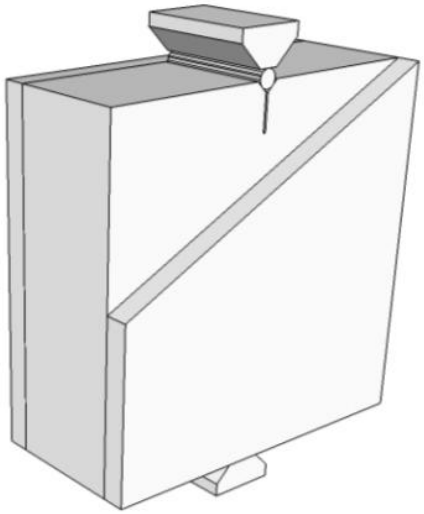

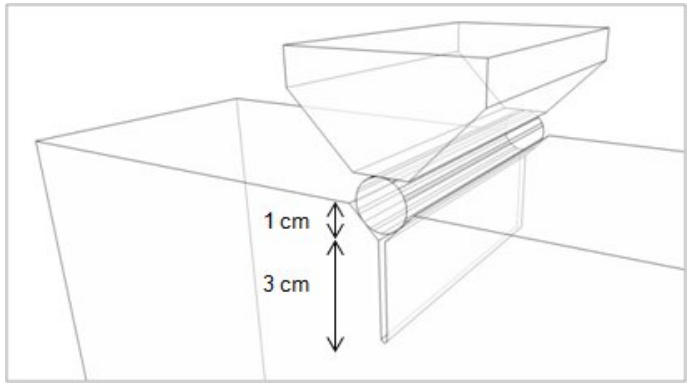

W = 0 mm

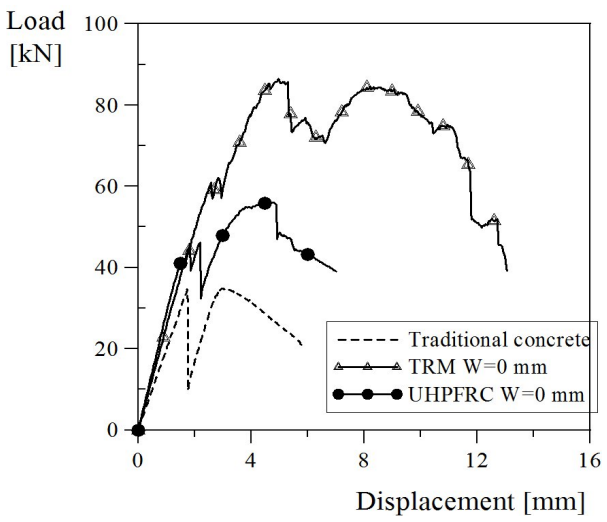

W = 0.3 mm

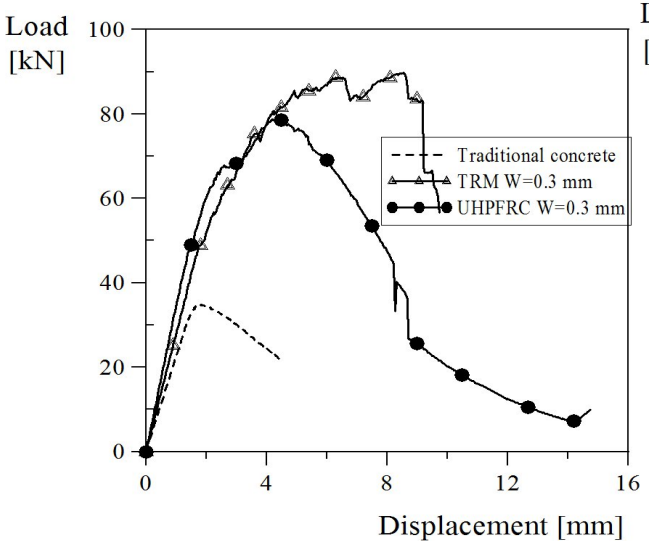

W = 3 mm

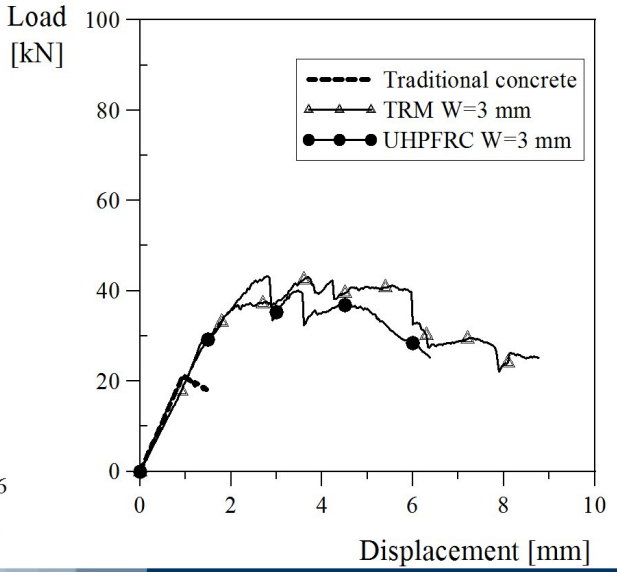

DEWS - TRC failure mechanism

Multicracking phenomenon guaranteed by the AR glass fabric.

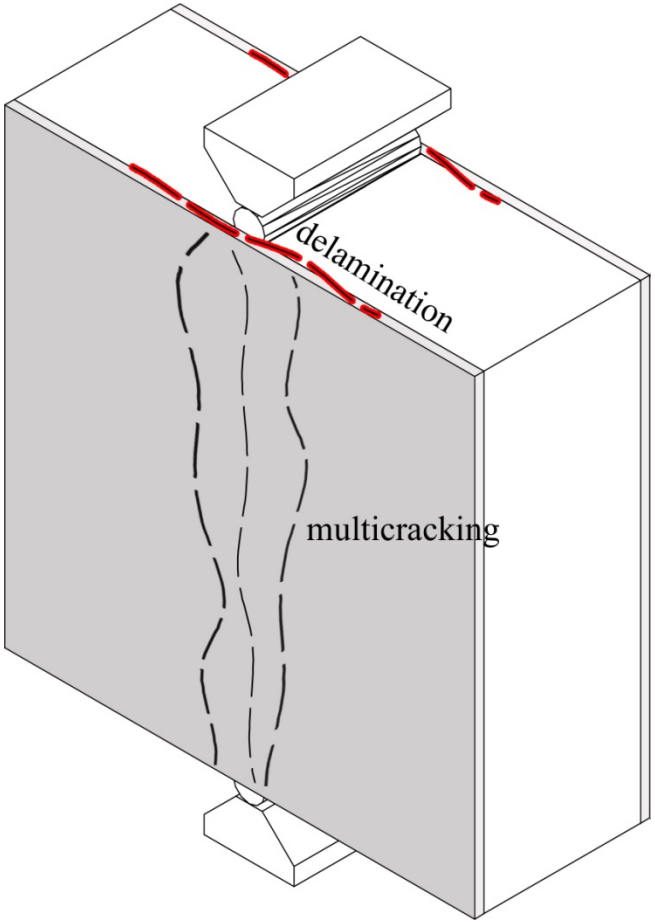

Detachment of matrix pieces

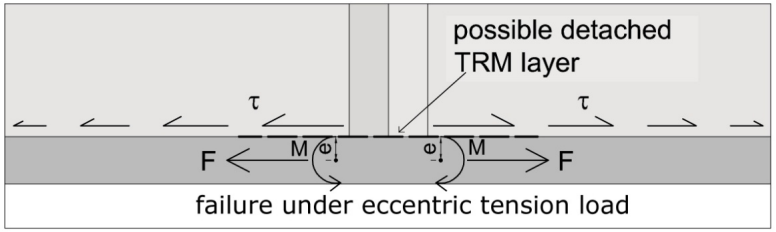

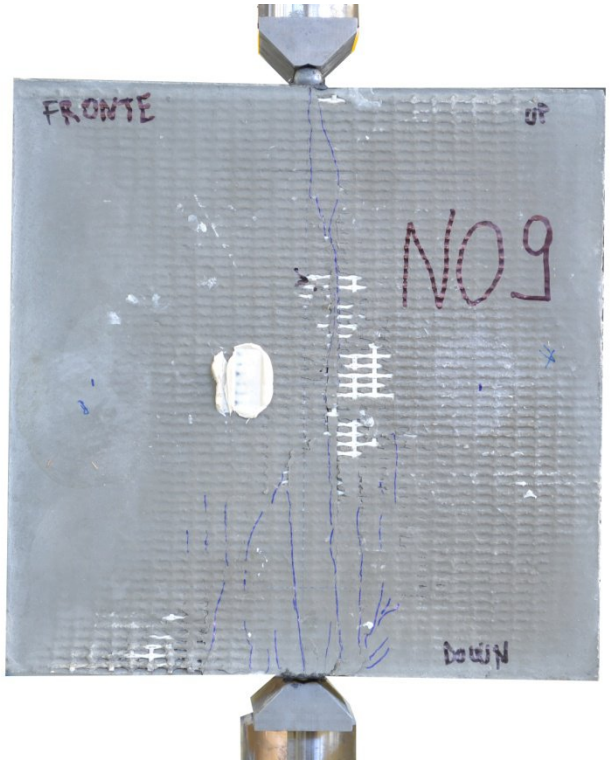

Double Edge Wedge Splitting test (DEWS): test preparation

Pre-cracking tests

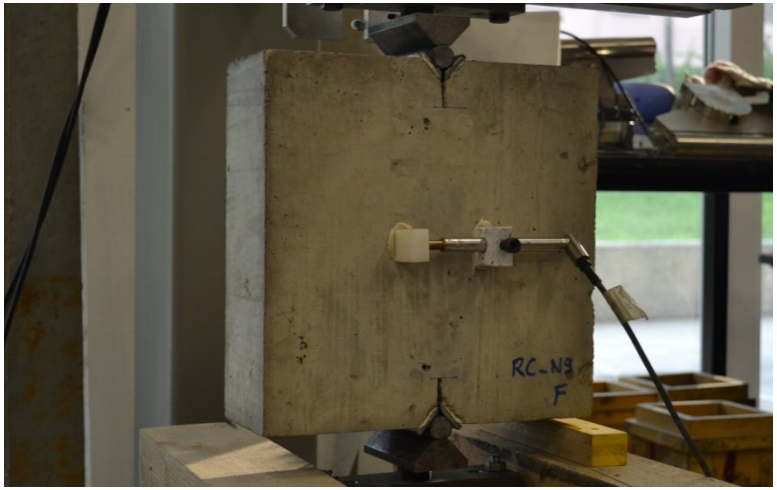

FRCM application (variable orientation)

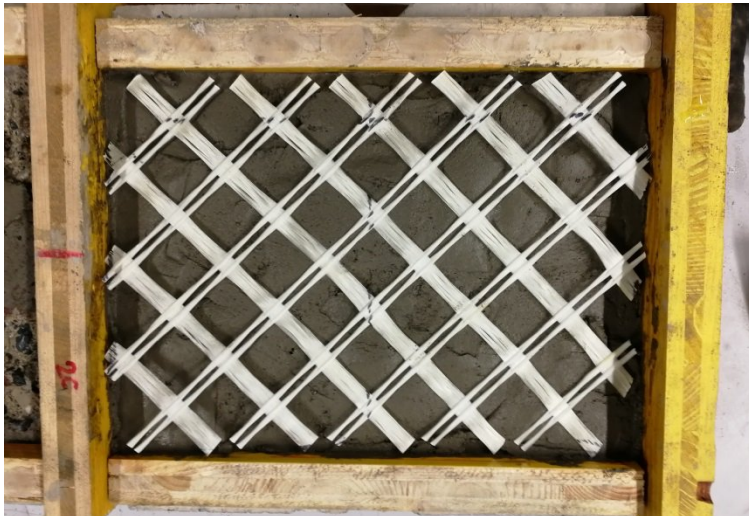

Retrofitted specimen

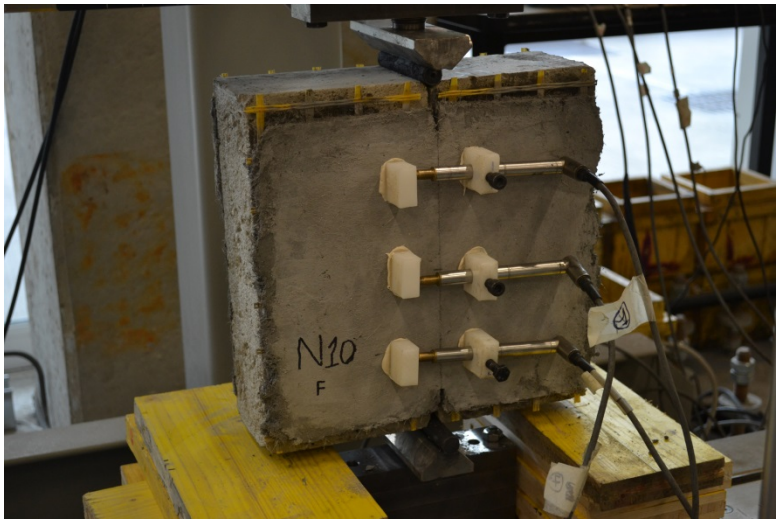

Ultrasonic measurements

Investigated RC elements:

Beams and slabs (out-of-plane loads)

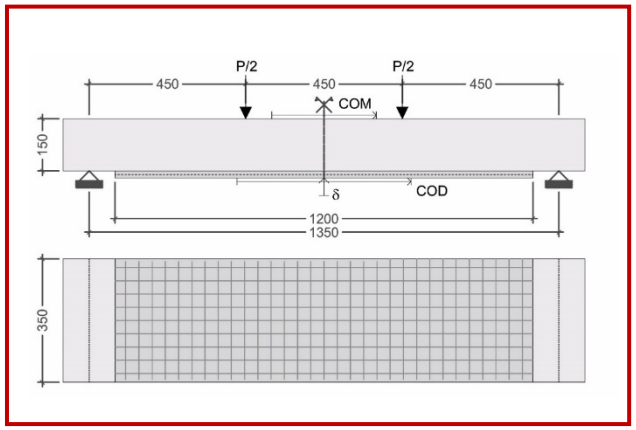

Presented at Ferro13

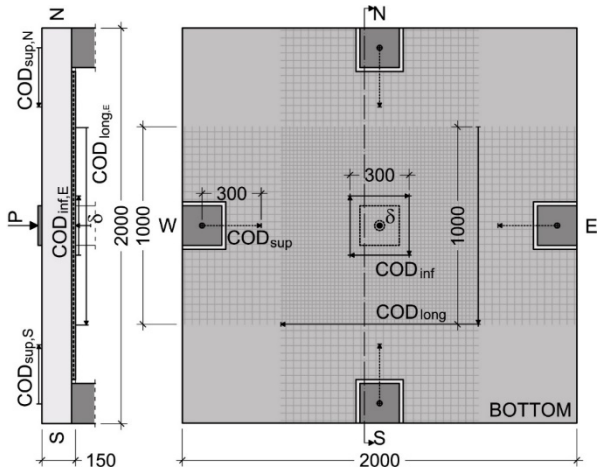

Coupling beams (in-plane loads)

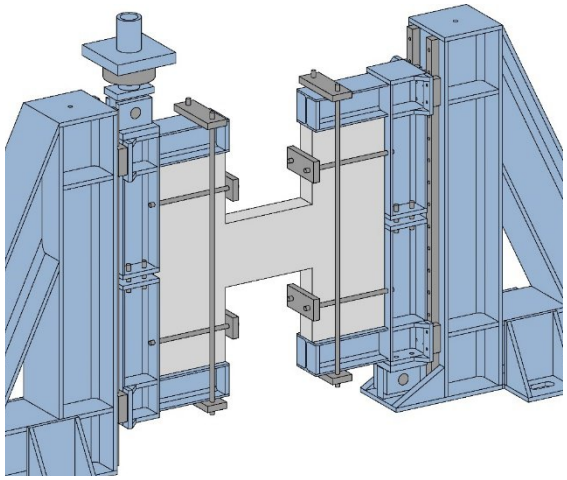

General procedure to assess the FRCM strengthening potential:

A) Preliminary steps:

Material level → FRCM to substrate interface → Meso-scale level

B) Structural elements investigation:

Full-scale tests → Interpretation of the results by means of simplified and numerical analyses → Design reccomendations and tools

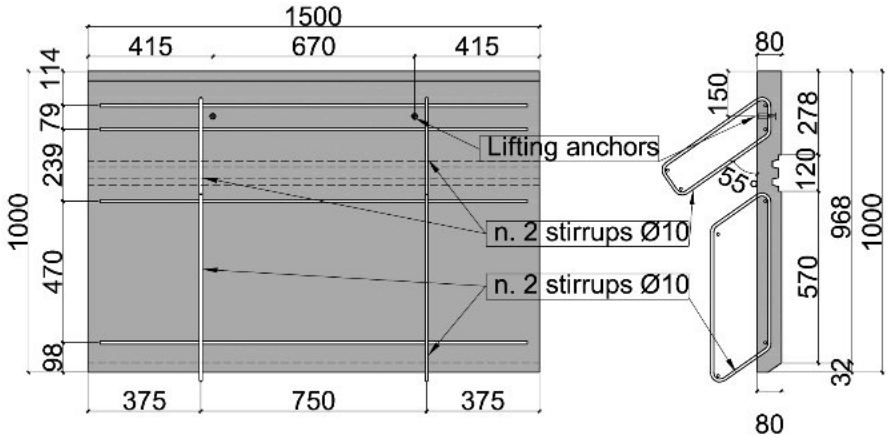

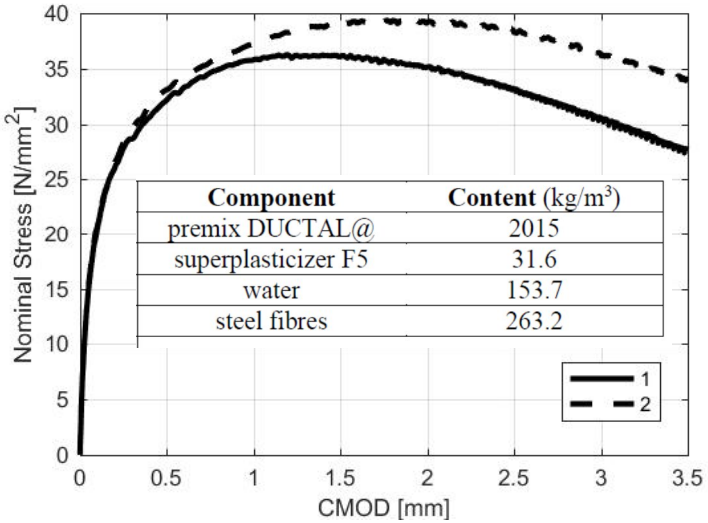

Component	Content (kg/m³)
premix DUCTAL@	2015
superplasticizer F5	31.6
water	153.7
steel fibres	263.2

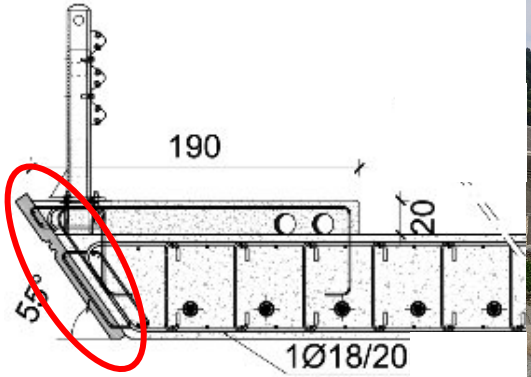

UHPFRC to strengthen half-joints

Research in progress …

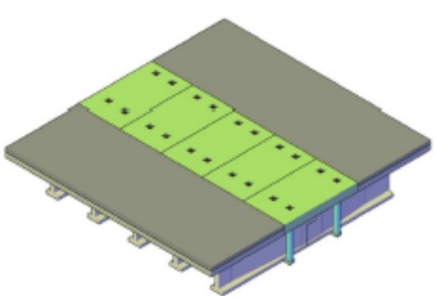

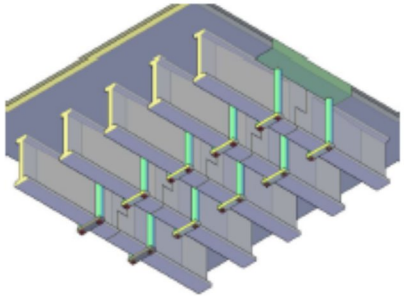

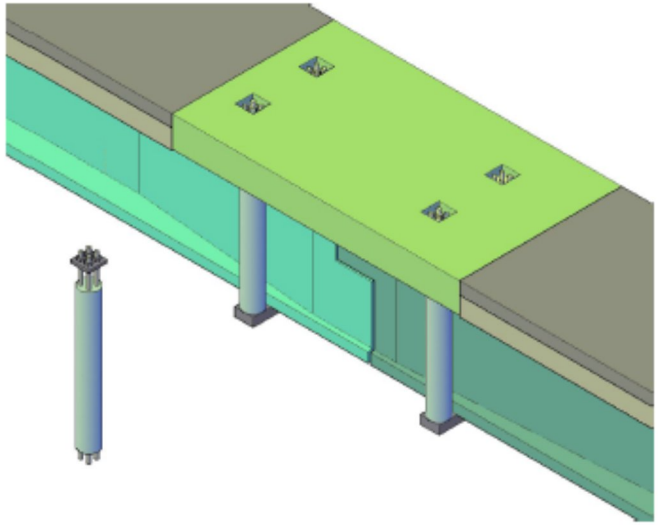

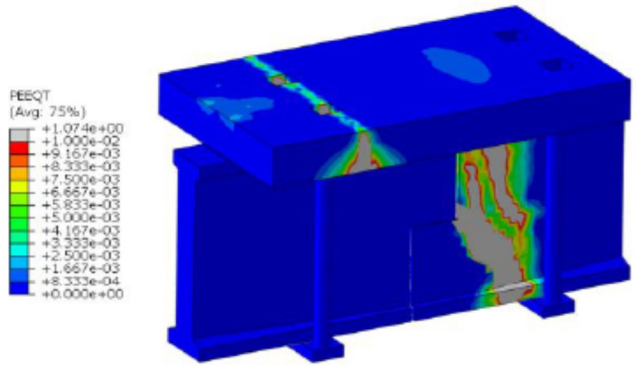

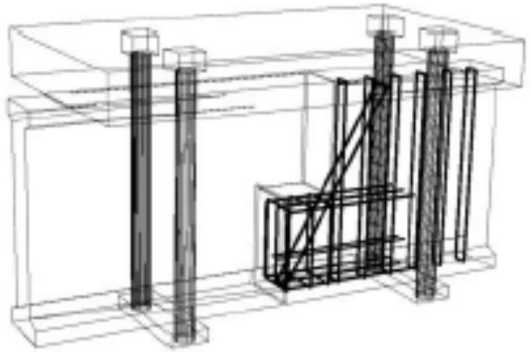

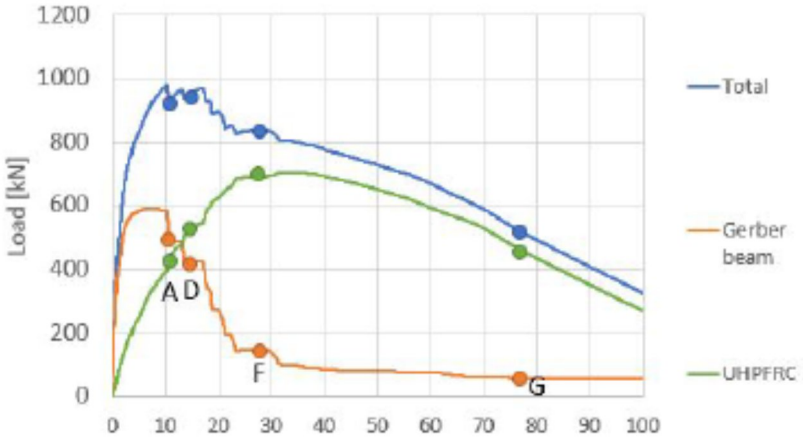

RESEARCH FRAMEWORK

POLITECNICO MILANO

A.C.C.I.DE.N.T

Funded by INTERREG

INTERREG
ITALIA-SVIZZERA ITALIE-SUISSE ITALIEN-SCHWEIZ

Advanced **C**ementitious **C**omposites **I**n **DE**sign and co**N**struction of safe **T**unnel

SUPSI
University of Applied Sciences of Southern Switzerland

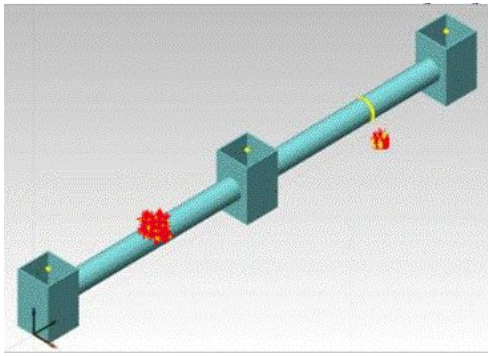

Research Aims

Response of a tunnel portion when inadequate mortar filling between the lining and the excavated surface takes place

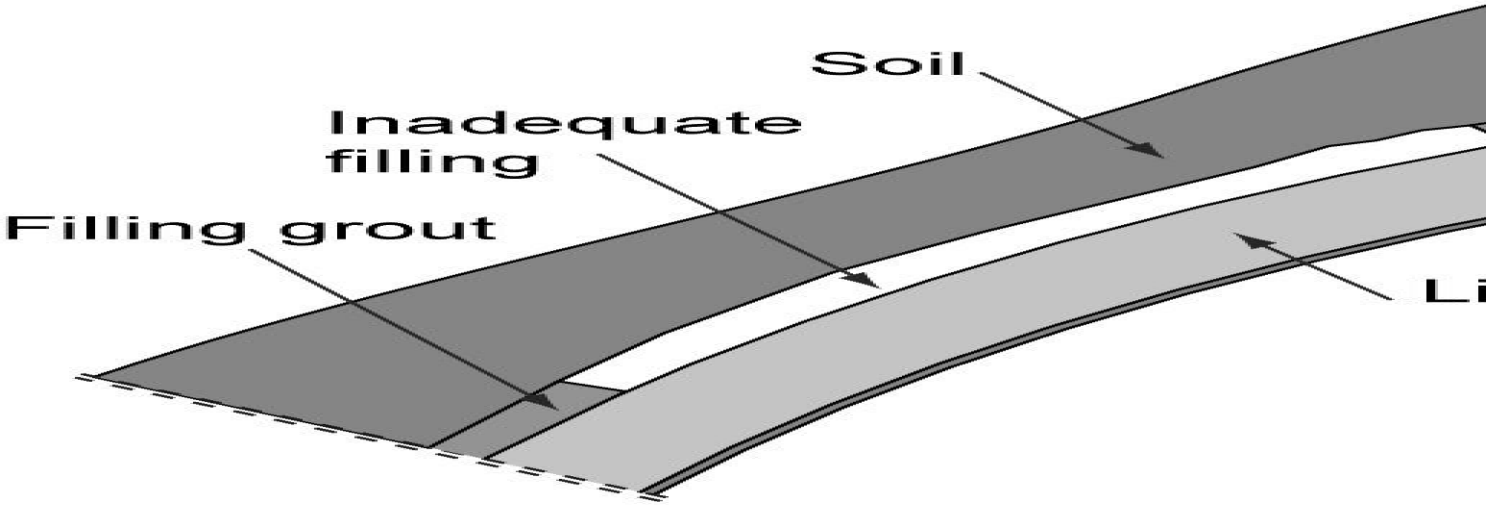

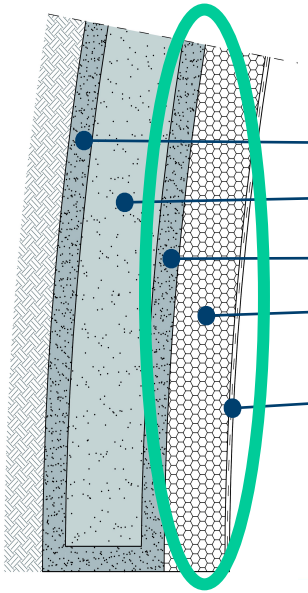

Possible solution

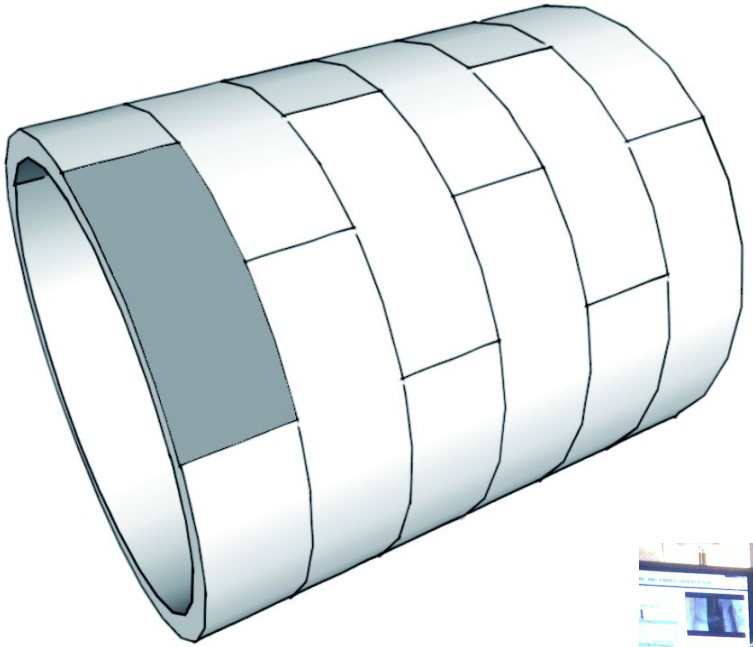

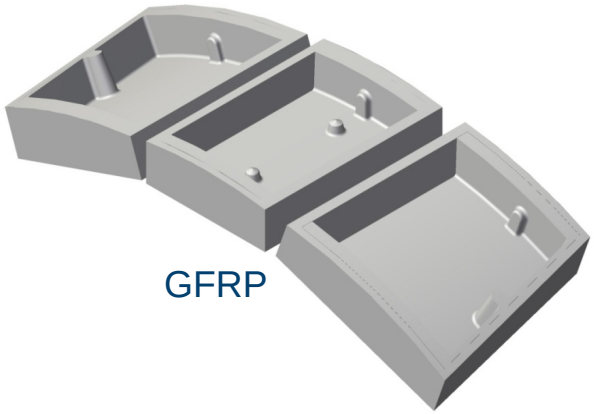

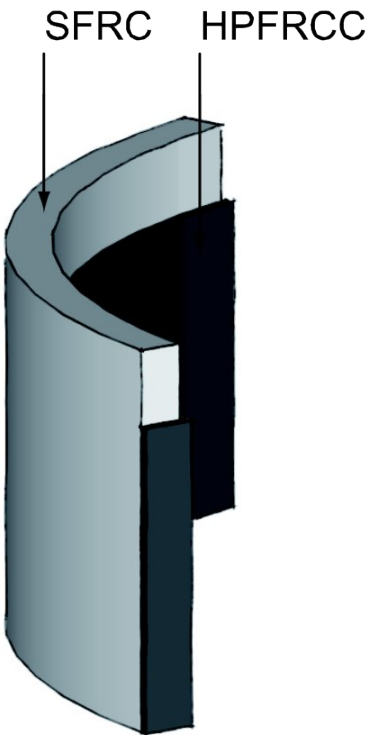

Final solution: 2 layers

EXPERIMENTAL PROGRAM: SYNOPSIS

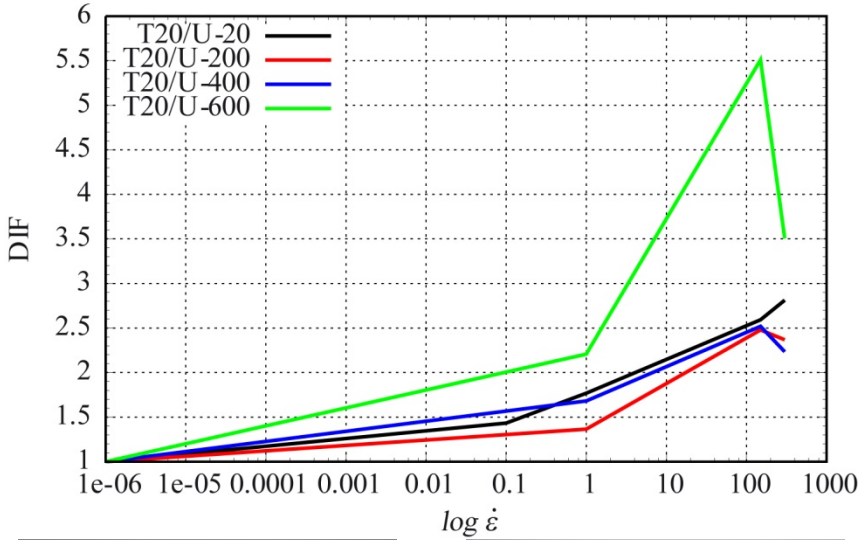

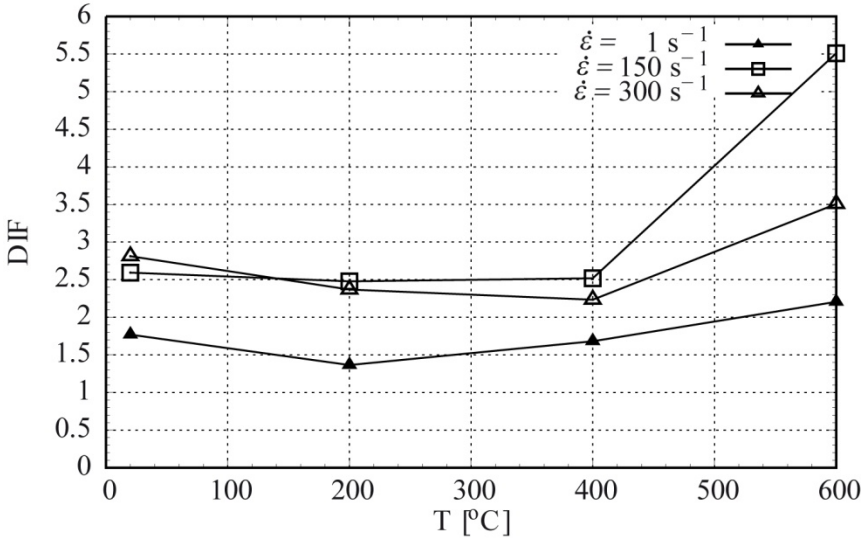

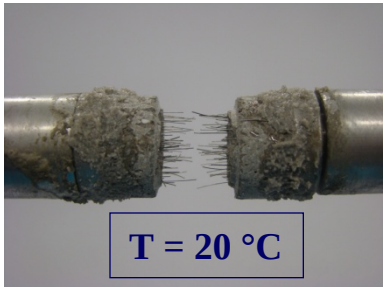

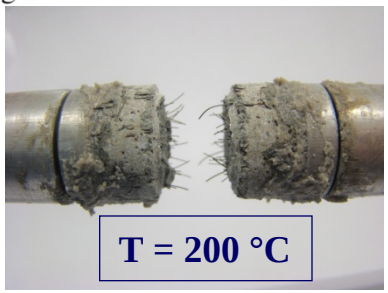

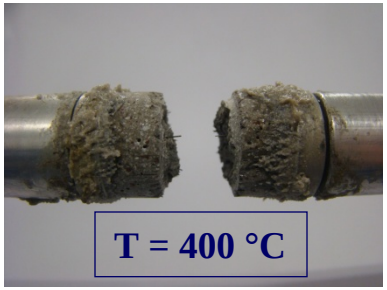

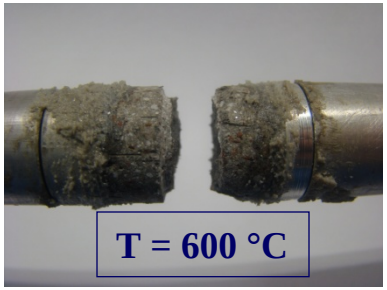

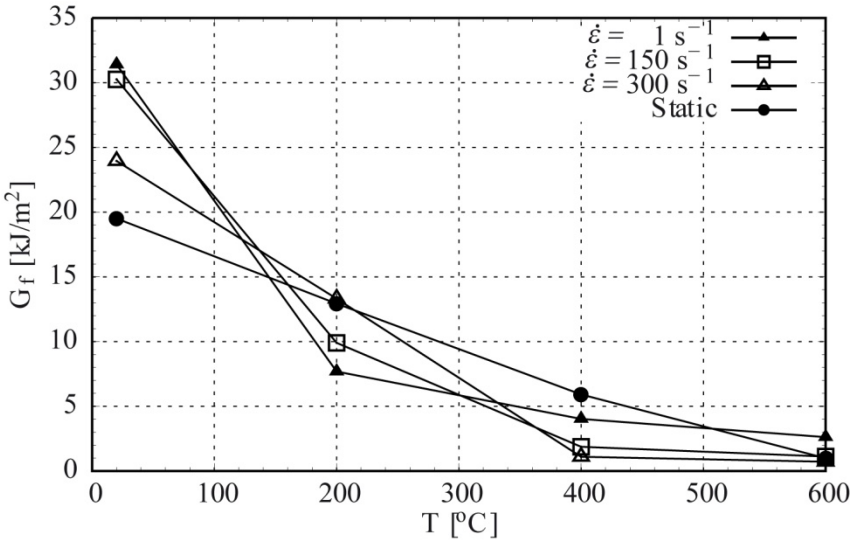

Specimen geometry and instrumentation

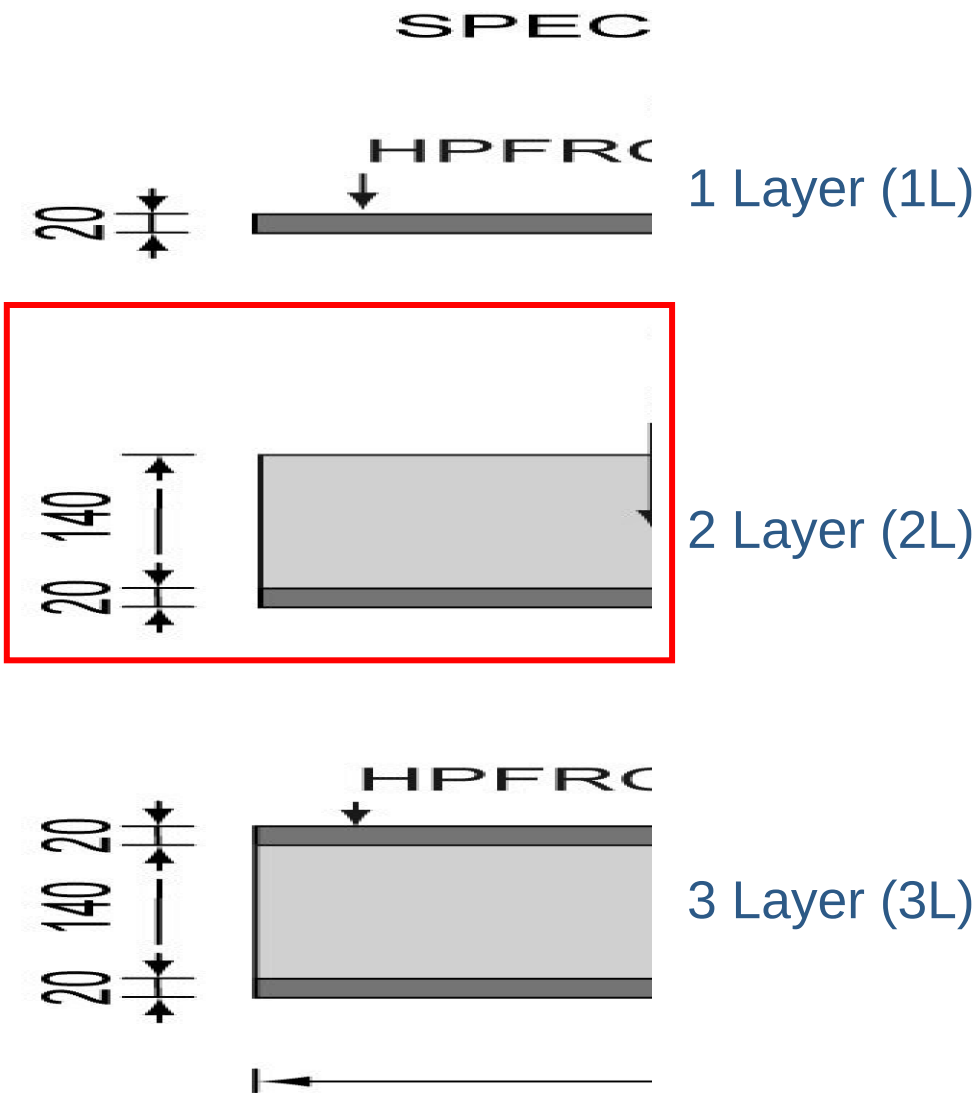

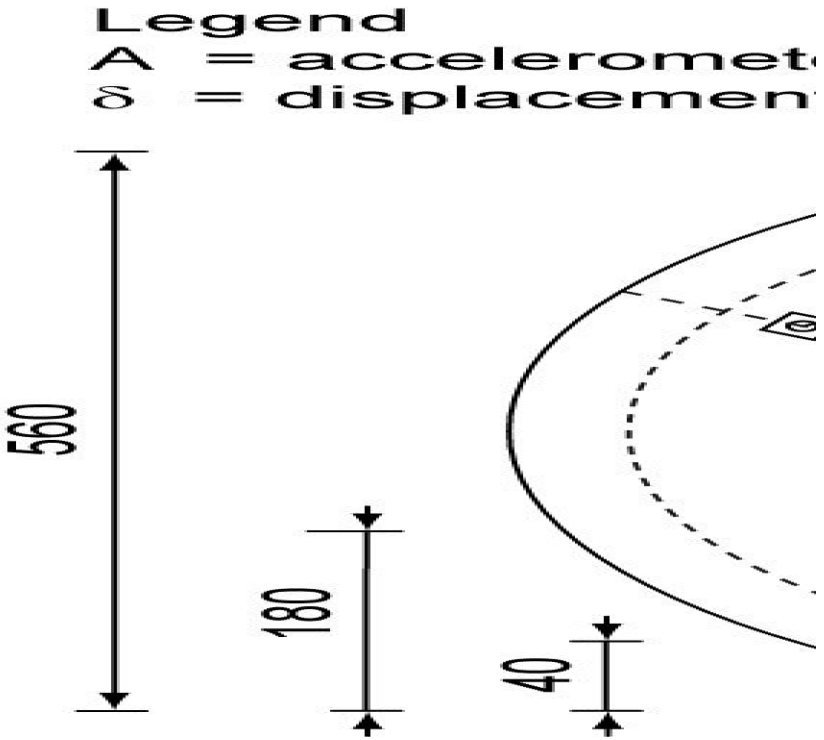

Experimental results

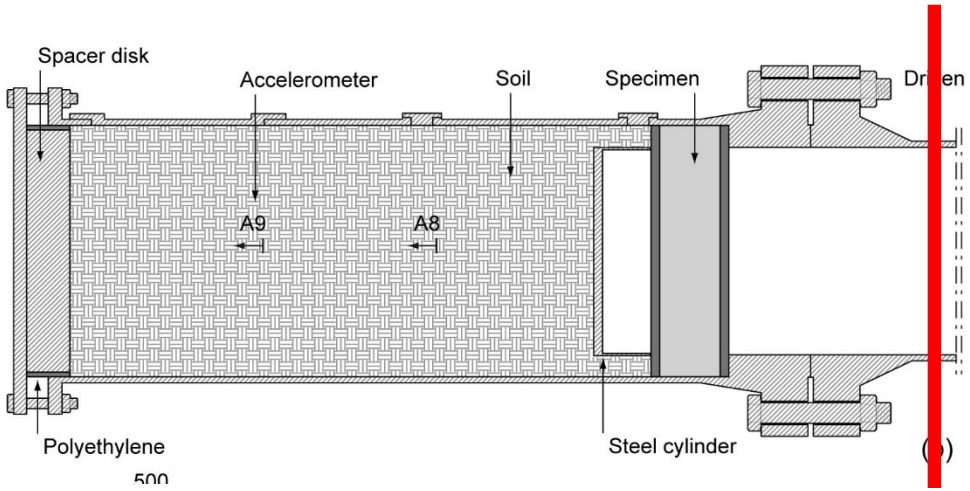

Pressure measurement cross section

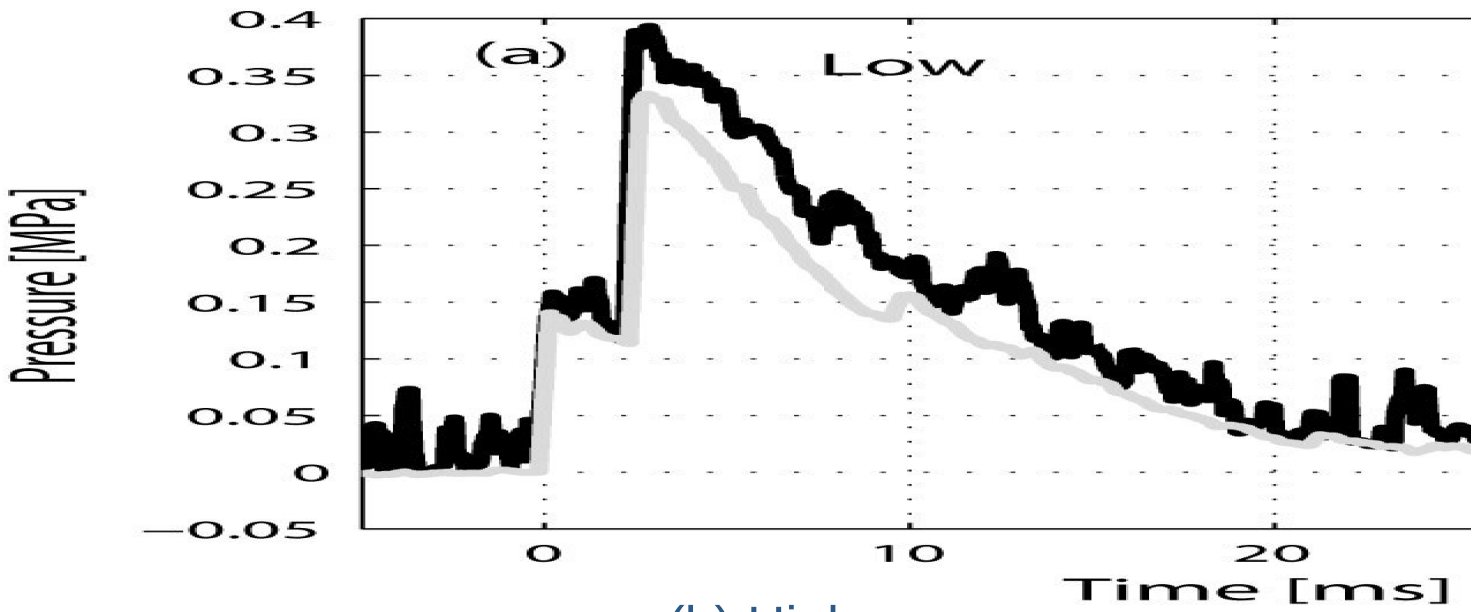

(a) Low pressure

(b) High pressure

Experimental results: crack pattern (1L-L)

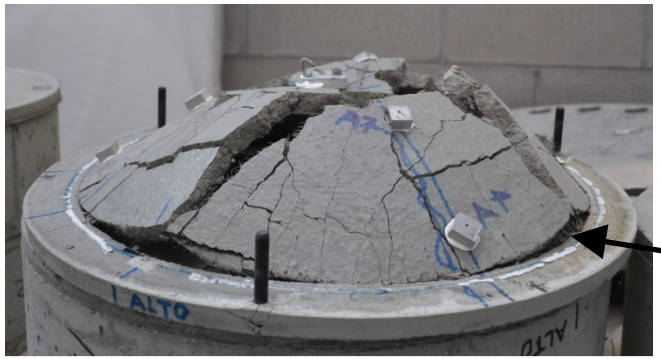

(a)

Lateral view

Plastic hinge at the support

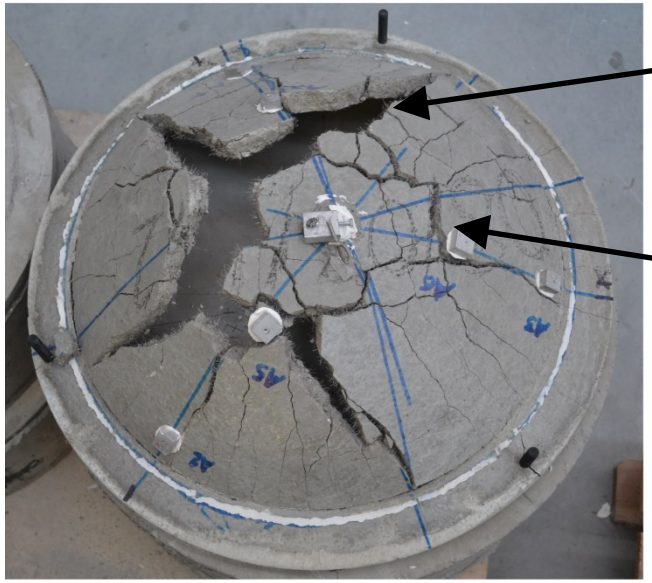

(b)

Radial crack

Circumferential crack

Unloaded face view

TUNNEL CROSS-SECTION: SEGMENT SOLUTION

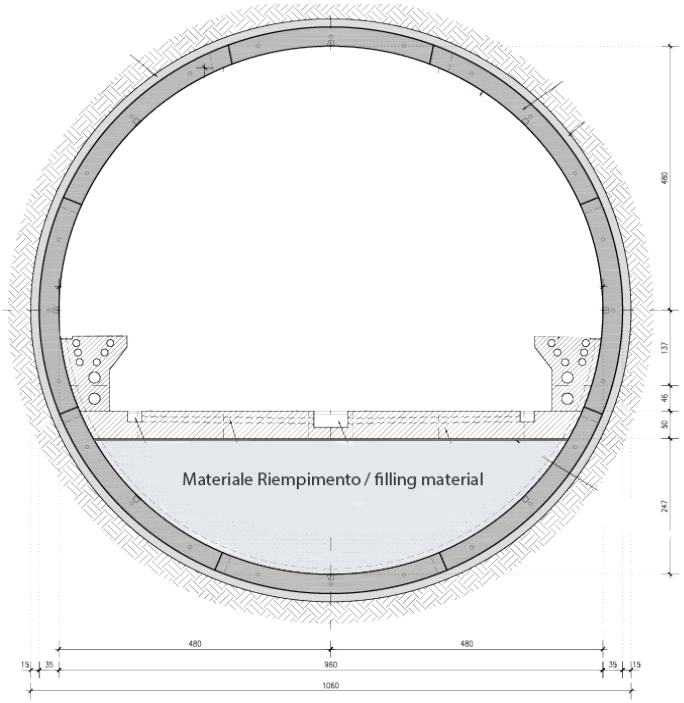

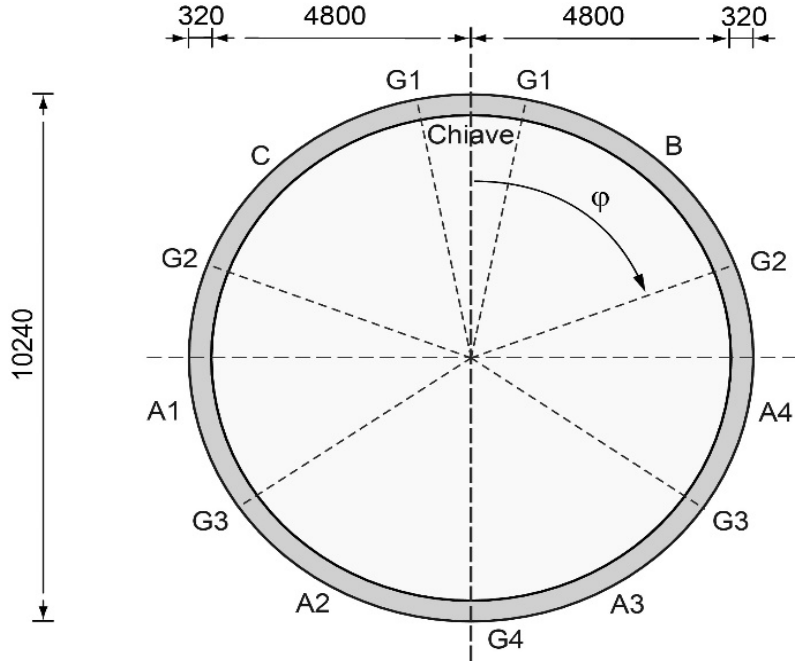

- 6+1 segments
- Concrete C50/60
- Steel rebar + fibres
- FRC class 4c

Structural solutions

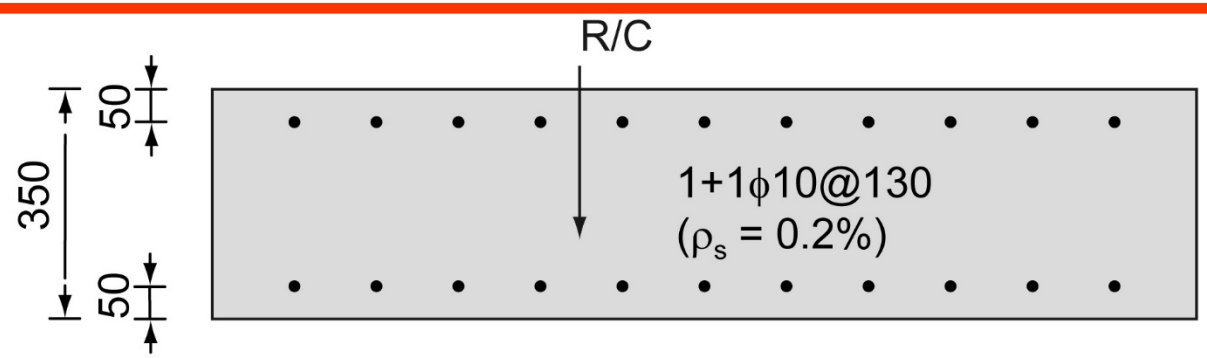

R/C solution

REFERENCE

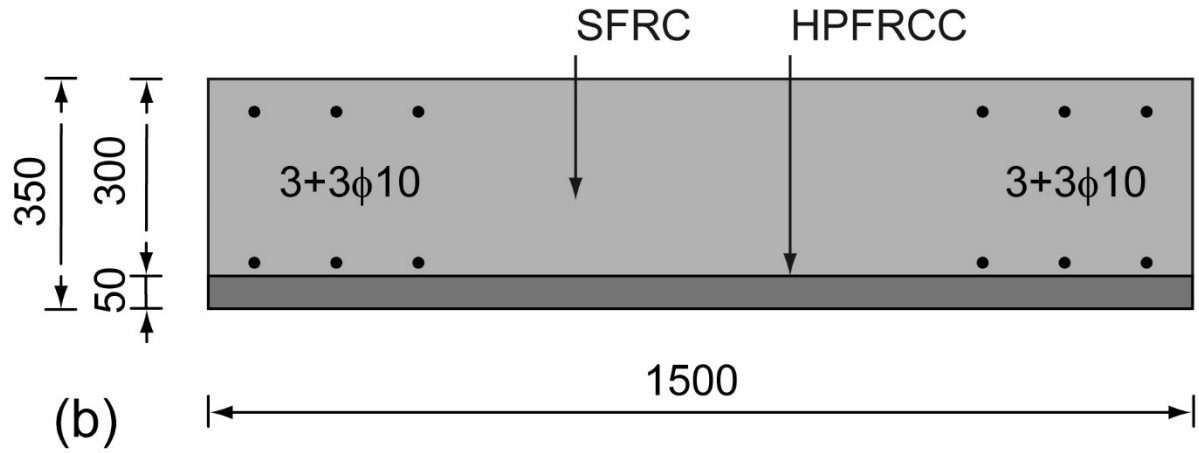

Layered solution

Pressure-impulse diagrams - Results

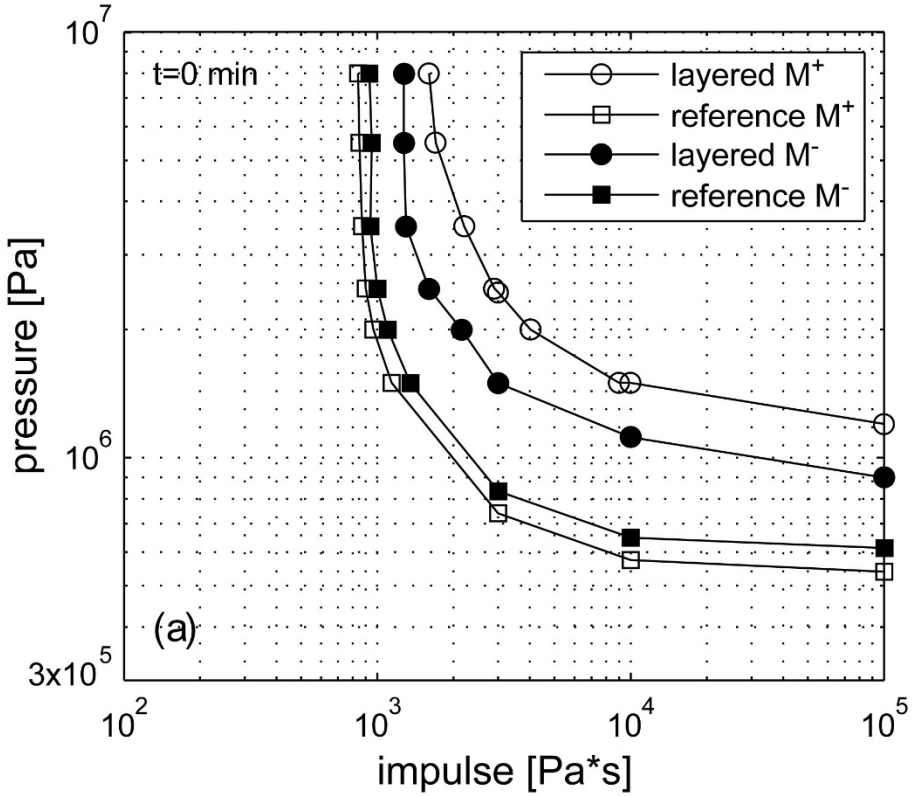

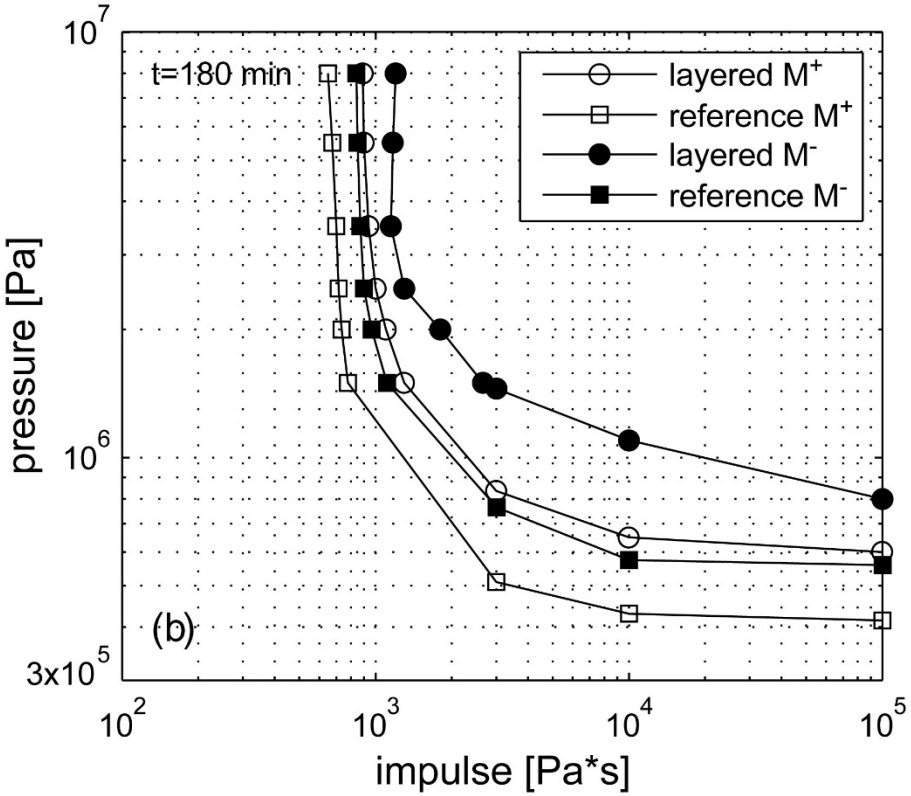

Practical advantage with layered solution

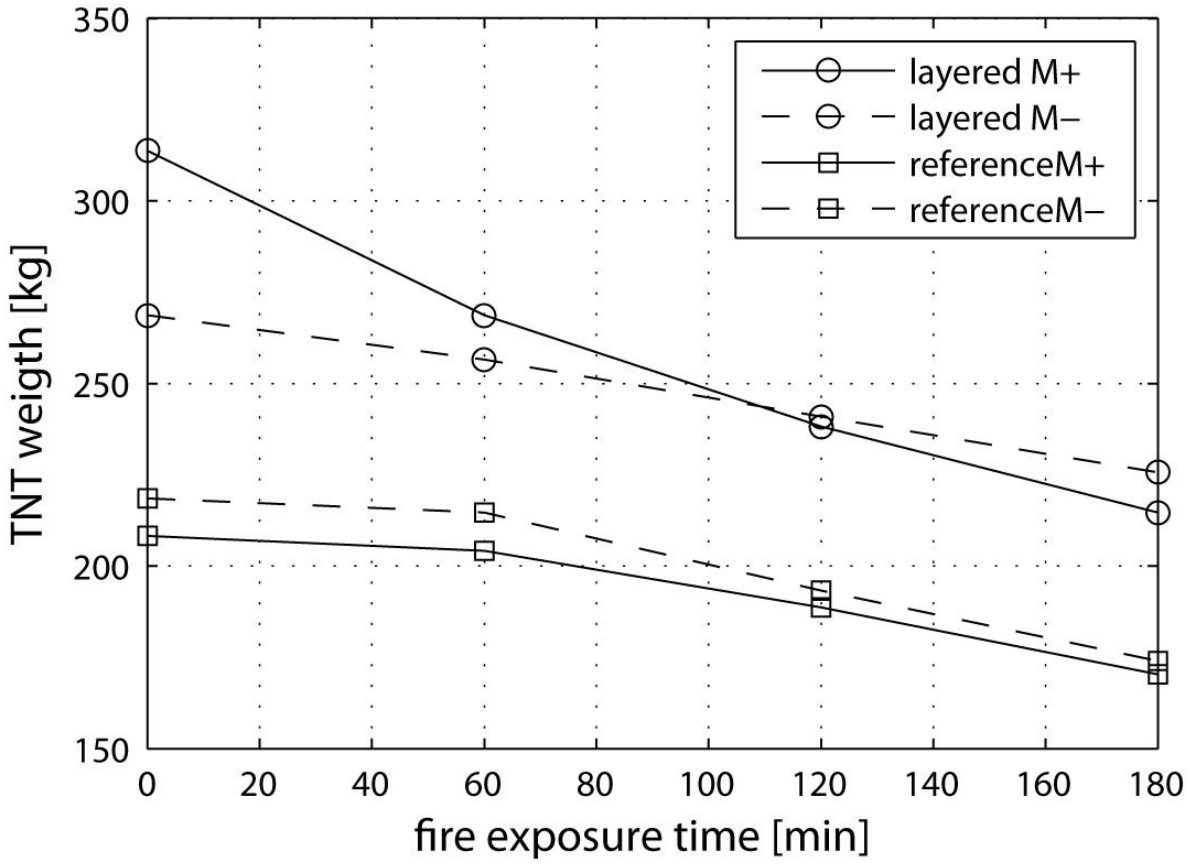

Concluding remarks (i)

- ✓ HPFRC optimized members can be regarded as a sustainable solutions mainly because of material weight reduction
- ✓ 4 point bending tests have exhibited how a fabric located in the thickness could play a very significant role from a structural point of view.
- ✓ Roof element proposed can solve at the same time seismic, energy performance and fire requirements
- ✓ Plane section approach for extremely thin-walled member can only be regarded as a rough approximation because it does not take into account the member deformability of the cross section
- ✓ F.E. modelling and design by testing can better approximate the experimental behaviour
- ✓ Also production process has to be improved to favour the industrialization and reduce the tolerances and the fibre distribution


Thank you for your attention!

References

di Prisco, M., Lamperti, M.G.L., Lapolla, S., Khurana, R.S. HPFRCC thin plates for precast roofing, (2011) Proc. 2nd Intl. Symp. on HPC, Kassel, March 2008.

di Prisco, M., Colombo, M. FRC thin-walled structures: Opportunities and threats, Fibre Reinforced Concrete - Challenges and opportunities (2012) BEFIB 2012, RILEM International Symp., Proc.

di Prisco, M., Ferrara, L., Lamperti, M., Lapolla, S., Magri, A., Zani, G., Sustainable Roof Elements: a proposal offered by cementitious composites, Innovative Materials and Techniques in Concrete Construction, 2012,167-181.

Muhaxheri, M., Spini, A., Ferrara, L., Lamperti, M.G.L., di Prisco, M., Strengthening/retrofitting of coupling beams using advanced cement based materials, Proc. of fib PhD Symposium, Quebec city, 2014, 495-501.

Zani, G., Colombo, M, di Prisco M., High performance cementitious composites for sustainable roofing panels, Proc. of fib PhD Symposiumf., Quebec city, 2014, 333-338.

Colombo, I.G., Colombo, M, di Prisco M., Pannello multistrato prefabbricato di facciata: ottimizzazione strutturale per l'adeguamento energetico, Proc. of CTE National Conf., 2014, 629-637.

Colombo, I.G., Colombo, M, di Prisco M., Multilayer precast façade: structural optimization for the energy retrofitting and for sustainable constructions, Proc. of fib PhD Symposiumf., Quebec city, 2014, 291-296.

Colombo, I.G., Colombo, M, di Prisco M., Bending behaviour of Textile Reinforced Concrete sandwich beams, accepted by Construction and Building Materials, 2015.